Design and Integration of Black-Start Service Provision by Offshore Wind Farms

To Assure Resilience in 100%-Renewable-based Future Power Systems

Pagnani, Daniela

DOI (link to publication from Publisher):
10.54337/aau539426786

Publication date:
2023

Document Version
Publisher's PDF, also known as Version of record

DESIGN AND INTEGRATION OF BLACK-START SERVICE PROVISION BY OFFSHORE WIND FARMS

TO ASSURE BETTER RESILIENCE IN 100%-RENEWABLEBASED FUTURE POWER SYSTEMS

BY
DANIELA PAGNANI

DISSERTATION SUBMITTED 2023

AALBORG UNIVERSITY
DENMARK

DESIGN AND INTEGRATION OF BLACK-START SERVICE PROVISION BY OFFSHORE WIND FARMS

TO ASSURE BETTER RESILIENCE IN 100%-RENEWABLE-BASED FUTURE POWER SYSTEMS

by

Daniela Pagnani

AALBORG UNIVERSITY
DENMARK

Dissertation submitted in 2023

Dissertation submitted: March 2023

PhD supervisor: Prof. Frede Blaabjerg,
Aalborg University

Assistant PhD supervisor: Prof. Claus Leth Bak,
Aalborg University

PhD committee: Associate Professor Sanjay Chaudhary
Department of Energy
Aalborg University, Denmark

PhD Christian Frank Flytkjær
Senior Manager, Grid Analysis, Energinet, Denmark

Professor Soledad Inmaculada Bernal-Pérez
Department of Electrical Engineering
Universitat Politècnica de València, Spain

PhD Series: Faculty of Engineering and Science, Aalborg University

Department: AAU Energy

ISSN (online): 2446-1636
ISBN (online): 978-87-7573-725-3

Published by:
Aalborg University Press
Kroghstræde 3
DK – 9220 Aalborg Ø
Phone: +45 99407140
aauf@forlag.aau.dk
forlag.aau.dk

Printed in Denmark by Stibo Complete, 2023

To my family for their unconditional love and support.

"Quando ti sembra che non ci sia via d'uscita, fermati, respira e cambia prospettiva."

"When you feel like there is no way out, stop, breath, and change your perspective."

- Samantha Cristoforetti

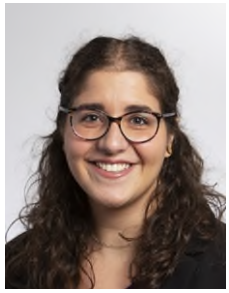

BIOGRAPHY

Daniela Pagnani was born in Caracas, Venezuela, in 1995. She obtained a B.Sc. in industrial engineering from the University of Cassino, Italy, in 2017 with a final mark of 110/110. In 2019, she completed an M.Sc. in electrical power systems and high voltage engineering from Aalborg University, Denmark (weighted average of 10.3). Since August 2019, she is with Ørsted, Gentofte, Denmark. In 2020, she started a Ph.D. degree at Aalborg University, in collaboration with Ørsted as the industrial partner. She was a visiting Ph.D. researcher at the Universitat Politècnica de València, Spain, at the Research Institute on Automatics and Industrial Informatics (Ai2), during the period from September to December 2021. In 2017-19, she volunteered in the IEEE Student Branch at Aalborg University. Since 2020, she volunteers on the Steering Committee of CIGRE Next Generation Network Denmark, and since, 2021 she is the Chair of the Steering Committee.
Her special fields of interest include power system analysis, renewable energy transition, grid-connected converters, black start, and island operation.

ENGLISH SUMMARY

Thanks to the consolidated practice in power system restoration, power systems in developed economies generally show a high level of resilience, having black-start sources able to restore the system after a blackout. Nevertheless, this practice strongly depends on conventional power plants, e.g., large thermal and hydro power plants. Sustainable goals entail the retirement of power plants based on fossil fuels and the large-scale deployment of renewable energy resources (RESs), which are interfaced by power electronic converters to the grid. This shift challenges the power system resilience, as power electronic-based resources do not have black-start capabilities yet. Integrating black-start capabilities into RESs represents a promising way to overcome the retirement of conventional black-start sources based on fossil fuels.

Offshore wind farms (OWFs) are considered one of the renewable-based resources that can overcome the challenge, thanks to their technological developments, large-scale deployment, and political support. However, differences in modeling, control, and application of novel types of converters, i.e., grid-forming converters, for black start create new bottlenecks for the stable operation of the OWF providing the black-start service. Moreover, the non-dispatchable nature of the wind entails the possibility to provide a black-start service only when the wind is available. The implementation of additional energy storage systems (ESSs) can counteract this issue.

Based on this, the focus of this Ph.D. project is to investigate the integration of grid-forming converters and ESSs into OWFs to provide black-start capabilities. To do this, black-start requirements for non-conventional power plants and the analysis of the challenges that these new requirements pose to current OWF design have been presented. Furthermore, the analysis of grid-forming control, as opposed to grid-following, and the different control topologies available in the state-of-the-art literature have been carried out. Finally, the black-start control and operational philosophy for the OWF have been outlined. Specifically, wind farm system configurations capable of performing a black start thanks to grid-forming control and ESSs are presented and compared. Two system configurations are investigated in detail with the use of electromagnetic transient (EMT) analysis and the overall black-start strategy is carried out. The two configurations apply grid-forming ESSs, like a battery ESS (BESS), working in parallel with grid-following wind turbines (WTs) (Configuration 1) and grid-forming WTs (Configuration 2). The main contributions of this thesis are: 1) A design methodology for future OWFs to provide black start equipped with grid-forming control and additional ESSs; 2) The analysis via EMT simulations of the complete operation; 3) The development of guidelines for the black-start procedure.

Overall, the findings of this Ph.D. project enable better integration of the black-start service provision into future OWF projects.

DANSK RESUMÉ

Takket være konsolideret praksis inden for genopretning af elsystemer, viser elektriske anlæg i de udviklede økonomier generelt en høj robusthed også pga. *black-start*-kilder, som kan genoprette systemet efter strømafbrydelse. Denne praksis afhænger i dag af konventionelle kraftværker (heriblandt både termiske kraftværker og vandkraftværker). Bæredygtighedsmål kræver en erstatning af fossile brændsler med vedvarende energikilder. Da mange vedvarende energikilder bruger konverter-teknologi, der består af effektelektronik, så er det også en udfordring for elsystemets robusthed, da konvertere endnu ikke har mulighed for at levere *black-start*-ydelser. Derfor er implementering af *black-start* kapacitet i konverter-baserede vedvarende energikilder yderst tiltalende, således man kan nå målsætningerne inden for den grønne dagsorden.

Særligt havvindmølleparker har et stort potentiale grundet den teknologiske udvikling, den store udbredelse og den politiske opbakning. Forskellige metoder inden for modellering, styring og anvendelse af nye typer af konvertere, særligt *grid-forming*-konvertere, udfordrer imidlertid den sikre og stabile drift af havvindmølleparker med *black-start* kapacitet. Desuden betinger vindens uregerlige karakter, at der kun kan leveres *black-start* ydelser, når vinden blæser. En eventuel implementering af energilagringssystemer kan afhjælpe dette problem.

Ph.d.-projektets fokus er på baggrund af dette at undersøge integrationen af *grid-forming* konvertere og energilagringssystemer til vindmølleparker med henblik på at levere *black-start* kapabilitet. For at opnå dette er krav til *black-start* på ikke-konventionelle kraftværker præsenteret, samt en analyse af de udfordringer som de nye krav giver for nuværende design af havvindmølleparker. Endvidere er der foretaget en sammenligning af *grid-forming*- og *grid-following*-reguleringsteknikker ud fra den nyeste litteratur. Dette sammenfatter en *black-start*-strategi og driftsfilosofi for havvindmølleparker, som også er fremlagt. Konkret præsenteres og sammenlignes systemkonfigurationer for vindmølleparker der kan levere *black-start,* takket være *grid-forming* kontrol og energilagringssystemer. To systemkonfigurationer undersøges ved brug af elektromagnetisk transient (EMT) analyse og overordnet *black-start* strategi fastsættes. De to konfigurationer anvender *grid-forming* med energilagringssystemer, som fx et batteri energilagringssystemer, som arbejder parallelt med *grid-following* havvindmøller (Konfiguration 1) og med *grid-forming* havvindmøller (Konfiguration 2). De vigtigste bidrag fra denne ph.d.-afhandling er: 1) En designmetodologi for fremtidige havvindmølleparker, der skal sikre *black-start* med *grid-forming* kontrol og yderligere energilagringssystemer; 2) EMT-analyser af den komplette operation; 3) retningslinjer for *black-start*-proceduren.

Alt i alt, fundene fra denne ph.d.-projekt muliggør bedre integration af *black-start* service i fremtidige havvindmølleprojekter.

SOMMARIO IN ITALIANO

Grazie alle pratiche consolidate nel ripristino delle reti elettriche, i sistemi elettrici nelle economie sviluppate dimostrano generalmente un alto livello di resilienza, avendo fonti di *black-start* in grado di ripristinare la rete dopo un blackout. Tuttavia, questa pratica si basa soprattutto sulle centrali elettriche convenzionali, ad esempio le grandi centrali termiche e idroelettriche. Gli obiettivi sostenibili comportano la chiusura delle centrali elettriche basate su combustibili fossili e la diffusione su larga scala di fonti energetiche rinnovabili, che si interfacciano alla rete tramite convertitori elettronici di potenza. Ciò sfida la resilienza del sistema elettrico, poiché le risorse basate sull'elettronica di potenza non hanno ancora funzionalità di *black-start*. L'integrazione delle capacità di *black-start* nelle fonti energetiche rinnovabili rappresenta un'idea promettente per superare la chiusura delle centrali convenzionali di *black-start* basate su combustibili fossili.

I parchi eolici offshore sono considerati una delle risorse rinnovabili in grado di superare questa sfida, grazie al loro sviluppo tecnologico, la loro diffusione su larga scala e al sostegno politico. Tuttavia, le differenze nella modellazione, nel controllo e nell'utilizzo di nuovi tipi di convertitori, cioè convertitori *grid-forming*, per il *black start* pongono nuovi problemi complessi per il funzionamento stabile dei parchi eolici offshore che devono fornire tale servizio. Inoltre, la natura del vento, il cui dispacciamento non può essere programmato, comporta la possibilità di fornire un servizio di *black-start* solo quando il vento è disponibile. Per contrastare problemi di questo tipo, si può pensare all'implementazione di sistemi aggiuntivi di accumulo di energia elettrica.

Basandosi su queste premesse, il focus di questo dottorato di ricerca è quello di indagare l'integrazione di convertitori *grid-forming* e di sistemi di accumulo dell'energia in parchi eolici offshore per fornire funzionalità di *black-start*. Per raggiungere questo obiettivo, sono stati presentati i requisiti di *black-start* per le centrali elettriche non convenzionali e l'analisi delle sfide che questi nuovi requisiti pongono all'attuale progettazione di parchi eolici offshore. È stata inoltre effettuata l'analisi del controllo *grid-forming*, in contrapposizione al *grid-following*, e le diverse tipologie di controllo disponibili nella letteratura all'avanguardia. Sono stati infine delineati la filosofia di controllo e la filosofia operativa per i parchi eolici offshore durante il *black-start*. Nello specifico, vengono presentate e confrontate configurazioni del sistema eolico in grado di eseguire un *black start* grazie al controllo *grid-forming* e ai sistemi di accumulo. Due configurazioni di sistema sono studiate in dettaglio con l'uso dell'analisi elettromagnetica transitoria e viene eseguita la strategia complessiva *black-start*. Le due configurazioni applicano sistemi di accumulo dell'energia con controllo *grid-forming*, ad esempio sistemi di accumulo dell'energia a batteria (BESS), che funziona in parallelo con turbine eoliche *grid-following* (Configurazione 1) e turbine eoliche *grid-forming* (Configurazione 2). I principali

contributi di questa tesi sono: 1) Una metodologia di progettazione per fornire servizi di *black start* per i futuri parchi eolici offshore dotati di controllo *grid-forming* e sistemi aggiuntivi di accumulo di energia elettrica; 2) L'analisi attraverso simulazioni dei transitori elettromagnetici dell'operazione completa; 3) Lo sviluppo di linee guida che descrivono in dettaglio la procedura *black-start*.

In conclusione i risultati di questo dottorato consentiranno, nel complesso, una migliore integrazione della fornitura di servizi di *black-start* nei futuri progetti eolici offshore.

RESUMEN EN ESPAÑOL

Gracias a las prácticas consolidadas para restaurar las redes eléctricas, los sistemas eléctricos en las economías desarrolladas generalmente muestran un alto nivel de resiliencia con las fuentes de *black-start*, que pueden restaurar el sistema después de un apagón. Sin embargo, esta práctica depende en gran medida de centrales eléctricas convencionales, como grandes centrales eléctricas térmicas e hidroeléctricas. Los objetivos sostenibles implican el cierre de centrales eléctricas basadas en combustibles fósiles y la implementación a gran escala de centrales eléctricas con fuentes de energía renovable, que se conectan a la red a través de electrónica de potencia. Esto desafía la resiliencia del sistema eléctrico, ya que las fuentes basadas en electrónica de potencia aún no tienen capacidades de *black-start*. La integración de las capacidades de *black-start* en fuentes de energía renovable es una forma prometedora de superar el desafío de retirar las fuentes convencionales de *black start* basadas en combustibles fósiles.

Los parques eólicos marinos se consideran unas de las fuentes renovables capaces de superar este desafío, gracias a sus avances tecnológicos, a la difusión a gran escala y al apoyo político. Sin embargo, las diferencias en el modelado, control y utilización de nuevos tipos de convertidores, es decir, convertidores *grid-forming*, para el *black-start* plantean nuevos problemas para el funcionamiento estable del parque eólico marino que proporciona el servicio de *black-start*. Además, la naturaleza no despachable del viento significa que solo se puede proporcionar un servicio de *black start* cuando hay viento disponible. La implementación de sistemas adicionales de almacenamiento de energía puede contrarrestar este problema.

Basándose en esto, este proyecto de doctorado se centra en investigar la integración de convertidores *grid-forming* y sistemas de almacenamiento de energía en parques eólicos marinos para proporcionar servicios de *black-start*. Para lograr este objetivo, se presentan los requisitos de *black-start* para las centrales de energía no convencionales y el análisis de los desafíos que estos nuevos requisitos plantean al diseño actual de parques eólicos marinos. Además, se realizan el análisis del control *grid-forming*, en contraposición a el *grid-following*, y las diferentes topologías de control disponibles en la bibliografía reciente. Por último, se describen la filosofía del control y la filosofía de funcionamiento del parque eólico marino durante el *black-start*. Específicamente, se presentan y comparan configuraciones de sistemas eólicos capaces de realizar un *black start* gracias al control *grid-forming* y los sistemas de almacenamiento de energía. Se estudian en detalle dos configuraciones del sistema eólico mediante análisis de transitorios electromagnéticos y se ejecuta la estrategia general de *black-start*. Las dos configuraciones utilizan sistemas de almacenamiento de energía *grid-forming*, como una batería, que funciona en paralelo con turbinas eólicas *grid-following* (Configuración 1) y turbinas eólicas *grid-forming* (Configuración 2). La contribución principal de esta tesis consiste en: 1) Una metodología de diseño para que los futuros parques eólicos marinos proporcionen el

servicio de *black-start* con control *grid-forming* y sistemas adicionales de almacenamiento de energía; 2) El análisis a través de simulaciones de transitorios electromagnéticos de la operación completa; 3) El desarrollo de directrices que detallan el proceso de *black-start.*

En definitiva, los resultados de este proyecto de doctorado permiten una mejor integración de la prestación de servicios de *black-start* en futuros proyectos eólicos marinos.

PREFACE

This thesis has been submitted to the Faculty of Engineering and Science at Aalborg University in partial fulfillment of the requirements for the Ph.D. degree in Electrical Energy Engineering. The research has been conducted at the Department of Energy at Aalborg University as well as in the Electrical System Design and Grid Integration Department in Ørsted. The collaboration has been in the form of this Industrial Ph.D. project, which implies that this research is industry-oriented, giving the chance to create benefits for both industry and academia.

This project has been conducted under the supervision of Prof. Frede Blaabjerg and Prof. Claus Leth Bak from Aalborg University and Dr. Łukasz Kocewiak and Dr. Jesper Hjerrild from Ørsted.

In this thesis, the software PSCAD has been used to model the system and perform the electromagnetic transient analysis to investigate and describe the black-start procedure carried out by an offshore wind farm with an integrated storage system. Furthermore, the software MATLAB has been used to design the grid-forming and grid-following controllers applied in the studied system.

Reading Guide:
This thesis is article-based, which means that it comprises two parts: the Extended Summary and the Appended Papers. The Extended Summary gathers the main points of this Ph.D. project in the form of a short report, where the related articles from the student are referenced and the complete manuscripts can be found in the Appended Papers.

The information referenced in the present work has been found in literature, web pages, and reports. Throughout this report, source notes will be appearing in square brackets. The source notes have been made using the IEEE notation; meaning that the notes in the text will be stating the number of appearances of the source in the text. The notes will refer to the complete literature list at the end of the report, where books are listed with the author, title, year, publisher, and ISBN, and web pages are put with the author, title, URL, and date.

Figures, equations, and tables are numbered in order of the chapter of their appearance. For example, the third figure in Chapter 4, will be numbered 4-3, the same goes for equations and tables. Every figure and table is provided with a caption, explaining its content.

ACKNOWLEDGMENTS

Words cannot express my gratitude to my supervisors Prof. Frede Blaabjerg and Prof. Claus Leth Bak from Aalborg University, and Dr. Łukasz Kocewiak and Dr. Jesper Hjerrild from Ørsted for their invaluable patience, mentorship, and expertise.
I would also like to acknowledge the support received from Dr. Troels Stybe Sørensen, who, although not being my supervisor, has certainly helped me very much over these three years. Special thanks also to Dr. M. Kazem Bakhshizadeh for introducing me to various practical and technical aspects of offshore wind projects. The knowledge sharing within the department of Electrical System Design and Grid Integration significantly contributed to the project development.
I owe all of you my deepest gratitude for the support and collaboration received in this type of project where academia and industry come together. I must underline the exceptional circumstances that we had to go through for more than two years of this project, being all forced to stay at home for long, intermittent lockdowns, avoiding meetings and travel, due to the COVID-19 pandemic. Even though it was tough, and we were completely unprepared, I would still go through this journey again. My most sincere gratitude.

Special thanks also to all the people in the Ai2 Research Institute hosted at the Universitat Politècnica de València, in Spain, for their kindness and hospitality once traveling was possible again. I would like to thank especially Prof. Ramón Blasco-Giménez and Prof. Jaime Martínez-Turégano for their significant contribution to the research and numerous professional discussions.

I also owe special thanks to all the academic and administrative stuff in the Department of Energy at Aalborg University. Aalborg University has a special place in my heart, as it is where my journey in Denmark started as an exchange student during my B.Sc. studies, and now, five years later, it is concluding with the third Thesis. I am also grateful to my academic colleagues, for their editing help, feedback sessions, and moral support, especially my fellow Ph.D. student and best friend, Monika Sandelic.

Thank you also to all my friends around the world. You are too many to be mentioned but to you goes my gratitude for making these years unforgettable.

I would be remiss in not mentioning my family, in Italy and Denmark, especially above all my mother, Paola. Their belief in me has given me strength and motivation during these years. Last but not least, I would like to thank the love of my life, Kasper, for his support and understanding. I would also like to thank our cat, Maxwell, for all the entertainment and emotional support.

Daniela Pagnani,
January 2023, Gentofte, Denmark

LIST OF FIGURES

Figure 1-1. a) Sustainable Development Goals established by United Nations and b) key target for goal no. 7.2 with a focus on renewable energy increase [1]. 3
Figure 1-2. A black start is an intermediate procedure to shift from a state of no power (due to a system shutdown) to a state of restored normal operation [C1], [3]. 4
Figure 1-3. Cumulative installed capacity of offshore wind power from 2000 to (forecasted) 2050 [5]. 5
Figure 1-4. Schematic of a Type-4 wind turbine (PMSG = permanent magnet synchronous generator). 5
Figure 1-5. Parallel between a typical controller structure and related bandwidth of a synchronous generator and a large Type-4 wind-turbine generator [9]. 6
Figure 1-6. Typical control topologies for grid-connected converters: (a) grid-following control and (b) grid-forming control (bold symbols refer to vectors)..... 7
Figure 1-7. Cumulative installed capacity of energy storage from 2020 to (forecasted) 2040 [18]. 9
Figure 1-8. Typical black-start procedure by a conventional power plant consisting of three main different steps [64]. 10
Figure 1-9. Traditional and new black start providers can bring benefits to society.17
Figure 1-10. Research activities of the Ph.D. project "Design and Integration of Black-Start Service Provision by Offshore Wind Farms". 19
Figure 1-11. Structure and corresponding appended papers of this Ph.D. thesis. 20
Figure 2-1. Schematic representation of (a) high voltage alternating current (HVAC) and (b) high voltage direct current (HVDC) transmission system for offshore wind farms [57]. 24
Figure 2-2. Offshore wind farm system configurations to provide black start by (a) synchronous generators (SGs), (b) energy storage systems (ESSs), and (c) new-generation wind turbines. 28
Figure 3-1. Schematic of the proposed wind farm system configuration consisting of a wind farm with integrated storage and the stages to achieve black start [J2], [61],[C3], [81]. 34
Figure 3-2. Flowchart describing stages and substages of the black-start procedure implemented by an offshore wind farm [J2], [61]..... 35
Figure 3-3. Implemented version of the power synchronization control (PSC) type of grid-forming including virtual inertia and damping [40], [J3], [95]. 38
Figure 3-4. Concept behind the power synchronization control structure of grid-forming control that represents two synchronous machines in AC system [39]. 39
Figure 4-1. Case study of the offshore wind farm with an integrated battery used for the black-start analysis [C4], [93]. 44
Figure 4-2. Aggregation of wind turbines and array cables: a) whole string and b) single wind turbine resulting from the aggregation..... 46
Figure 4-3. Inverter equivalent circuit and controller. 48
Figure 4-4. Converter topology used in the system for: a) the battery storage and b) for the wind turbine [C4], [93]. 48

Figure 4-5. Grid-forming control based on power synchronization control implemented for the energy storage system and the wind turbines in the benchmark model [J3], [95]. 50
Figure 4-6. Grid-following control implemented for the wind turbines in the benchmark model [J3] [95]. 51
Figure 4-7. Two configurations to perform black start services by offshore wind farms with integrated battery storage [J3], [95]. 52
Figure 4-8. Bumpless transfer between the phase-locked loop and the power synchronization control implemented in the wind turbines [39], [C4], [93]. 52
Figure 4-9. Flowchart schematizing the main steps of the implemented black-start procedure for the wind farm operator [C3], [81]. 53
Figure 4-10. Case study of the offshore wind farm with an integrated battery used for the black-start analysis for Configuration 1 and 2 with related stages (CB =circuit breaker). 54
Figure 4-11. Three-phase electrical measurements for Stage 1.1 of the black-start procedure seen from the battery storage point of connection; a) voltage, b) current; c) active power (blue), and reactive power (orange). 57
Figure 4-12. Three-phase electrical measurements for Stage 1.2 of the black-start procedure seen from the battery storage and the wind turbine point of connection; a) battery storage voltage, b) wind turbine voltage, c) battery storage current, d) wind turbine current, e) battery storage active power (blue) and reactive power (orange), and f) wind turbine active power (blue) and reactive power (orange). 59
Figure 4-13. Three-phase electrical measurements for Stage 2.1 of the black-start procedure seen from the battery storage and the wind turbine point of connection; a) battery storage voltage, b) wind turbine voltage, c) battery storage current, d) wind turbine current, e) battery storage active power (blue) and reactive power (orange), and f) wind turbine active power (blue) and reactive power (orange). 61
Figure 4-14. Three-phase electrical measurements for Stage 2.2 of the black-start procedure seen from the battery storage and the wind turbine point of connection; a) battery storage voltage, b) wind turbine voltage, c) battery storage current, d) wind turbine current, e) battery storage active power (blue) and reactive power (orange), and f) wind turbine active power (blue) and reactive power (orange). 62
Figure 4-15. Black-start strategy performed with the offshore wind farm in Configuration 1 (grid-forming battery and grid-following wind turbines) showed from the battery terminals: a) voltage; b) current and c) active (blue) and reactive (orange) power [J3], [95]. 64
Figure 4-16. Black-start strategy performed with the offshore wind farm in Configuration 1 (grid-forming battery and grid-following wind turbines) showed from the turbine terminals: a) voltage; b) current and c) active (blue) and reactive (orange) power [J3], [95]. 65
Figure 4-17. Three-phase electrical measurements for black-start procedure in Configuration 1 without inertia emulation in the grid-forming controller seen from the battery storage and the wind turbine point of connection; a) battery storage voltage, b) wind turbine voltage, c) battery storage current, d) wind turbine current, e) battery

storage active power, f) wind turbine active power, g) battery reactive power, and h) wind turbine reactive power. 67
Figure 4-18. Comparison of the frequency swings during block loading (Stage 2.2) in Configuration 1. 67
Figure 4-19. Three-phase electrical measurements for Stage 1.2 of the black-start procedure for Configuration 2 seen from the battery storage and the wind turbine point of connection; a) battery storage voltage, b) wind turbine voltage, c) battery storage current, d) wind turbine current, e) battery storage active power (blue) and reactive power (orange), and f) wind turbine active power (blue) and reactive power (orange). 70
Figure 4-20. Three-phase electrical measurements for Stage 2.1 of the black-start procedure seen from the battery storage and the wind turbine point of connection; a) battery storage voltage, b) wind turbine voltage, c) battery storage current, d) wind turbine current, e) battery storage active power (blue) and reactive power (orange), and f) wind turbine active power (blue) and reactive power (orange). 72
Figure 4-21. Three-phase electrical measurements for Stage 2.2 of the black-start procedure seen from the battery storage and the wind turbine point of connection; a) battery storage voltage, b) wind turbine voltage, c) battery storage current, d) wind turbine current, e) battery storage active power (blue) and reactive power (orange), and f) wind turbine active power (blue) and reactive power (orange). 73
Figure 4-22. Black start strategy performed with the offshore wind farm in Configuration 1 (grid-forming battery and grid-following wind turbines) from the battery terminals: a) voltage; b) current and c) active (blue) and reactive (orange) power [J3], [95]. 74
Figure 4-23. Black start strategy performed with the offshore wind farm in Configuration 2 (grid-forming battery and grid-forming wind turbines) from the turbine terminals: a) voltage; b) current and c) active (blue) and reactive (orange) power [J3], [95]. 75
Figure 4-24. Energization of wind turbine transformer separately from the soft-charge seen from the battery storage: a) voltage, b) current, c) active power, and d) reactive power. 77
Figure 4-25. Soft-charge in 0.05 s: a) voltage, b) current, c) active power, and d) reactive power. 78
Figure 4-26. Soft-charge in 0.2 s: a) voltage, b) current, c) active power, and d) reactive power. 78
Figure 4-27. Soft charge in 0.8 s: a) voltage, b) current, c) active power, and d) reactive power. 79
Figure 4-28. Energization of 100 km overhead line during Configuration 1: a) battery voltage, b) battery current, c) battery active power, d) battery reactive power, e) wind turbine voltage, f) wind turbine current, g) wind turbine active power and h) battery reactive power. 80
Figure 4-29. Energization of 100 km overhead line during Configuration 2: a) battery voltage, b) battery current, c) battery active power, d) battery reactive power, e) wind

turbine voltage, f) wind turbine current, g) wind turbine active power and h) battery reactive power. 81
Figure 4-30. Three-phase electrical measurements for the battery storage application of single-pole switching to energize the onshore transmission grid transformer; a) voltage, b) current, c) active power, and d)reactive power. 82
Figure 4-31. Three-phase electrical measurements for the battery storage application of single-pole switching to energize the onshore transmission grid transformer; a) voltage, b) current, c) active power, and d)reactive power. 83

LIST OF TABLES

Table 1-1. Comparison of selected features between a synchronous generator and a grid-forming converter [17]. 8
Table 1-2. Overview of selected large-scale blackouts in terms of affected customers (in chronological order) [21-29]..... 11
Table 2-1. Extension of the black start requirements to non-traditional sources presented by National Grid Electricity System Operator in Great Britain in 2021 [C1], [3]..... 26
Table 2-2. Overview of methods to achieve black start in offshore wind farms [C1], [3]..... 32
Table 3-1. Comparison of grid forming control strategies to achieve offshore wind farm black start [J1], [30]..... 38
Table 4-1. Ratings of the equipment implemented in the studied system [C4], [93]. 47
Table 4-2. Converter hardware parameters implemented in the battery model..... 49
Table 4-3. Converter hardware parameters implemented in the wind turbine model. 49
Table 4-4. Controller parameters implemented in the grid-forming converters..... 50
Table 4-5. Controller parameters implemented in the grid-following converters. ... 51
Table 4-6. Events simulated for the base case of Configuration 1 (grid-forming battery storage and grid-following wind turbines) of the black-start procedure [J3], [95]... 55
Table 4-7. Events simulated for the demonstration of Configuration 2 (grid-forming battery storage and grid-forming wind turbines) of the black-start procedure [J3], [95]. 68

LIST OF ABBREVIATIONS

automatic voltage regulator (AVR) 4

battery energy storage system (BESS) 9

direct power control (DPC) 16

electromagnetic transient (EMT) 12

flexible AC transmission system (FACTS) 24

grid-following (GFL) 6

grid-forming (GFM) 7

high voltage (HV) 23

maximum power point tracking (MPPT) 6

National Grid Electricity System Operator (NGESO) 12

offshore substation (OSS) 29

offshore wind farm (OWF) 4

onshore substation (OnSS) 29

overhead line (OHL) 14

permanent magnet synchronous generator (PMSG) 5

phase-locked loop (PLL) 6

photovoltaic (PV) 12

point of wave (POW) 82

power synchronization control (PSC) 15

proportional-integral (PI) 48

rate of change of frequency

	(RoCoF) 4
renewable energy source	(RES) 4
short-circuit ratio	(SCR) 15
static compensator	(STATCOM) 24
synchronous generator	(SG) 4
synchronous machine	(SM) 36
transmission system operator	(TSO) 4
uninterruptible power supply	(UPS) 30
United Kingdom	(UK) 13
virtual synchronous machine	(VSM) 13

TABLE OF CONTENTS

Title Page ..... **i**
Biography ..... **v**
English Summary ..... **vi**
Dansk Resumé ..... **vii**
Sommario in Italiano ..... **viii**
Resumen en Español ..... **x**
Preface ..... **xii**
Acknowledgments ..... **xiii**
List of Figures ..... **xv**
List of Tables ..... **xix**
List of Abbreviations ..... **xx**
Table of Contents ..... **xxii**
Part I – Extended Summary **1**
1. Introduction **3**
1.1. Background 3
1.1.1. Black Start from Conventional Sources 9
1.1.2. Black Start from Non-Conventional Sources 11
1.2. Project Objectives and Limitations 18
1.2.1. Research Questions and Objectives 18
1.2.2. Project Limitations 19
1.3. Thesis Outline 20
1.4. List of Publications 21
2. Requirements and Wind Farm System Configurations for Black Start **23**
2.1. Modern Offshore Wind Farms 23
2.1.1. Common Energization Procedure of Offshore Wind Farms 24
2.2. Technical Requirements for Black-Start Provision by Offshore Wind Farms 26
2.2.1. Challenges for Current Wind Farm Design 27
2.3. Wind Farm System Configurations to Provide Black Start 28
2.4. Design Guidelines for Future Wind Farms Providing Black-Start Services 32

2.5. Summary 33
3. Black-Start Functionality and Grid-Forming Control in Offshore Wind Farms 34
3.1. Black-Start Functionality Analysis 34
3.2. Grid-Forming Control Concept 36
3.2.1. Grid-Forming Control Applied to Black Start 37
3.2.2. Overview of Different Grid-Forming Strategies 37
3.3. Principles of the Selected Grid-Forming Control 38
3.3.1. Principle of Power Synchronization 39
3.3.2. Virtual Synchronous Machine (VSM) Variation 40
3.4. Summary 42
4. Operational and Control Philosophy for Wind Farms as Black-Start Providers 43
4.1. Black-Start Study Methodology and Modeling 43
4.1.1. System Model 44
4.1.2. Converter Models 47
4.2. Black-Start System Configurations 52
4.3. Black-Start Operational and Control Philosophy 53
4.4. Configuration 1: Grid-Forming Battery and Grid-Following Wind Turbines 54
4.4.1. Stage 1: Wind Farm Power Island 55
4.4.2. Stage 2: Black Start Power Island 60
4.4.3. No Inertia Emulation in the Grid-Forming COntrol 66
4.5. Configuration 2: Grid-Forming Battery and Grid-Forming Wind Turbines . 68
4.5.1. Stage 1: Wind Farm Power Island 68
4.5.2. Stage 2: Black Start Power Island 71
4.6. Strategy Variations and Sensitivity Analysis 76
4.6.1. Energization of Wind Turbine Transformer Separately from Soft-Charge 76
4.6.2. Soft-Charge with Different Time Rates 77
4.6.3. Energization of Longer Transmission Line 79
4.6.4. Application of Single-Pole Switching to Energize the Onshore Transmission Grid Transformer 82
4.7. Summary 84

5. Conclusions 86
5.1. Overall Summary 86
5.2. Main Contributions 87
5.3. Future Work 88
Literature List 91
Part II – Appended Paper 99

PART I – EXTENDED SUMMARY

1. INTRODUCTION

This chapter introduces the background and motivation of the presented Ph.D. work. It comprises a small overview of the current development of wind power, system restoration, and expected future grids with high integration of power electronic devices. Subsequently, the thesis objectives are described. To conclude, this chapter includes an overview of the report structure and the contents of each chapter.

1.1. BACKGROUND

Nowadays, energy represents the main player in climate change since it accounts for approximately 60% of the total CO_2 emissions [1]. The United Nations established Sustainable Development Goals to call for urgent action by all countries in a global partnership. As shown in Figure 1-1, Goal no. 7 focuses on renewable energy, stating the need of increasing substantially the share of renewables by 2030 [1].

a) b)

Figure 1-1. a) Sustainable Development Goals established by United Nations and b) key target for goal no. 7.2 with a focus on renewable energy increase [1].

This transition towards renewable-based power systems entails the retirement of conventional power plants based on fossil fuels. Consequently, new challenges arise for the resilience and planning of system restoration strategies, as many of these conventional power plants are also black-start service providers.

A black start is defined as the process of restoring an electric power plant or a part of an electric grid to normal operation without relying on the external power transmission network to recover from a total or partial blackout [2]. In other words, a black start is an intermediate procedure to shift from a state of no power to a state of restored normal operation, without the support of an already energized network. This is schematized in Figure 1-2.

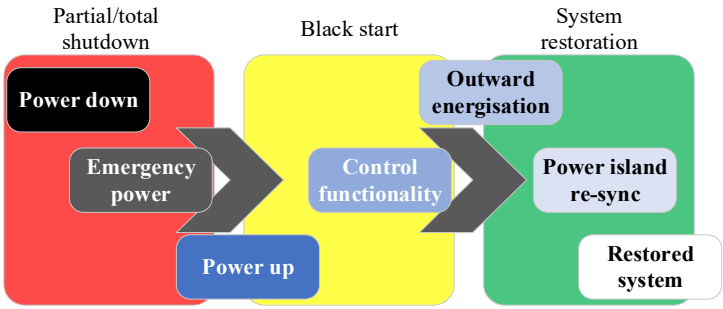

Figure 1-2. A black start is an intermediate procedure to shift from a state of no power (due to a system shutdown) to a state of restored normal operation [C1], [3].

The black-start procedure involves the creation of a local grid, islanded from the main transmission system, where the energization of both passive and active components must be carried out. Traditionally, there are multiple methods of commencing a black start of the power grid: diesel generators, open-cycle gas turbines, hydroelectric dams, etc. [2]. According to the transmission system operator (TSO), different approaches can be chosen following criteria such as the availability of local resources (e.g., suitable valleys for dams), costs, risks, the presence of a neighboring generating network, complexity, and the time necessary for the black-start process [4]. Apart from hydro power, no renewable-based resources can perform black-start services, as of today. Therefore, new non-conventional black-start sources must be designed and integrated into power systems to replace the conventional sources that are being phased out, to protect future power systems in the instance of a blackout.

Among renewable energy sources (RESs), offshore wind farms (OWFs) are one of the fastest-growing large-scale generation technologies [5]. Thus, they can play a major role in this transition to non-conventional black-start providers due to their increasing installation rate and sustainable nature. Figure 1-3 illustrates the global cumulative installed capacity of offshore wind power from 2000 with forecast to 2050, showing its exponential growth [5]. Global installations are forecasted at approximately 1000 GW in 2050. Wind power levels of the extent seen in Figure 1-3 are not trivial for power system operations, as they exhibit different behavior than traditional sources based on synchronous generators (SGs).

In the past, power systems were dominated by SGs with relatively slow controllers, namely, the automatic voltage regulator (AVR) and the governor. In SGs, the rotor offers large physical inertia, which is a favorable behavior in containing performance parameters such as the rate of change of frequency (RoCoF) and the frequency nadir during disturbances. Thus, SGs can actively control frequency and voltage while having automatic power sharing, i.e., without additional centralized controllers. At the same time, SGs can deliver a large short-circuit current, typically up to 5-10 times their rated value [6]. On the other hand, wind power systems are the collection of

multiple wind turbines (WTs), which are units based on power electronics. The electrical interface between the mechanical system of a Type-4 WT and the grid is equipped with a generator, normally a permanent magnet synchronous generator (PMSG), and a back-to-back converter, i.e., an AC/DC converter (rectifier) and a DC/AC converter (inverter) linked by a capacitor on the DC side (DC-link), which offers a decoupling stage, in theory ideal, from the generator to the grid [7].

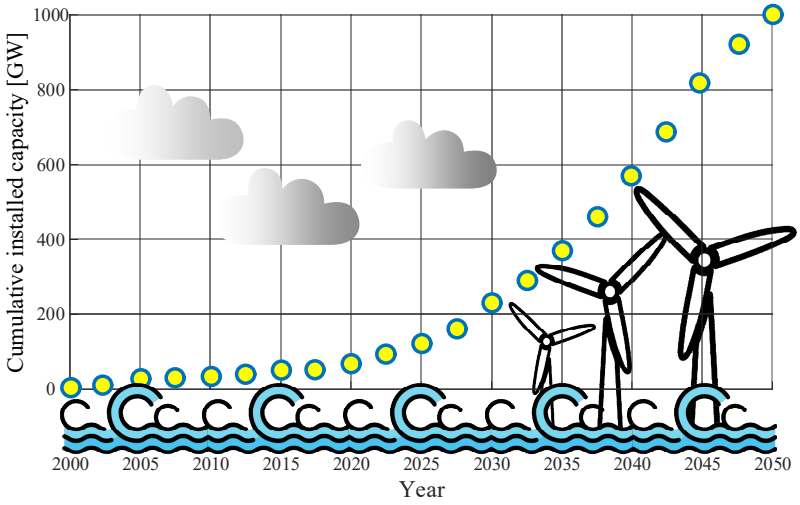

Figure 1-3. Cumulative installed capacity of offshore wind power from 2000 to (forecasted) 2050 [5].

A schematic of a Type-4 WT is shown in Figure 1-4, where the rectifier is named the machine-side converter, and the inverter is the grid-side converter. Contrarily to SGs, power electronic converters can be controlled faster and with more flexibility [8]. Together with their many advantages, power electronic converters in WTs also exhibit some disadvantages when compared to conventional generators, like the well-established black-start provision and the overcurrent capability.

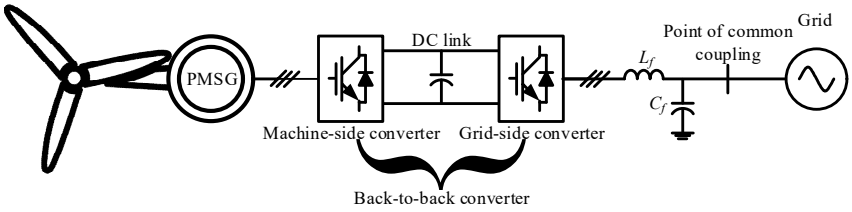

Figure 1-4. Schematic of a Type-4 wind turbine (PMSG = permanent magnet synchronous generator).

Furthermore, converters are fundamentally different from rotating machines in terms of electrical dynamics. Converter-based systems feature discontinuous, non-linear, and time-varying dynamics within a wide range (from Hz to kHz) due to the high

switching and control bandwidth of these converters, which can interact with the electrical grid and result in various instability issues [9, 10]. A comparison between the frequency range of a grid-connected converter used in Type-4 WTs and an SG is shown in Figure 1-5. Therefore, there may be a higher chance to excite resonances in power electronic-dominated systems due to the higher presence of converters compared to SGs.

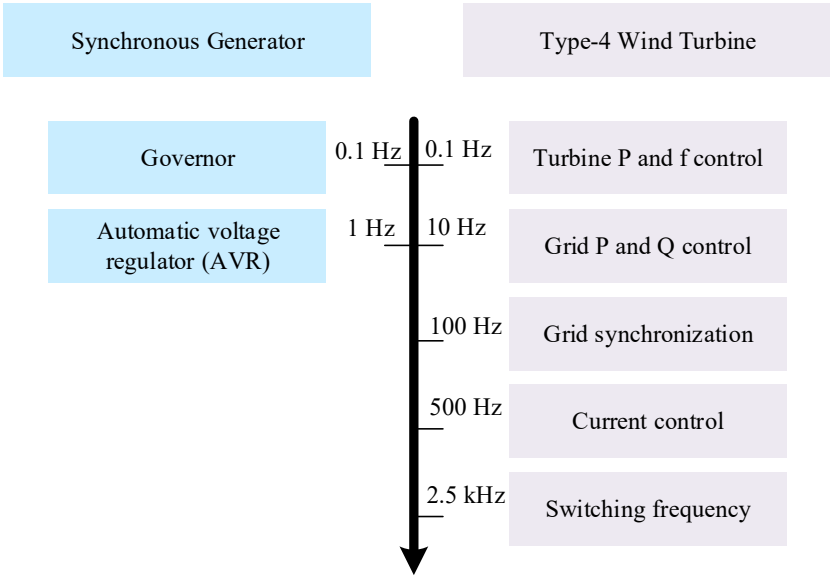

Figure 1-5. Parallel between a typical controller structure and related bandwidth of a synchronous generator and a large Type-4 wind-turbine generator [9].

Commonly, inverters for grid-connected applications (i.e., the grid-side converter for a WT) use grid-following (GFL) control [11]. From a control perspective, a GFL converter behaves like a controlled current source. Thanks to its high bandwidth, it can achieve fast power tracking. Moreover, RESs are normally controlled to inject the maximum active power available at every instant, following a strategy called maximum power point tracking (MPPT), which transfers all the energy available to the grid [12]. GFL control depends on the power grid, normally applying a phase-locked loop (PLL), which performs best when connected to a strong[1] grid [9]. However, there have been cases in so-called weak grids, where interactions between the converters, and between the converters and the power grid have caused stability-related issues. For example, these incidents concern the loss of synchronization of the converter unit as well as harmonic stability, which are events not anticipated by the

[1] The concept of system strength is not well defined in the literature; however, the behavior of a strong grid is considered as one that can maintain a stable voltage magnitude, frequency, and phase despite external events. This concept is often quantified by means of the short-circuit ratio. [15]

traditional stability analysis [10, 13, 14]. Due to the decrease in conventional SGs connected to the grid, the weakening (/reduction of short-circuit ratio (SCR)) of the grid is a condition often seen [15]. Therefore, these stability-related challenges are an increasing concern. Thus, the concept of grid-forming (GFM) control has gained interest as a mitigation to the poor performance of GFL control in weak grids, often intending to imitate SGs [11]. Figure 1-6 shows a diagram of generic control structures for GFL and GFM converters for comparison.

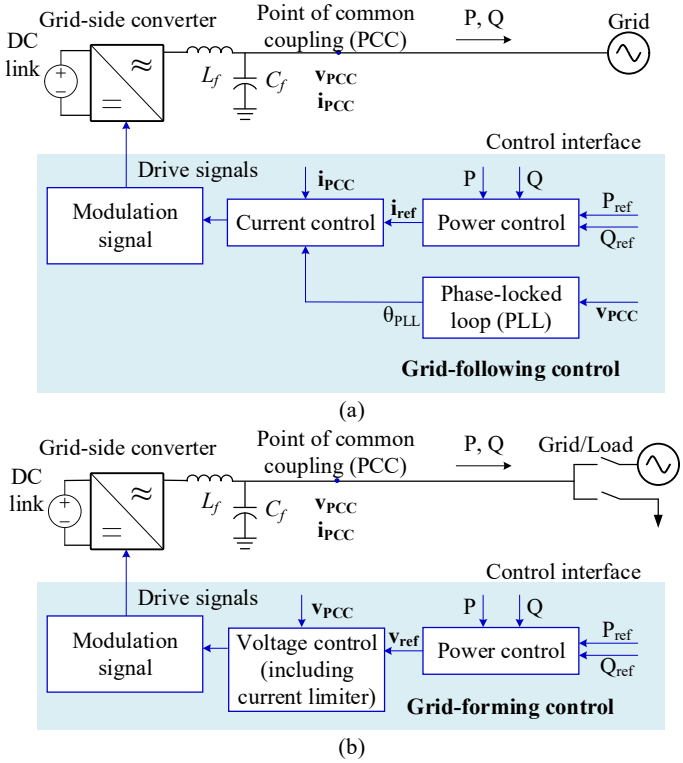

Figure 1-6. Typical control topologies for grid-connected converters: (a) grid-following control and (b) grid-forming control (bold symbols refer to vectors).

GFM control allows the outputs of power electronic-based resources to emulate the terminal characteristics of an SG, i.e., behave like a voltage source, regardless of the differences in the fundamental hardware. A GFM converter can operate in both islanded and grid-connected modes, thus being an important asset in the case of black start. Therefore, the focus on the application of GFM converters is needed to realize black start by OWFs, if no fuel-based resources, like SGs, are to be applied. To behave like an SG, a GFM converter applies specific control topologies and hardware upgrades. The controller usually aims to mimic the AVR and governor regulation, as well as the inertia provision by the rotor. Furthermore, the converter DC source intends to provide an energy buffer. Meanwhile, the power electronic switches of the converter restrain its short-circuit capability. Another fundamental aspect of GFM

control is that it may not have an explicit current controller, as to replicate the SG. However, the current flowing through the power electronic switches must be always monitored and limited for protection purposes, due to their low overcurrent capabilities. This makes the application of GFM control less trivial [16]. Nevertheless, GFM converters have also advantages over SGs, for example, a GFM control can have higher flexibility as its performance depend highly on its controls, while the SG is highly determined by its physical components. Hence, a GFM controller does not need to replicate complex models of the SG, governor, and AVR to introduce the relevant features [17]. Table 1-1 presents a few of the differences between SGs and GFM converters. Overall, GFM converters are a relevant solution for mitigating the challenges arising from the phaseout of fuel-based black start sources, and they are expected to have an increasing number of applications in the future. Before that, there are several issues in both the performance and practical implementation of GFM converters, which need to be investigated.

Table 1-1. Comparison of selected features between a synchronous generator and a grid-forming converter [17].

Features		**Synchronous generator**	**Grid-forming converter**
Black start	Energy	Internal supply	DC source (e.g., DC-link capacitor, storage, reserve of renewable energy)
	Realization	Mature	To be consolidated
Inertia	Energy	Kinetic energy in the rotor	DC source (e.g., DC-link capacitor, storage, reserve of renewable energy)
	Realization	Physical rotor	Control algorithm
Regulation	Energy	Governor and automatic voltage regulator (AVR)	Control algorithm
	Realization	Prime mover	DC source
Overcurrent capability		High	Low
Modeling		Physical dynamics	Control algorithm
Controllability		Low	High

Due to the fluctuant nature of non-dispatchable RESs like wind and solar, energy storage systems (ESSs) applications are also rising in terms of the installed capacity worldwide as shown in Figure 1-7. These may also interface the grid via an inverter, as in the case of a battery energy storage system (BESS), and for example, may apply GFM control to be a self-starter in a black-start of the grid. Thus, an ESS may be integrated into OWFs and be a part of the black-start solution.

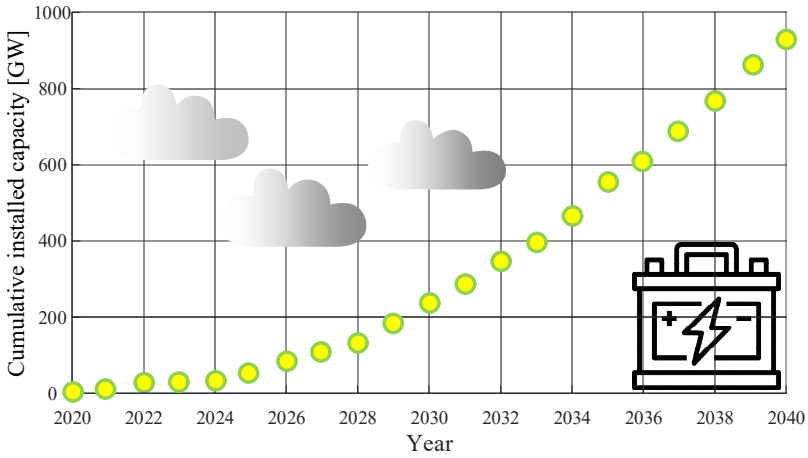

Figure 1-7. Cumulative installed capacity of energy storage from 2020 to (forecasted) 2040 [18].

For OWFs to become new black-start service providers, there is the need to study and design new methods for control and operation of the system, since OWFs do not possess the black-start capability as per the current design. This new type of operation needs to be analyzed carefully as the black start of the grid is a scenario where the local grid must be formed only by local resources, i.e., without the presence of the main transmission grid which represents a strong source to be connected to, and its successful outcome may impact millions of consumers.

The goal of this thesis is to investigate the implementation of black-start capabilities from the point of view of wind farm developers, considering the challenges they may face and the solutions available nowadays in designing future OWFs capable of providing black-start services.

1.1.1. BLACK START FROM CONVENTIONAL SOURCES

As explained above, the current power system restoration practice strongly relies on conventional power plants, e.g., large thermal power plants equipped with diesel generators/gas turbines, which today are closing and/or being taken out of operation

to accommodate a larger share of renewables [19]. These power plants can deliver emergency services, and among those, the black start is of focus.

To study the capabilities of non-conventional black start technologies, the trends seen in several conventional operations have been collected briefly through this review for the following items: 1) Experiences in black start and restoration in actual power systems, 2) Historical data on large-scale power outages.

Many countries have commonly chosen auxiliary gas turbines or diesel engines as black-start generators [2]. In a conventional power plant designed for black start operation, there may be a small diesel generator that can be used to energize larger generators, even of several MW capacity. These in turn can be used to start the main power station generators. Therefore, the actual black start of the transmission grid will be carried out by the main (large and robust) power plant generators. This structure is illustrated in Figure 1-8.

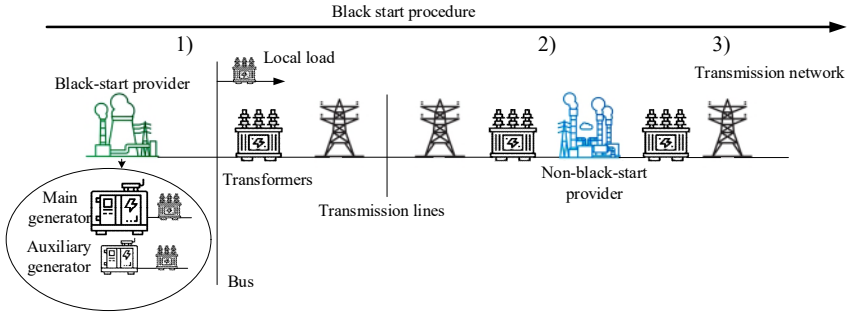

Figure 1-8. Typical black-start procedure by a conventional power plant consisting of three main different steps [63].

As shown in Figure 1-8, this procedure consists of three main steps: 1) The black-start provider starts its black-start generator (self-start unit) to energize the main generator and creates a power island[2] disconnected from the main grid; 2) The black-start provider black-starts the power grid to restore the electricity supply to block loads (which also include other generators that are non-black-start providers); 3) The black-start and non-black-start power plants gradually energize the transmission system until full restoration is accomplished. In the instance of a large blackout, multiple black-start procedures may be started simultaneously, creating several power islands. Once each power island has restored the area of the transmission grid that is assigned to them, they will be synchronized and interconnected to complete the system restoration [4].
Historically, a large-scale blackout occurs every two years or less somewhere in the developed world [20]. The consequences of such large-scale blackouts are

[2] The term power island is used to indicate an isolated power station, i.e., working disconnected from the main power grid, together with complementary demand.

catastrophic and can result in loss of capital by businesses and private customers, as well as human deaths due to missing power for vital medical equipment. Examples of extensive blackouts that happened in the last decades and their impact on the number of affected customers are shown in Table 1-2.

Table 1-2. Overview of selected large-scale blackouts in terms of affected customers (in chronological order) [21-29].

Event location and date	Affected customers
North-eastern USA and Canada, 14 August 2003	50 M
Southern Sweden and eastern Denmark, 23 September 2003	5 M
Italy, 28 September 2003	56 M
Northern and eastern India, 30-31 July 2012	620 M
South Australia, 28 September 2016	850,000
Venezuela, 7 March 2019	30 M
Argentina, Paraguay, and Uruguay, 16 June 2019	48 M
Texas, USA, 10-27 September 2021	4.5 M
Ontario and Quebec, Canada, 21 May 2022	1.1 M

These examples show the negative impact of blackouts on a large number of customers, and these events can have a considerable time extent (days/weeks). Thanks to the integration of RESs with black-start capability, the implementation of novel restoration strategies can reduce the impact of large-scale blackouts. An example of a problematic restoration strategy based on conventional generation was seen in South Australia in 2016, where the conventional black-start sources were not able to provide the service, and after several attempts, the restoration strategy had to change and the power was restored by a neighboring area [J1], [30]. This is given as an exemplary case since the South Australia region is prominent in RESs, which did not contribute to the restoration on that occasion, as they did not possess the capability to black start.

1.1.2. BLACK START FROM NON-CONVENTIONAL SOURCES

In order to propose a successful black-start strategy based on OWFs, a review of the state-of-the-art literature on the most innovative technologies for system restoration has been carried out. Recent research on novel black start methods has been focused on the use of resources at the distribution level, microgrids[3], onshore wind farms, or HVDC systems (with a focus on HVDC based on voltage-source converters (VSCs))

[3] The IEC 62898-1:2017 guidelines define a microgrid as a "group of interconnected loads and distributed energy resources with defined electrical boundaries that acts as a single controllable entity and is able to operate in both grid-connected and island mode" [97].

to reduce restoration time and provide block load capability. Previous research on black start focused on OWF is also presented.

Distribution-Level Resources, Microgrids, and Onshore Wind Farms

Contrary to the application discussed for OWFs, which takes place from the transmission level, some research proposes system restoration by distributed generation (located at the distribution level). This is a non-conventional approach since usually, the transmission grid (not the distribution grid) acts first in case of a large-scale blackout. However, this research field aims at proposing the smaller RESs to be the main drivers of the restoration to achieve faster restoration of consumer loads, which are located at lower voltage levels [31].

In [32], the investigation of the black-start and islanding capabilities of a 30-kV microgrid is analyzed. The microgrid consists of WTs, and passive and motor loads and it is equipped with a lithium-ion BESS rated at 2.6 MVA with the exact purpose of providing the black-start service. Both analytical simulation and field tests are performed, and the chosen control philosophy is based on the master-slave approach. In their control philosophy, the BESS is the only GFM unit in the microgrid, and thus, acts like the master unit. The operational philosophy consists of the BESS gradually ramping up its voltage while the passive components of the microgrid, i.e., lines and transformers are connected. This procedure is often referred to as soft charge. Afterward, the WTs are synchronized to the islanded grid and the procedure is completed with the black start of a motor load. This study presents another case of promising application of non-conventional resources to provide black-start services. Nevertheless, this is also for lower power and voltage levels than for large OWFs.

A feasibility study based on electromagnetic transient (EMT) simulations is carried out in [33] regarding the black-start capability of a 51-MW onshore wind farm with an integrated BESS sized at 15.3 MVA. The BESS provides power to the pitch and yaw systems and energizes the WTs. The wind farm energizes transmission lines, then it powers the auxiliary motors and the 150-MW thermal power plant in the test network. Therefore, the operational philosophy of the system consists of the BESS having the main role in the energization procedure, while the wind farm supports the restoration strategy with the additional power. This shows the capability of non-conventional resources to provide a black start, even if at a lower power rating, and the simulation gives an estimation of the behavior that may take place during the actual procedure. However, the authors in [33] do not elaborate in detail on the control applied to the units during the island mode and subsequent black start.

In 2019, National Grid Electricity System Operator (NGESO), the transmission system operator of Great Britain, concluded the project “Black Start from Non-Traditional Generation Technologies” [31]. In this project, the possible application of distributed RESs, i.e., onshore wind farms, photovoltaic (PV) power plants, and hydroelectric power plants are detailed and the challenges and barriers that currently inhibit reliable participation are identified as: the missing self-start

capability, to be prone to instability due to operation in a weak system and low service availability in the case of missing natural resources [31]. The project also investigated microgrids.
It has been proposed that the main challenges faced by microgrids as black-start sources, e.g., voltage and frequency stability, could be mitigated by using a BESS and WTs acting as a virtual synchronous machine (VSM) [31]. The project did not consider OWFs, since they are mainly located at the transmission level due to their size.
This project showed the need and interest for TSOs to have non-conventional energy resources to join the black-start market. Furthermore, a statistical case specifically tailored to onshore wind farms located in Great Britain to provide sufficient availability is studied. The analysis suggested using the aggregation of two or more wind farms to black-start 500 MW. This analysis focused on the wind variability to reflect on the service availability, showing that the wind farms selected can deliver a constant power output for up to five days with a level of fluctuations of around 0.1%. Nevertheless, it was seen that the longer the time extent requested, the lower the power output that could be guaranteed, especially maintaining such a small fluctuation of the power output. The analysis also showed that if the wind farm must provide 500 MW for a black start following the black-start requirements, an actual wind farm of 30 to 40 times the rated power capacity, i.e., 15-20 GW (which is an extremely high-power capacity), should be used.
This study showed a concrete interest from the TSO in having wind power being part of the future restoration planning. Nevertheless, it may require the wind farm to work with an integrated ESS to avoid low service availability when the wind is not blowing. Another consequence points in the direction of relaxing the grid codes, especially in terms of the availability requirement, since more RESs can enter the market and work together to complete the black-start procedure. All in all, the project did conceptual and statistical analyses only, without the application of simulations and field testing.

The project “Black Start from Non-Traditional Generation Technologies” has been followed up by the newest project “Distributed ReStart”, again by NGESO, with the addition of live network testing [34]. One of the most relevant parts of the project is the testing that took place at the Redhouse trial site in the United Kingdom (UK). This live trial focused on testing the GFL and GFM ability of a BESS rated at 11.6 MVA. This was connected in a test network at the local distribution level (33 kV), which in turn was connected at the transmission level (132 kV). The test showed complete support from the BESS when responding to frequency deviations, in particular stabilizing the system in GFM mode.
Another interesting part of the project Distributed ReStart is related to the several tests that involved an onshore wind farm connected at the transmission level. The wind farm used for trial was the Dersalloch wind farm in Scotland, UK, which features 23 WTs (Type-4), each rated at 3 MW, for a total wind farm capacity of 69 MW. Using the VSM type of GFM converter control scheme applied to the WTs, successful trials were completed in 2019 to demonstrate the performance of inertial response. Trials

taking place in 2020 aimed at operating the wind farm in islanded mode by having a few WTs in GFM mode supporting most of the WTs in GFL mode. During these trials, the wind farm also achieved a re-synchronization from islanded to grid-connected mode. Additional trials focused specifically on black-start capability, having 4 WTs equipped with GFM control and 125 kV external diesel generators to supply the WTs auxiliary loads to perform the energization.
The remaining turbines within the wind park were run in the conventional GFL control. This number of WTs was selected as in combination there was enough reactive power capacity to cover the requirements for the wind park network, plus a 90 MVA, 33/132 kV transformer, connecting 10 km overhead line (OHL) and cable, and a 240 MVA 132/275 kV transformer. The black start procedure implemented a soft charge approach for the WT energization. During soft charge, the voltage at the WT terminals ramped up from 0 to 1 pu in 14.25 s. These trials demonstrate the potential for wind farms to provide a black start, especially based on GFM WT technology. Nevertheless, diesel generators were used to create the initial grid for the onshore WTs to be synchronized, which represents a non-sustainable alternative.

A case of an operating GFM BESS supporting also an onshore wind farm to address grid challenges and provide a black start is presented in [35, 36]. A 30 MW/8 MWh BESS (also known as ESCRI-SA) located at Dalrymple on the Yorke Peninsula of South Australia is installed and performs both grid-connected and islanded services. The main purpose of this BESS is to strengthen the grid, especially via the provision of fast power, inertia, and fault current. The business case for the BESS covers both energy and system security services, e.g., fast frequency response, reduction of unserved energy, and energy arbitrage. The used GFM algorithm is also based on VSM control. Together with a 91 MW Wattle point onshore wind farm and distributed solar PV, the BESS is capable to transition from grid-connected to islanded mode and maintain a power supply for local customers. The BESS is connected at the end of a 132-kV line, North of the wind farm (not co-located). ESCRI-SA can also deliver black-start services to the local 33-kV distribution grid, having the BESS apply a soft charge to energize its six local 6-MVA transformers and one of the 25-MVA transformers in its substation. Afterward, the energization of the 33-kV system can take place. This is another relevant example of how a BESS with GFM control can be exploited for providing black-start services and further ancillary services in grid-connected mode.

HVDC Transmission

HVDC systems represent a very useful technology in terms of 100% power-electronic-based systems able to provide a black start. HVDC interconnections can be used to perform a restoration top-down approach (in contrast to bottom-up as a black start), where the HVDC link transmits power from its energized end to the end where there is a blackout. Some discussions can already be found around the application of HVDC systems as black-start service providers in comparison to conventional sources [37]. Moreover, an investigation of possible start-up methods can be found in [38]. In

[37], it is proven for the first time that the HVDC provided a black-start source for starting a large thermal unit. Furthermore, possible unsuccessful energization of transformers can also be avoided with HVDC applying a soft charge.

Offshore Wind Farms

In the literature, it can be found that some research has already explored the concept of black start using OWFs to a certain extent. Some of the research outcomes are derived from large projects, thus the grouping of this review is done following the selected projects.

Project "IBESS"

The project "IBESS" (Integrated Battery Energy Storage and STATCOM for the Optimal Operation and Control of Wind Power Plants in Power Systems) has investigated the design of a new device, a BESS with integrated STATCOM capabilities, to operate together with OWFs to provide additional services. Both operations in GFL and GFM modes are investigated. If equipped with GFM control, this component could be a valid resource for the OWF to help to deliver different services, like the black start. The GFM control applied is known in the literature as power synchronization control (PSC) and it was chosen thanks to its industrial maturity and flexibility, as it can also feature additional inertia and damping terms with characteristics similar to the VSM [39, 40]. In [41, 42], it is shown how the IBESS equipped with GFM control can form an islanded network with the OWF (HVAC connected) equipped with only GFL WTs and black start the onshore transmission grid. Further studies show the stability boundaries of the system for small-signal perturbations [43, 44]. Control interaction studies for small-signal stability assessment show that a virtual resistance added to the GFM control has positive damping effects when interacting with the OWF, therefore it is recommended for the GFM topology. Furthermore, strong grids have destabilizing effects on the GFM BESS [43]. Thus, the recommendation is to tune and assess the GFM controller for the highest SCR predicted rather than in the typical low SCR/weak grid scenario for GFL converters. A similar analytical study comparing the operation of the IBESS with GFM and GFL control proves that the GFM control offers a higher stability margin and damping to the OWFs, especially in weak grids, which are superior to the GFL performance [44]. Hence, it suggests that the GFM BESS has the potential to stabilize the system also in grid-connected applications. This project, nevertheless, has not investigated the application of new-generation WTs having GFM capabilities.

Project "PROMOTioN"

The "PROMOTioN" (Progress on Meshed HVDC Offshore Transmission Networks) project investigated in one of their work packages the use of HVAC- and HVDC-connected OWFs to deliver black start and islanded operation (defined house-load operation in its literature) when applying GFM WTs. This is a different procedure compared to the one investigated by the IBESS project, as the energization procedure starts from the WTs, which means that starts from offshore to onshore, conversely to

the common energization procedure of the OWF when the grid is available. The concept originated from the damage that may happen in a WT if left without electricity for a certain amount of time, due to a blackout or during commissioning, for example [45]. Therefore, the WTs are used as the main power source for the OWF to avoid or reduce the use of external/mobile power supply [46]. It is shown that this configuration could be advantageous when the OWF is connected via HVDC transmission, especially if the offshore converter station is not a full bi-directional converter, but a diode rectifier unit [47, 48]. The main outcomes of the project are related to the comparison of different GFM controllers in the implemented strategy, the amount of needed GFM WTs to achieve successful islanded operation, and black start and stability analysis.
In [49], four GFM control strategies, namely the VSM, the PSC, the distributed PLL [50], and the direct power control (DPC) [51], are applied to an HVDC-connected OWF to do black start for an onshore load. The simulation results present successful stable operation for the four different controllers, being able to maintain a stable voltage and frequency at the offshore terminal. It is shown that the performance of voltage controllers, such as the ones in PSC and DPC, is better given the absence of decoupling terms, as weak grids present more coupling compared to the conventional relations for active power/frequency *P/f* and reactive power/voltage magnitude *Q/V*.

Research presented in [52] deals with the application of both GFM and GFL WTs in a black-start operation performed by an OWF. The background concerns the reduction of the additional cost related to the new GFM WT to be installed on a system, allowing considerations to apply both types of controllers. The used study case is an HVAC-connected OWF rated at 400 MW. It is seen that only 25% of GFM WTs can start up and maintain the system, especially taking into account a long export cable (75 km long) and the load rejection capability, i.e., the maximum load step and voltage drop allowed.
Another part of the project dealt with the small-signal stability and fault performance of an OWF with both GFM and GFL WTs connected via an HVDC-diode rectifier [53]. In this paper, the operation of both GFL and GFM WTs is assessed when connected to a common diode rectifier-based HVDC link. The offshore AC grid is restored by applying the soft charge to the system. The controllers for both GFM and GFL WTs include the fault-ride-through capability. Droop control is used as a GFM strategy. It is shown that fault onset and fault clearance detection are carried out by the individual WTs successfully in the simulations. This project has not clarified whether the use of additional storage may be needed to prepare a black start in the case of no wind conditions for the OWF.

Carbon Trust
As part of the Carbon Trust organization, the program Offshore Wind Accelerator (OWA) launched several projects looking into different implementations for black start services by OWFs. The most relevant is the project “E-BLAST” (Black Startable Offshore Wind Turbine), which concluded in 2019, where the main outcomes have

been a technology and market assessment of the technology and simulation studies of an OWF made of 100% GFM WTs. In [54], the case study of a 400-MW OWF connected via HVAC cables to the grid is presented. The paper shows that the system can black-start the transmission system made of one OHL and two transformers where 50-MW block loads are connected, for a total of 380 MW, almost the same as the OWF rating. The project successfully shows the implementation of an OWF system able to do black start. However, it does not mention the necessary upgrades to current WTs to become able to black start in terms of hardware updates, assuming the software updates are the main concern. A new project by OWA is "HVDC BLADE" (HVDC Black Start Demonstrator), which has recently started and has the main objective of building a demonstrator of HVDC converters for the black start laboratory test. The project is ongoing and there are no new results to cite at the time of writing this thesis.

General Outcome

As examined, several sources point towards the inclusion of new technologies based on power electronic converters to participate in the system restoration strategy as black-start sources. In the current and future scenario, where renewable energy generation is predominant, it is also uneconomical to provide such a large standby capacity from the conventional black-start stations, so black-start power can be provided over designated tie lines after a blackout scenario. However, this weakens the resilience of the power system in the case of a blackout, as there are no black-start sources ready to re-energize the grid in this scenario.

Therefore, both social and economic concerns indicate research on black-start service providers based on power electronics. Direct consequences will include also the increased competition on the black-start market and the lowering of the costs for electricity consumers. Additionally, the black-start provision will be a further revenue stream for the new black-start power plant operator. This is illustrated in Figure 1-9.

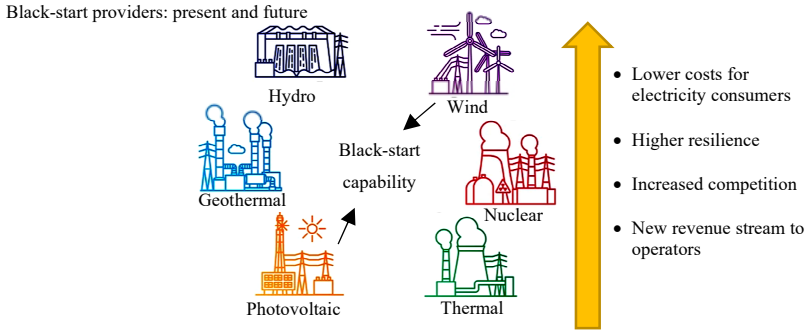

Figure 1-9. Traditional and new black start providers can bring benefits to society.

1.2. PROJECT OBJECTIVES AND LIMITATIONS

1.2.1. RESEARCH QUESTIONS AND OBJECTIVES

Motivated by the gaps in the existing research and the increasing trend in the development and construction of OWFs discussed above, this Ph.D. project focuses on the following main question.

"Can black-start functionalities of offshore wind farms be designed, integrated, and analyzed to create a system that can ensure stable dynamic behavior between all its components?"

This main question introduces the following sub-questions:

- What are the grid code requirements that non-conventional black start providers, such as offshore wind farms, may have to comply with, and what challenges are introduced for current offshore wind farm design?
- What are the possible system configurations and control topologies that may be able to comply with these new requirements?
- How can an offshore wind farm with integrated energy storage be controlled and operated to provide a black start?

Based on these questions, the following objectives of this Ph.D. project are defined:

- **Compare and analyze different offshore wind farm system configurations and controllers to allow black start by offshore wind**
  Various types of equipment with different black-start capabilities could be needed to be introduced in the common offshore wind farm design and must be compared with each other. Furthermore, when performing the black-start strategy by power electronic converters, the different topologies for grid-forming control need to be investigated to understand the advantages and disadvantages.

- **Investigate improved methods for energization of large offshore wind farms in islanded mode and black start**
  Since forming a power island is the first step to achieving a black start by offshore wind farms, its current energization strategy has to be updated as it will not depend on the onshore grid, which is shutdown. Therefore, energization methods to enable the new procedure must be proposed and validated, e.g., soft charging of the passive system.

- **Compare procedures for black start by offshore wind farms**
  Since a new service translates into a new operation to be performed, select the most attractive solution for the provision of black start by a wind farm and compare the different procedures to select the optimal criteria.

- **Develop guidelines and recommendations for the design and analysis of energization and black start procedures**
  When a new offshore wind farm must be designed and the black start service has to be integrated, design engineers should be able to have an overview of the requirements to be addressed and the best options to be implemented. This will ease the design procedure and analysis of the needed service.

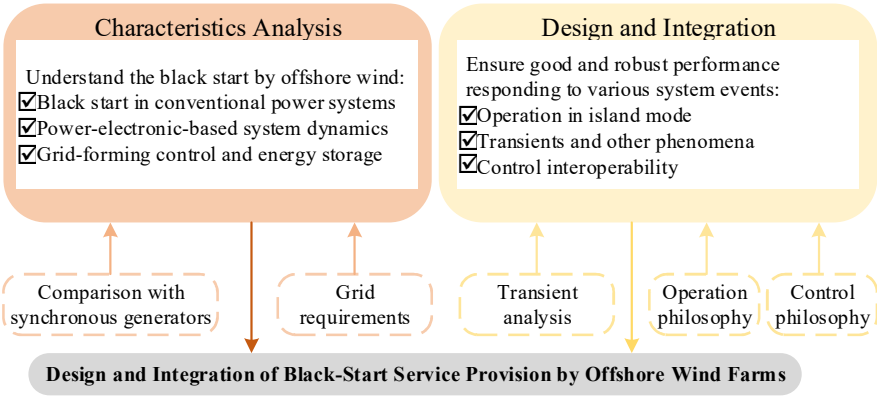

Figure 1-10. Research activities of the Ph.D. project "Design and Integration of Black-Start Service Provision by Offshore Wind Farms".

An overview of the research activities of this Ph.D. project is graphically shown in Figure 1-10, which has two main pillars: "Characteristic Analysis" and "Design and Integration".

1.2.2. PROJECT LIMITATIONS

A list of the limitations defined during this three-year research project is presented in this section. The specified limitations are:

- An aggregated representation of the OWF is used in this work, as it simplifies the EMT modeling work and reduces the computational time.
- The DC-source dynamics of the WTs and BESS are not modeled. It has been assumed that the power from the DC link could be extracted at any point in time. The converters are modeled as average voltage sources with added sampling and modulation delays.
- The variation of wind speed and its impact on the DC-link control of the WTs is not considered. It is assumed that the time constants of the transients considered are very small in comparison to the timescales of wind speed variation. Furthermore, the fluctuations of wind speed could be smoothed out in a large OWF since these are spread across a large area.
- No protection settings have been implemented in the analyzed power system, which also means circuit breakers implemented are simple open/closed

switches, controlled to close at a specified instant. Neither fault-ride-though capabilities have been implemented nor tested on the generation sources. Therefore, fault performance has not been considered.

- The applied control of the controllers used in the system is realized in the synchronous *dq* reference frame (SRF) only.
- No internal losses have been considered in the model of the auxiliary systems of the WTs and BESS.
- Only an HVAC type of system structure has been considered. Nevertheless, the results of the operation are generic and can be used as a first guideline for the analysis of HVDC-connected OWFs.

1.3. THESIS OUTLINE

The outcome of this project is summarized in this Ph.D. thesis as a collection of the articles published as the outcome of the research was carried out. The thesis consists of two main parts: ***Extended Summary*** and ***Appended Papers***. Figure 1-11 presents the structure of this Ph.D. thesis, where the corresponding selected publications of each chapter are indicated as well.

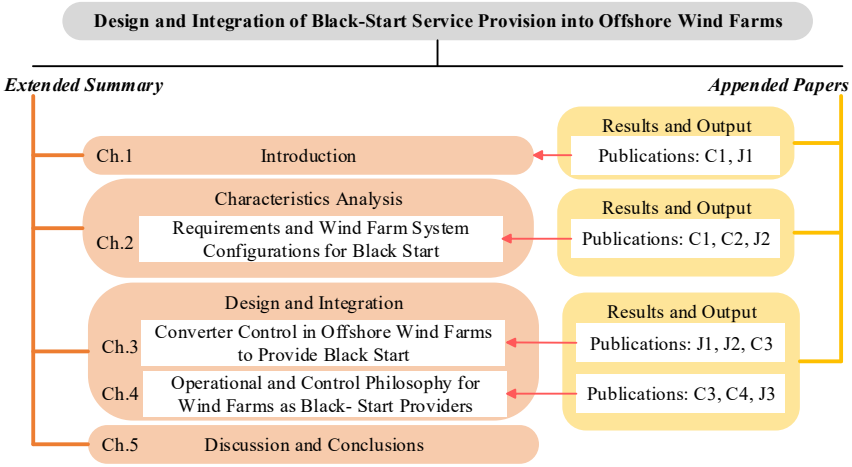

Figure 1-11. Structure and corresponding appended papers of this Ph.D. thesis.

In *Chapter 1*, an introduction about the background, motivation, and objectives of this Ph.D. thesis is given. The following two chapters study the fundamental characteristics of the black-start service, where *Chapter 2* presents an extension of black-start requirements from the considered TSO and a comparison of possible wind farm system configurations to implement to provide a black start. *Chapter 3* is focused on the analysis of the black-start procedure carried out by an OWF and on the converter control to provide the black start and the interoperability of grid-forming and grid-following controllers. Afterward, *Chapter 4* presents the operational and control philosophy implemented for the two selected wind farm configurations for the

black start. Additional variations to the two configurations are also discussed. The conclusions, main contributions, and future work are included in *Chapter 5*.

1.4. LIST OF PUBLICATIONS

The results and outcomes during this Ph.D. study are included in several publications as listed in the following, and they are integrated into this Ph.D. thesis as shown in Figure 1-11.

Conference Papers

[C1] **D. Pagnani**, Ł. Kocewiak, J. Hjerrild, F. Blaabjerg and C. L. Bak, "Overview of Black Start Provision by Offshore Wind Farms," in *IECON 2020 The 46th Annual Conference of the IEEE Industrial Electronics Society*, 2020, pp. 1892-1898, doi: 10.1109/IECON43393.2020.9254743.

[C2] **D. Pagnani**, Ł. Kocewiak, J. Hjerrild, F. Blaabjerg and C. L. Bak, "Challenges and Solutions in Integrating Black Start into Offshore Wind Farms," in *19th Wind Integration Workshop*, Energynautics GmbH, 2020, pp. 1-8.

[C3] **D. Pagnani**, Ł. Kocewiak, J. Hjerrild, F. Blaabjerg and C. L. Bak, "Control Principles for Island Operation and Black Start by Offshore Wind Farms integrating Grid-Forming Converters," in *2022 21st European Conference on Power Electronics and Applications (EPE '22 ECCE Europe)*, 2022, pp. 1-11.

[C4] **D. Pagnani**, Ł. Kocewiak, J. Hjerrild, F. Blaabjerg, C. L. Bak, R. Blasco-Gimenez and J. Martínez-Turégano, "Power System Restoration Services by Grid-Forming Offshore Wind Farms with Integrated Energy Storage," in *2023 IEEE Power and Energy Society General Meeting*, Accepted, pp. 1-5.

[E1] N. Halwany, **D. Pagnani**, M. Ledro, O. E. Idehen, M. Marinelli and Ł. Kocewiak, "Optimal Sizing of Battery Energy Storage to Enable Offshore Wind Farm Black Start Operation," in *21st Wind Integration Workshop,* Energynautics GmbH, 2022, pp. 1-10.

Journal Papers

[J1] **D. Pagnani**, F. Blaabjerg, C. L. Bak, F. M. Faria da Silva, Ł. Kocewiak and J. Hjerrild, "Offshore Wind Farm Black Start Service Integration: Review and Outlook of Ongoing Research," *Energies*, vol. 13, no. 23, p. 6286 (1-24), 2020, doi: 10.3390/en13236286.

[J2] **D. Pagnani**, Ł. Kocewiak, J. Hjerrild, F. Blaabjerg and C. L. Bak, "Integrating Black Start Capabilities into Offshore Wind Farms by Grid-Forming Batteries," *IET Renewable Power Generation*, vol. (Early View), issue (Early View), pp. 1-12, 2023, doi: 10.1049/rpg2.12667.

[J3] **D. Pagnani**, Ł. Kocewiak, J. Hjerrild, F. Blaabjerg, C. L. Bak, R. Blasco-Gimenez and J. Martínez-Turégano, "Wind Turbine and Battery Storage Interoperability to Provide Black Start by Offshore Wind Farms," *CIGRE Science and Engineering*, pp. 1-19, 2023, in review.

[E2] L. Huang, C. Wu, D. Zhou, L. Chen, **D. Pagnani** and F. Blaabjerg, "Challenges and Potential Solutions of Grid-Forming Converters Applied to Wind Power Generation System – An Overview," in *Frontiers in Energy Research*, vol. 11, pp. 1-14, 2023, doi: 10.3389/fenrg.2023.1040781.

2. REQUIREMENTS AND WIND FARM SYSTEM CONFIGURATIONS FOR BLACK START

In this chapter, the generic structure of offshore wind farms is explained, to later introduce their current energization procedure. Afterward, the grid requirements for non-conventional sources are reviewed to show the main challenges that current wind farm design may face when performing a black start. Finally, an analysis of relevant configurations for wind farm black start is proposed and a list of main design requirements is presented.

2.1. MODERN OFFSHORE WIND FARMS

Among RESs, offshore wind power has been selected to provide a significant portion of renewable energy for the future 100%-renewable power system [55]. Offshore as well as onshore wind farms have different characteristics from conventional power plants, especially due to the fluctuating nature of wind, the operation in weak power systems, the power-electronic-based generation, and the many small-scale units that work in parallel.

Nowadays, the trend with OWFs is to connect them far away from shore and to have increased capacities. For example, the world's largest OWF in operation at the moment is Hornsea Two, located in the UK waters, approximately 89 km off the Yorkshire coast in the North Sea. It comprises 165 8-MW turbines, for a nominal capacity of approximately 1.4 GW [56]. In general, the complex type of infrastructure of OWFs gives rise to several challenges in the wind power industry concerning aspects like the control and operational philosophy, grid connection, construction, installation as well as transmission of the generated energy. Nevertheless, it allows for the exploitation of suitable offshore locations, which have high wind speed and ample space, so that many WT units can be installed.

Usually, WTs are connected through a widespread medium-voltage cable system, also known as the array system, and connected to the transmission grid using long high-voltage (HV) cables, i.e., the export system, which often has a sea, and a land cable parts. The export system can be implemented as HVAC or HVDC transmission, often depending on the distance to shore and related economic considerations. For both types, transformers are used to step up the voltage from the WT voltage level to the array and export system, and finally to the onshore transmission grid level. In HVDC systems, the AC power produced by the WTs is rectified by an offshore converter station, which transmits the power onshore into DC form, where it is then inverted and sent to the power grid. In HVAC systems, passive filters and reactive power compensation are often employed to comply with grid codes and optimize the power

flow and voltage levels in the OWF. Currently, it is very common to also employ flexible AC transmission system (FACTS) devices such as static compensators (STATCOMs) for dynamic reactive power compensation. Normally, project-specific considerations lead to the direction for the choice of one transmission type or the other for the OWF design. A schematic of the two types of structure is shown in Figure 2-1.

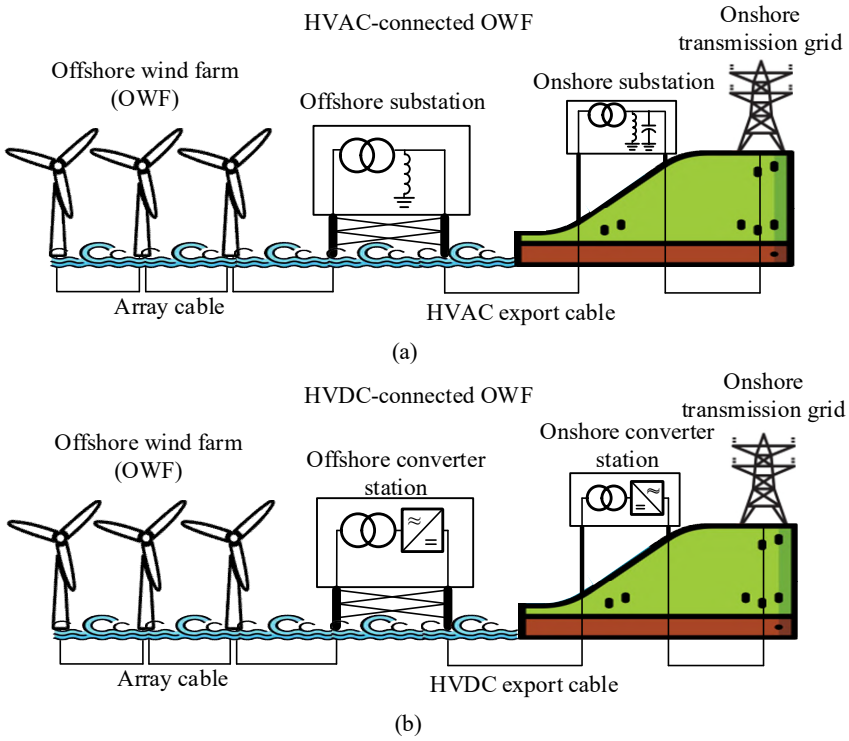

Figure 2-1. Schematic representation of (a) high voltage alternating current (HVAC) and (b) high voltage direct current (HVDC) transmission system for offshore wind farms [57].

Currently, OWFs do not possess black-start capabilities, therefore, black-start sources must be integrated into their design to provide the service. Since a black-start procedure may be similar in practice to a common energization, in order to fully understand the status of the start-up procedures of OWFs, a brief review of common energization practices for OWFs is presented.

2.1.1. COMMON ENERGIZATION PROCEDURE OF OFFSHORE WIND FARMS

Normal Operation

Considering the stage where an OWF is fully ready to produce power, the common energization procedure involves the closing of a main circuit breaker (CB) connecting the OWF to the transmission network, while all the other CBs in the system are open.

From this point on, the system is energized from the onshore transmission network with a sequential procedure, where one piece of equipment is energized at a time. Auxiliary components may be added to ease the procedure as well as special settings of elements such as tap changers of transformers and passive reactive compensation. In this method, the energization power therefore comes from the transmission grid, i.e., starts onshore and ends offshore, with the WTs being the last components to be energized. Usually, dedicated studies are implemented to take care of the challenges that may arise during switching events of this type, such as inrush currents, temporary overvoltages, converter control interactions, etc. Once these analyses have been concluded, the final operational philosophy for the OWF energization is determined and applied.

Abnormal Operation

During the installation and commissioning of an OWF, there may be a significant amount of time from the moment when the first WT has been installed to the moment when the wind park is completed. Moreover, in emergencies, such as when a blackout takes place, the WTs may experience a long time before the power is restored. Hence, the WT may be left without electricity to power up its auxiliaries and may thereby be subject to damage. The main concerns arising in this situation may be [46]:

- Damage due to freezing due to low temperature offshore.
- Moisture damage in the nacelle and the tower of the WT, especially concerning the power electronic components (e.g., the power converter) because of low temperature and rain.
- Mechanical damage due to vibrations at the natural frequency of the tower caused by unfavorable wind and the unfortunate orientation in the yaw axis.
- Loss of hydraulic control as a result of a reduction in pressure caused by any slow leakage.
- Other unwanted effects of no power, depleted backup, standstill, etc.

To avoid this harm to the system, the deployment of external/mobile auxiliary power supplies, like diesel generators, is a common practice during the OWF installation procedure. These auxiliary supplies are normally used to provide emergency power supply to WT systems that need to be kept operating, e.g., dehumidifiers, heaters, and ventilation [46]. The use of mobile diesel generators for emergency power supply is costly and unwanted from a CO_2 emission perspective, and hence there is currently a development towards using power produced by the WTs themselves when the wind is available.

Both for normal and abnormal operation, the energization procedure of an OWF has elements that can be considered for the design of the new service of interest, i.e., black start. These are the use of diesel generators as black start units and energization power originated onshore.

2.2. TECHNICAL REQUIREMENTS FOR BLACK-START PROVISION BY OFFSHORE WIND FARMS

There are no official black-start requirements involving OWFs as of today. However, the TSO in Great Britain, i.e., NGESO, has proposed an extension of the existing grid code for non-conventional technologies [58], and this is specified in Table 2-1.

Table 2-1. Extension of the black start requirements to non-traditional sources presented by National Grid Electricity System Operator in Great Britain in 2021 [C1], [3].

Requirement and Definition	**Minimum Requirement**
Time to connect: Time taken to start up the restoration station, and to energize part of the transmission system, after receiving the instruction.	≤ 2 hours
Service availability: The ability to deliver the contracted restoration service over the defined time of a year.	≥ 90%
Voltage regulation: Ability to create a voltage source and remain connected within acceptable limits during energization/block loading.	±10%
Frequency regulation: Ability to manage frequency level when block loading.	47.5 – 52 Hz
Resilience of supply (restoration service): When instructed, the minimum time for the service to be delivered.	≥ 10 hours
Resilience of supply (restoration auxiliary unit): Run continuously at the output required to support/deliver the contracted restoration service.	≥ 72 hours
Block loading size: Capability to accept instantaneous loading of demand blocks.	≥ 20 MW
Reactive capability: Ability to energize part of the transmission system, managing voltage with leading or lagging capability whilst active power is zero.	≥ 100 MVAr (leading)
Sequential restoration attempts: Ability to perform sequential start-ups.	≥ 3
Short-circuit level (following the start of a system disturbance): Injection of reactive current I during a disturbance. t : time after disturbance start. U : voltage level.	t≤80ms: $I \geq \frac{240\,[MVA]}{\sqrt{3}\cdot U[\mathrm{kV}]}$ [kA] t>80ms: $I \geq \frac{100\,[\mathrm{MVA}]}{\sqrt{3}\cdot \mathrm{U}[\mathrm{kV}]}$ [kA]
Inertia value: Stored energy available for immediate release in response to changes in power levels, either physical or virtual.	≥ 800 MVA.s

As can be seen from Table 2-1, some requirements are very unfamiliar for OWFs, for example, the self-start capability and the availability requirement, which are crucial for the black-start service. Moreover, other requirements like the provision of inertia and the short-circuit capability are new black-start requirements introduced especially for renewable-based sources, as these capabilities cannot be taken for granted with power-electronic-based sources and are, therefore, added as an extension of the black-start requirements. A detailed analysis of the requirements is presented in [C1], [3]. It should be mentioned that these requirements are a work in progress, and they have been modified by NGESO during the time of this doctoral study. The requirements presented in Table 2-1 are not the latest, which are the ones discussed in [C1], [3] and used as a reference for this project. In late 2022, another revision of these requirements adapted to wind power systems was published [58]. Some of these requirements in [58] are slightly relaxed in comparison to the ones presented in Table 2-1 and, therefore, are considered less challenging for OWFs to prove the capability to black start. This is a sign in the right direction from the TSO, which shows the willingness to recognize the challenges that rose from the original requirements proposed. An overview of these challenges is explained in the following section.

2.2.1. CHALLENGES FOR CURRENT WIND FARM DESIGN

Since OWFs have not been designed to restore a black network so far, many new challenges arise in their design and operation when the requirements listed above must be fulfilled. The main challenges identified are explained in [C2], [59] and [J2], [60] and listed below.

- **Self-start capability**: OWFs have usually no equipment able to self-start.
- **Service availability**: High availability requirements may be tricky as the nature of wind is fluctuant.
- **Inertia provision**: There are no rotating masses connected directly to the OWF system, and thus no physical inertia is normally provided by the system.
- **Control, stability, and interoperability**: OWFs are made of many small-size units working in parallel, in contrast to large black-start traditional units, and this makes control, stability, and interoperability more challenging for the OWF.
- **Transient behavior**: The stresses introduced by the switching operations involved in the energization procedure may hinder the success of the operation if maybe the voltage and current limits are exceeded, or dynamic interactions are excited.
- **Harmonic performance**: The power quality of the system may be compromised in case the harmonic levels of the system may be excessive.
- **Communication settings**: Both in grid-connected mode and autonomously in the black start and islanded mode, the communication must be flexible and

resilient. The use of non-central communication could improve the resilience of the system, for example, by applying a droop setting for voltage and frequency control.

- **Protection settings**: Introducing the islanded operation and the low short-circuit may challenge the protection of the system

This thesis has focused on proposing solutions to these challenges, mainly based on the system-level performance to establish the operational and control philosophy of the OWF with an integrated storage system for the black-start procedure. Further work for harmonic studies, protection coordination, and control communication is recommended.

2.3. WIND FARM SYSTEM CONFIGURATIONS TO PROVIDE BLACK START

Many different configurations can be imagined for integrating black-start capabilities into OWFs. As presented above, a device with the capability to self-start must be integrated into the system in order to form the initial grid and start the black-start procedure. These different configurations that have been considered will be presented in this section based on the type of self-start unit, i.e., synchronous generators, ESSs, and new-generation WTs, as seen in Figure 2-2. Furthermore, the application of additional equipment such as STATCOMs and synchronous condensers will be discussed too. Further details are presented in [C1], [3].

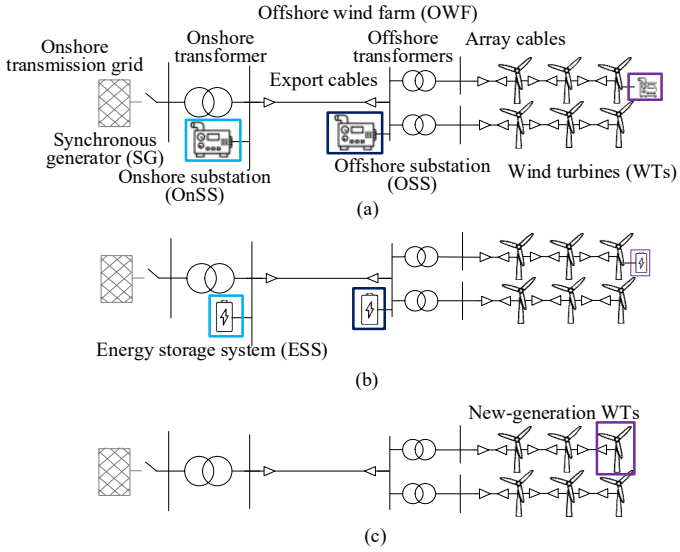

Figure 2-2. Offshore wind farm system configurations to provide black start by (a) synchronous generators (SGs), (b) energy storage systems (ESSs), and (c) new-generation wind turbines.

A literature review has been carried out to uncover all the relevant research that is published in this area. Several manufacturer documents, journals, research papers, and a review of patents that have been filed worldwide have been considered. There is limited publicly available information from manufacturers on their latest solutions about black start from converter-based resources. Research is being carried out by a wide range of companies and academics at the moment on different topics related to black-start provision by wind farms. When reviewing the patents, it is seen that all suppliers are developing commercial systems to produce power with no grid connection, and the suppliers seem to be developing similar solutions at a high level.

Use of Synchronous Generators

As presented in the previous chapter, some black-start power plants have small SGs, e.g., diesel generators, designed specifically to provide a black start. These generators will in turn energize the main power plant generators so, the power plant can proceed as a whole to black start the onshore transmission system. Normally, a diesel generator is present in the offshore substation (OSS) of both HVAC- or HVDC-connected OWFs, to power up the auxiliary loads of the OSS [46]. Its application can be expanded for black-start purposes. As described in [61], a diesel generator located in the OSS can first energize one or a group of WTs. As presented in [J1], [30], a self-start unit like an SG could be placed in the onshore substation (OnSS), as to replicate the energization from the onshore transmission grid that happens from onshore to offshore. Furthermore, one or several WTs can have an integrated diesel generator, as proposed in [62]. Therefore, an SG can be located in three different locations in the OWF as shown in Figure 2-2-a: in the OnSS, in the OSS, and/or in the single WT. SGs will increase the black-start service availability as they can dispatch power according to their fuel capacity. An advantage of the use of SGs is that they are a mature technology, with well-known characteristics like overcurrent capability and inertia provision. A disadvantage consists in the fossil fuel that powers the SG, e.g., diesel, which is non-renewable and thus, against the vision of a future 100% renewable power system. Biomass-powered SGs could represent an alternative, however, they are found mainly in small sizes, which will not be relevant for OWFs.

Use of Energy Storage Systems

Another option, discussed in the previous chapter, is the integration of energy balancing interfaces, such as ESSs like BESSs, supercapacitors, or hydrogen fuel cells. If equipped with a GFM converter, ESSs can be the self-start unit of the system [63]. The integration of such devices can increase the system availability and flexibility, as not only will have extra energy to supply like a diesel generator but can also store the surplus energy if the wind is available. In particular, GFM BESSs have been tested in the field as GFM and black-start units of the system [64], [65]. Similar to SGs, BESSs can be placed as centralized or decentralized, as shown in Figure 2-2-b. The centralized unit could be located on the OSS or the OnSS. On the other hand, a decentralized BESS can be equipped in the WTs. Decentralized BESSs have the flexibility to be completely independent of each other if one has a failure, thus, allowing the system to carry on with the black-start procedure. Ref. [66] analyzes the

optimal OWF system with integrated BESS to provide black-start, and according to this article, the optimal solution is the use of BESSs in the WTs. However, this research did not consider operation and maintenance costs for these extra units offshore. The application of a centralized BESS could be potentially favorable in terms of costs for operation and maintenance as acquiring space onshore is usually cheaper than building the space in the OSS. Furthermore, the cost associated with reaching the offshore location is always larger than onshore. Some research is found on the application of a centralized BESS located onshore to allow OWFs to provide the black-start [33], [67], [68]. Moreover, the use of a single large unit onshore allows to replicate to some extent the typical energization procedure that starts from the grid, with the advantage to have a controllable unit like a BESS to ramp-up the voltage slowly, i.e., do a soft charge. Additionally, this centralized BESS can also work with a VSM-like algorithm allowing the provision of virtual inertia for the requirements.

Use of Wind Turbines

Usually, WTs have an uninterruptible power supply (UPS) that is used to power up critical loads of the WT like its controllers, and switchgear for not more than an hour [46]. The UPS could be replaced with a larger BESS so that the WTs could be able to self-start and energize array cables, the rest of the wind farm, and black-start the grid. This must be done together with an upgrade of their converter to be GFM. These new-generation WTs, i.e., GFM WTs with enhanced UPS, have the advantage to have a full power-electronic interface, which can be controlled to soft-charge and provide virtual inertia [69]. An example of this structure is shown in Figure 2-2-c. Ref. [E2], [70] gives an overview of the challenges and potential solutions of GFM control applied to WTs. It shows that there are several challenges for this technology, such as sizing the DC-link capacitor for stable GFM operation and reducing mechanical stresses from the WT, especially in low-power operation. Suppliers are working on different solutions for this future technology; thus, it is considered relevant. Island operation and black-start for HVDC-connected OWFs using GFM WTs would be especially convenient when the offshore converter is a passive unit, such as a line-commutated converter or diode rectifier, although the latter has been never realized in practice yet.

Support from Complementary Devices

In addition to the self-start unit, support from extra devices can enhance the chances of a successful black-start strategy. Especially, given the need for a large reactive power regulation capability in a complex transmission network for an OWF with large reactive components like cables and transformers. Normally, STATCOMs are added to the OWF design for dynamic voltage/reactive power *V/Q* regulation. VSM-like control algorithms have been applied to STATCOMs for inertia emulation [71]. Some suppliers have been researching the enhancement of the STATCOM DC source, via integration with a BESS like in the IBESS project, or with supercapacitors, referred to as E-STATCOM [42, 72].

Synchronous condensers have also been considered more and more for OWFs for both provision of inertia and *V/Q* regulation. These can help with the inertia requirements

since they are SMs [73]. Although, the inertial support is less compared to an SG of the same size since the synchronous condenser shaft spins freely, not being connected to anything [74, 75], which implies that the inertial contribution from the physical prime mover is absent. Some research analyzed and compared the inertia provision of a large synchronous condenser against a smaller storage unit, for example, supercapacitors or BESSs, concluding that their inertia provision can be relatable [76, 77, 78]. When selecting a supercapacitor, its time constant is the main factor in contributing to the stability of the grid and the inertial contribution [72]. Different is the performance of a STATCOM, where the inertia provision can be adjusted by adjusting its controller gain and depends on the converter power rating [73]. On the other hand, neither STATCOMs nor supercapacitors have the overloading capability that can be achieved in a synchronous condenser [73]. In [79], it is proposed to apply a synchronous condenser to strengthen the grid. The synchronous condenser also showed better fault-ride-through performance, having faster voltage recovery. All in all, the use of STATCOMs seems more attractive for black-start purposes, as its interface is fully controllable and can be integrated with ESSs to work as a unit with enhanced active and reactive power capabilities, like in the project IBESS.

Overall Comparison

Table 2-2 presents the key features of the devices presented in this section to provide black start by OWFs. The challenges described in Section 2.2 can be overcome to different extents by the discussed devices, i.e., SGs, ESSs, GFM WTs, and complementary devices. Conventional SGs, like a diesel generator, are already part of the typical OWF design, even though they do not have the purpose of black start. Further research is needed to consider an SG as the best self-starter to provide OWF black-start, as it is not a solution ever applied. Furthermore, the trend in modern power systems is to move away from fossil fuels to boost sustainability goals. Integrating a GFM BESS and/or GFM WTs as self-starters for the OWF appears to be a preferable choice given the sustainability discussions. GFM BESSs have been tested on the field to provide a black-start, so they are considered a more mature choice concerning GFM WTs in the present time. Additionally, the black-start service availability could suffer by the use of GFM WTs only, as the service availability will depend solely on the wind. The use of a GFM BESS as a central self-starter in combination with GFL and/or GFM WTs is proposed. These configurations can potentially achieve higher availability than having only GFM WTs, and higher revenue due to the several ancillary services that a BESS can supply also in grid-connected services. Furthermore, a STATCOM can be integrated with the BESS to support the large reactive power requirements and the *V/Q* regulation in the OWF. Nevertheless, the control and interoperability for the OWF need to be analyzed, especially focusing on GFM control. Given the nature of this system as a hybrid power plant, performing a new procedure like a black start, the definition of control and operational philosophies is a critical milestone.

Table 2-2. Overview of methods to achieve black start in offshore wind farms [C1], [3].

	Synchronous Generator	**Battery Energy Storage Systems**	**Wind Turbine**	**STATCOM**	**Synchronous Condenser**
Type of device	Conventional	Power electronic based	Power electronic based	Power electronic based	Conventional
Application	Dynamic compensation, overloading capabilities	Fast dynamic compensation	Fast dynamic compensation	Fast dynamic compensation and voltage recovery during faults	Dynamic compensation and voltage recovery during faults, overloading capabilities
Black-start service availability	Fuel	Stored energy	Wind	DC-link buffer (with grid-forming control)	/
Inertia provision	Real	Virtual	Virtual	Virtual	Real

2.4. DESIGN GUIDELINES FOR FUTURE WIND FARMS PROVIDING BLACK-START SERVICES

Based on the state-of-the-art review of different black-start units, grid code requirements, and presented challenges for non-conventional black-start sources, the following list aggregates the design guidelines that are critical for OWFs with black-start capability:

- The capability of self-start is a major feature that must be integrated into the OWF. This can be integrated via equipment such as a diesel generator, or based on power electronics, such as BESS, WTs, or STATCOM with GFM capabilities.
- Given the service availability requirement of a minimum of 90% together with the requirements of the resilience of supply of the restoration service of at least 10 hours, and resilience of supply of the restoration auxiliary unit of a minimum of 72 hours, the level of continuous power/energy available must be considered. Furthermore, the black-start system must be able to start-up a minimum of three times. An additional source of energy storage may be considered, such as a BESS.
- The final goal of the restoration strategy is the energization of block loads; thus, a minimum capability of 20 MW must be ensured.

- A large part of the transmission system may be restored, and this implies that passive reactive components must be energized as well. Thus, a minimum capability of 100 Mvar has to be included in the design.
- Voltage and frequency control play a significant role in the successful realization of the black start. Thus, the voltage must be maintained in the ±10% range, while the frequency in the 47.5-52 Hz range. Dedicated control loops in the power electronic converters and auxiliary equipment, such as shunt reactors and transformer tap changers, may be included in the design.
- Because of the significance of the short-circuit level following a system disturbance, a source capable of injective reactive current following Table 2-1 must be guaranteed.
- The provision of inertia became also a key feature. A source capable of supplying either virtual or real inertia must be integrated and capable of supplying at least 800 MVA.s. This may be supplied by the converters.

2.5. SUMMARY

This chapter has focused on the needs of the OWF system to be able to perform a black start. Firstly, the overview of a common, modern OWF structure is given. After that, a brief discussion on the current energization procedure that can take place in today's OWFs is given. Black start by RESs is not ready for industrial deployment yet, however, some TSOs have started researching it. This is why an overview of recent grid code requirements for black start by NGESO in Great Britain is presented and discussed. These requirements highlight the gaps that current OWFs have concerning the performance of black start. Therefore, a discussion of possible wind farm system configurations to overcome these gaps and do the black start is given, where the use and placement of SGs, ESSs, and GFM WTs are considered. Additionally, support functions from complementary devices like STATCOMs and synchronous condensers are discussed. Overall, the most interesting solutions to apply are ESSs, like for example BESSs, given their increased popularity in power system applications. Furthermore, these can be integrated with a STATCOM, providing a reduction in costs and space compared to having two separate units. Moreover, the use of next-generation WTs with GFM capabilities has been analyzed, showing promising solutions for implementing black-start capabilities in OWFs. Therefore, the relevant system configurations to investigate further are considered; GFM BESS (with integrated STATCOM), in combination with GFL WTs, i.e., the BESS is the only self-start unit, and in combination with GFM WTs, that means that the OWF will be 100% based on GFM control. These configurations of OWF+BESS represent a hybrid power plant, which has to be studied to define the optimal interoperability strategy to provide a robust black start.These two system configurations must follow certain guidelines to be grid compliant, thus a brief list of design guidelines for the system is presented. Once the system configurations for OWF black start are selected and their key features are designed, the next step is to analyze how the system will operate and be controlled. This will give the full overview to perform black start by OWFs.

3. BLACK-START FUNCTIONALITY AND GRID-FORMING CONTROL IN OFFSHORE WIND FARMS

This chapter presents the different stages that comprise a black start by an offshore wind farm with an integrated energy storage system. Furthermore, the concept of grid-forming control applied to black start is clarified and a review of the control topologies for grid-forming control is given, as well as the control principles for the selected control methods, i.e., power synchronization control.

3.1. BLACK-START FUNCTIONALITY ANALYSIS

As discussed earlier, the process of black start can be split into three different stages, that start from the system completely shut down, OWF included, to the normal operation of the power grid.
The first stage is represented by the energization of the sole OWF in islanded mode, i.e., disconnected from the main power grid. This stage is named Wind Farm Power Island. The following stage (Stage 2) entails the actual black-start of the onshore power grid with the OWF being the black-start source. This stage is referred to as Black Start Power Island. Once the black-start of a part of the power grid that the TSO assigns to the OWF is completed, the synchronization with other external power islands must take place until the full system is synchronized and restored. This last stage is called Power Island Re-Sync. The complete analysis of the three stages is given in [J2], [60].
These stages are shown in Figure 3-1, for an OWF equipped with battery storage as it is here studied.

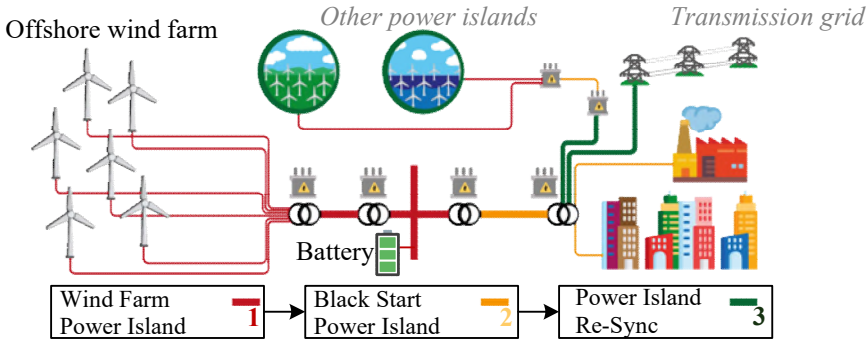

Figure 3-1. Schematic of the proposed wind farm system configuration consisting of a wind farm with integrated storage and the stages to achieve black start [J2], [60],[C3], [80].

Figure 3-2 gives the different steps of the black-start procedure to be implemented.

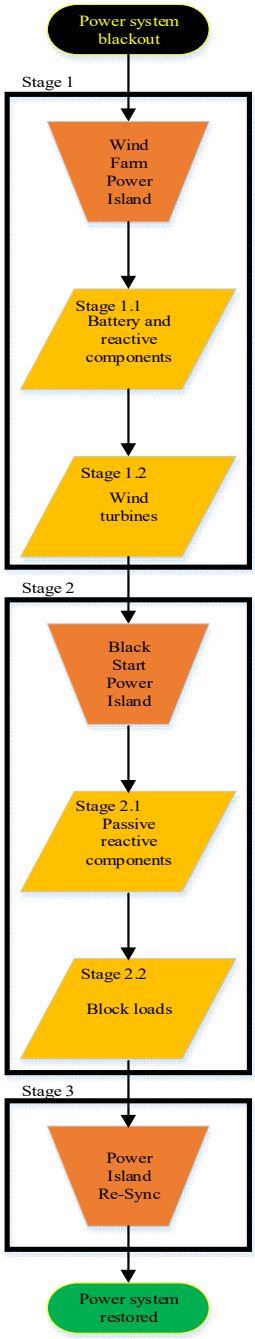

Figure 3-2. Flowchart describing stages and substages of the black-start procedure implemented by an offshore wind farm [J2], [60].

In the flowchart shown in Figure 3-2, it can be seen that the three black-start stages are divided into substages. In Stage 1, i.e., Wind Farm Power Island, the BESS self-starts itself and the main reactive components of the OWF using soft charge. This is defined as Stage 1.1. Once this is completed, the connection and energization of the WTs can take place, so this is defined as Stage 1.2. Afterward, when the TSO gives the signal that the onshore transmission network can be restored, Stage 2 begins, i.e., Black Start Power Island. During this stage, both the passive components of the transmission network, like transmission lines and transformers, and block loads, such as other power plants without black-start capabilities or consumers, have to be black-started. The black start of passive reactive components is referred to as Stage 2.1, while block loads as State 2.2. Nevertheless, these two stages do not happen sequentially in a real black-start scenario, as modern transmission systems are meshed and interconnected, and the energization of transmission lines and cables will lead to different block loads and so on.

To make the black-start procedure possible in 100% converter-based systems, the concept of GFM control is of fundamental importance. Thus, it will be presented in the following.

3.2. GRID-FORMING CONTROL CONCEPT

When moving towards the black start by fully power-electronic-based power systems using VSCs, the study of GFM converter control is crucial, as discussed in Chapter 1. GFM converter control is a concept that is mature for UPS applications and that, in the last decades, has been developed broadly to integrate grid-connected converters to the grid [11]. Applications of GFM control to PV systems in microgrids have been available for nearly 25 years for low-power applications, and for around 15 years for higher power levels (>MW) [81]. In the last decades, research on GFM control has been expanded to different technologies, like BESSs and WTs, and many different GFM strategies have been proposed, e.g., droop-based control, VSM, and PSC [C1], [3], [J1], [30].

The term *grid-forming* has no universally accepted definition yet, however, it generally refers to an inverter control that creates its internal voltage phasor and can be the only source in the grid to which it is connected, or it can coexist with other GFL and GFM inverters, as well as with SGs [82]. A GFM converter that co-exists with other GFM and SGs has also been referred to as a GFM grid-supporting converter [11, 82]. In general, a GFM control does not need a voltage vector reference, e.g., as the PLL does, to be the main loop to create its voltage phase reference and synchronize itself to the grid but it can create its own [C3], [80]. Thus, GFM control is different from GFL control, as GFL control only “follows” the grid reference and is unable to create its own.

GFM control is mainly based on the synchronization mechanism of synchronous machines (SMs), in contrast to vector-current control, which uses the grid voltage as a reference to control active and reactive power injection, often via a PLL for synchronization [83]. In the past, this type of converter control was the sole applied

to VSC-HVDC systems, whose key application was to connect systems to very weak AC systems, where the thyristor-based HVDC was incapable [39]. Nevertheless, VSC-HVDC based on vector-current control reported challenges in weak systems [84, 85]. The low-frequency resonance usually present in the power grid can represent a problem for the vector-current control, due to unbalance of power demand and power available at a time [39]. This low-frequency resonance in the grid can interfere with the fast current controller and hinder the performance of the converter control [86, 87]. The second main problem is related to the PLL, as PLL-related instability phenomena have been reported in weak AC systems [84], [87], [88]. To avoid stability issues and allow more and more converter-based technology to be connected to the power grid, the concept of GFM control is more and more applied [C3], [80].

3.2.1. GRID-FORMING CONTROL APPLIED TO BLACK START

Since GFM converters can be designed to work without the main power grid /in island mode, they are important for the black-start service provided by an OWF, as a power electronic unit located in the OWF can form the grid even if the main power grid is shutdown [C3], [80]. Furthermore, the GFM converter must have the capability to actually self-start itself [C3], [80]. Therefore, a GFM converter must be specifically tailored for black-start purposes [C3], [80]. The GFM concept used in this project seeks a converter capable of both self-start “black-start itself” and forming the grid [C3], [80].

A variety of different GFM controllers have been developed in the literature. An overview of different GFM control topologies is briefly discussed in the following section. Ref. [J1], [30] gives more details on the different control strategies for further reference.

3.2.2. OVERVIEW OF DIFFERENT GRID-FORMING STRATEGIES

An overview of the state-of-the-art literature on different control topologies related to GFM control has been executed. These topologies have been applied to different technologies, i.e., HVDC systems, PV power plants, BESSs, etc., and for different purposes, for example, weak grid conditions, black-start operation, virtual inertia provision, etc. Nevertheless, these all have the potential to be applied to OWF to black start. A comparison of these presented methods is shown in Table 3-1, where the main advantages and disadvantages of each are outlined. A further overview is given in [J1], [30].

Table 3-1. Comparison of grid forming control strategies to achieve offshore wind farm black start [J1], [30].

Grid-Forming Control Strategy	Advantage	Disadvantage
Basic [11]	Simplicity	Requires higher-level control to set reference values
Droop-based [11]	Automatic power-sharing	Can cause steady-state errors
Virtual Synchronous Machine [89]	Explicit inertia emulation	Numerical instability
Power Synchronization Control [39]	Specifically designed for weak grid applications and is found in many industrial applications.	May cause steady-state errors
Distributed Phase-Locked Loop [90]	Plug-and-play capability	Not mature technology
Direct Power Control [51]	Able to work in weak grids	Complex

Thanks to the well-established guidelines on the PSC, as presented in [39, 40], and its popularity in applications [41, 42, 49], this has been selected as the GFM structure for this Ph.D. project. The disadvantage of causing steady-state errors may be corrected by a higher-level controller that adjusts the PSC references to align with its output. While the advantage of the VSM of having explicit inertia emulation can be merged into the PSC thanks to its VSM variation to the first proposed controller, as seen in [40]. The principles and main points of the PSC will be discussed in the next section.

3.3. PRINCIPLES OF THE SELECTED GRID-FORMING CONTROL

The selected GFM control applied is based on PSC with virtual inertia and damping, as shown in Figure 3-3.

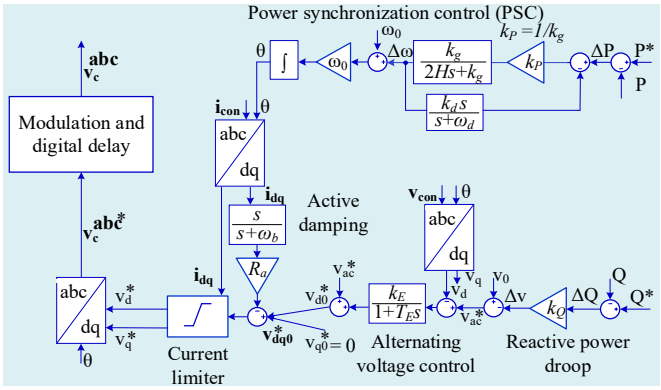

Figure 3-3. Implemented version of the power synchronization control (PSC) type of grid-forming including virtual inertia and damping [40], [J3], [95].

As explained, this has been chosen as it is an established control topology, where the additional contribution of inertia and damping is implemented (VSM variation of the PSC). As seen, the controller is made of different blocks. Firstly, the principles behind PSC will be explained. Secondly, the applied variations will be discussed.

3.3.1. PRINCIPLE OF POWER SYNCHRONIZATION

The core concept of the PSC is to reproduce the equations that describe the self-synchronizing mechanism of SMs in the converter algorithm. The principle behind this mechanism is now briefly presented. Figure 3-4 shows an AC system made of two SMs connected via a reactance *X*.

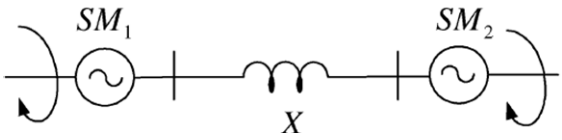

Figure 3-4. Concept behind the power synchronization control structure of grid-forming control that represents two synchronous machines in AC system [39].

It is assumed that the SM to the left SM_1 is a generator, while the SM to the right SM_2 is a motor. Furthermore, the reactance X connecting the two SMs is the result of SM reactances and a power line. To only focus on the principle behind PSC, all the resistances of the system and damping are not considered. The steady-state equations of the system are now drawn: the line-to-line equivalents of the inner emfs are assumed as two phasors of the two SMs E_1 and E_2, respectively. Assuming that the two emfs are constant, even in transient conditions, the electric power P transmitted from SM_1 to SM_2 is given by [40]:

$$\boldsymbol{P = \frac{E_1 E_2 \sin \theta}{X}} \tag{3-1}$$

where θ is the electrical phase angle between the two emfs E_1 and E_2. Given this new power flow given by Equation 3-1, the mechanical torque T_{m1} of SM_1 has a temporary increase in its magnitude, to then return to the original value. This change in the magnitude of T_{m1}, causes the rotor of SM_1 to move forward and therefore increase its mechanical angle, following the swing equation [40]:

$$\boldsymbol{J_1 \frac{d\omega_{m1}}{dt} = T_{m1} - T_{e1}} \tag{3-2}$$

where J_1 is the total inertia of the shaft system, ω_{m1} is the rotor speed, and T_{e1} is the electromagnetic torque of SM_1. The change in the mechanical angle of the rotor of SM_1 causes an increase in the phase of E_1. This implies that there is a higher phase difference between the two emfs. According to Equation 3-2, electric power is sent

from SM_1. Consequently, the electromagnetic torque T_{e2} of SM_2 is increased. Assuming that SM_2 has a constant load torque T_{m2}, the rotor of SM_2 starts to accelerate as given by [40]:

$$\boldsymbol{J_2 \frac{d\omega_{m2}}{dt} = T_{m2} - T_{e2}} \tag{3-3}$$

where J_2 is the total inertia of the shaft system of SM_2 and, ω_{m2} is the mechanical angular velocity of SM_2. This causes a rotor acceleration in SM_2, which translates into an advance in phase for E_2, bringing the two phasors to their initial position (after a transient involving some damping).

With these equations, the concept of synchronization employing active power transient is illustrated. This synchronization mechanism is well-known and adopted by SMs. This is replicated by the PSC. This controller differs from the general structure of a VSM as the mechanical angular velocity ω_m is the derivative of the angular position, so, a double integration is required to calculate the angular position based on the electric power/torque. For the control system, the double integration translates into a reduced phase margin, leaving the controller prone to instability [91]. Thus, the main difference between PSC and VSM, i.e., employing only a single integration to achieve synchronization, is explained.

The PSC principle is expressed as [40]:

$$\boldsymbol{\frac{d\theta}{dt} = k_p(P_{ref} - P)} \tag{3-4}$$

where P_{ref} is the reference for the active power, P is the measured active power output from the converter, k_p is the controller gain and $\frac{d\theta}{dt}$ is the output of the controller. Therefore, integrating Equation 3-4, the phase angle θ is extrapolated. This type of controller is not compatible with an inner current control loop as the current is not an output of the control system. The active power is instead controlled directly by the power-synchronization loop, and the reactive power (or alternating voltage) is controlled by adjusting the magnitude of the voltage like a conventional SG. Consequently, an inner current loop is not necessary [91]. However, a current limiter can be implemented in the system to avoid overcurrents and damage to the power electronic switches of the converter, as it is chosen to apply in this thesis.

3.3.2. VIRTUAL SYNCHRONOUS MACHINE (VSM) VARIATION

By adding the VSM variation to the PSC, the provision of virtual inertia and damping can be applied. Inertial provision can be mimicked with the addition of a low-pass filter to the PSC control law (the term ω_f in the following equations) [40]. The virtual inertia supplied requires an additional energy buffer on the DC side of the converter, so it is assumed that this is implemented in the system. Virtual inertia can be added

by emulating the swing equation of a synchronous machine as shown in Equation 3-5 [40].

$$\frac{d\theta}{dt} = \omega_g; \qquad M\frac{d\omega_g}{dt} = P_g - P - k_d(\omega_g - \omega_f) \tag{3-5}$$

where M is the virtual inertia scaled by the grid frequency ω_1, ω_g is the virtual machine speed and the local angular grid frequency of the converter, P_g is the virtual governor power, k_d is the virtual mechanical damping constant, and ω_f is the low-pass filtering of ω_g through $\omega_d/(s+\omega_d)$, where ω_d is the damping angular frequency. Thus, the previous Equation 3-5 can be re-written and transformed in the Laplace domain as [40]:

$$\theta = \frac{1}{s}\omega_g; \qquad \left[Ms + \frac{k_d s}{s+\omega_d}\right]\omega_g = P_g - P \tag{3-6}$$

The virtual inertia M is also be re-written in terms of the inertia constant H and the rated apparent power of the converter S_{base} as shown in Equation 3-7 [40].

$$M = \frac{2H\,S_{base}}{\omega_1} \tag{3-7}$$

Furthermore, the virtual governor power P_g does not carry the physical lag of the real SM, and so can be regulated by adding a droop characteristic to adjust it based on the active power reference P_{ref} and the angular frequency $\omega_1 - \omega_g$ [40]:

$$P_g = P_{ref} + k_g(\omega_1 - \omega_g); \qquad k_g = \frac{S_{base}}{\sigma\omega_1} \tag{3-8}$$

where σ represents the droop parameters in pu of the converter power rating.

Thus, the overall power-synchronization loop with VSM variation is implemented as seen in Equation 3-9, and it is shown in Figure 3-3.

$$\Delta\omega = \frac{1}{2Hs + \frac{k_d s}{\omega_d + s} + k_g}\Delta P \tag{3-9}$$

The design of this control strategy is done in the Laplace domain following [40], and its parameters are explained in the next chapter, together with the overall model in PSCAD.

3.4. SUMMARY

In this chapter, a differentiation in the different stages of the black-start by an OWF is presented. This is used to explain the different characteristics that distinguish each stage. Stage 1, Wind Farm Power Island, consists of the energization of the OWF, that can be started by the self-start and soft charge by the BESS, with the local OWF working in island mode. Stage 2, Black Start Power Island, comprises of the actual power system restoration of the onshore transmission grid, and carries also the unknown of energizing components outside of the OWF. This stage can be challenging as the actual extent of the blackout is unknown, and so, is the equipment to be black-started. Furthermore, a flowchart describing how these stages look in the operation is shown.

Subsequently, a key concept for the black-start by power electronic-based systems, i.e., the GFM control, is analyzed. A distinction between GFM converters for grid-connected applications and GFM converters for black-start purposes is presented. Afterward, a brief comparison between GFM control topologies is given, and the selection of the PSC algorithm is justified. Furthermore, the core principle that distinguishes a PSC from PLL-based controllers and other GFM controllers is explained thanks to the main equations related to SM synchronization. The explanation of how to integrate a VSM variation into PSC is explained and the final equation implemented in the controller is presented.

The selected GFM control, PSC with additional VSM characteristics, is used to show a black-start strategy made from an OWF with integrated BESS. This is presented in the next chapter.

4. OPERATIONAL AND CONTROL PHILOSOPHY FOR WIND FARMS AS BLACK-START PROVIDERS

This chapter presents the study performed to prove the capability of offshore wind farms to provide black-start services. Two wind farm system configurations for black start by offshore wind farms with integrated grid-forming storage are presented. Both strategies apply a grid-forming storage system, where the first strategy uses grid-following wind turbines, while the second uses grid-forming wind turbines.

4.1. BLACK-START STUDY METHODOLOGY AND MODELING

The provision of black-start services dictates a new operation philosophy to be followed. A similar concept is for the control coordination of the OWF during the black start. Both philosophies are especially important as the proposed OWF is integrated with another generation source, i.e., the BESS. Therefore, a new black-start operational and control philosophy is proposed in this chapter.

To present the new operational philosophy and the new control philosophy, black-start studies are performed in this chapter to prove the interoperability of the OWF+BESS system. This black-start study applies EMT simulations that allow the analysis of the non-linear time-domain dynamics of the OWF and the power grid during the black-start procedure. This analysis is conducted with the EMT tool PSCAD.

The analysis applies a benchmark model for the wind farm inspired by CIGRE Working Group C4.49 “Multi-frequency stability of converter-based modern power systems” [10]. The OWF system resembles a scaled-down version of a modern, large OWF like the ones seen in the UK, and described in the previous chapters [56]. The OWF system will be described in the next section.

Following the design guidelines expressed in Chapter 2, the OWF benchmark model has been equipped with an additional ESS to show the proposed OWF system configurations and their operational and control philosophies. The ESS is assumed to be a lithium-ion BESS, due to their suitable use for short- and medium-term applications, with high efficiency and long cycle lifetime and calendar lifetime, just to mention a few of the reasons for their increased popularity in applications together with RESs [18]. The model applied is inspired by the project “IBESS”, which has proposed a lithium-ion battery with integrated STATCOM capabilities for OWF applications [42]. The IBESS, in the following referred to simply as BESS, plays the

main role of the black-start unit in the proposed case study and thus, is always in GFM mode. To show the capability of the OWF+BESS system to do black start on the onshore transmission network, a model of the onshore power grid has been assumed. For simplicity, it has a radial structure, and it is made of both passive reactive components and block loads of different sizes. Further details are given in the following section.

4.1.1. SYSTEM MODEL

As mentioned, the OWF system is based on the CIGRE WG C4.49 benchmark [10], where the BESS has been integrated into the OWF as in [42]. The onshore transmission network is a radial system, and the overall system is depicted in Figure 4-1.

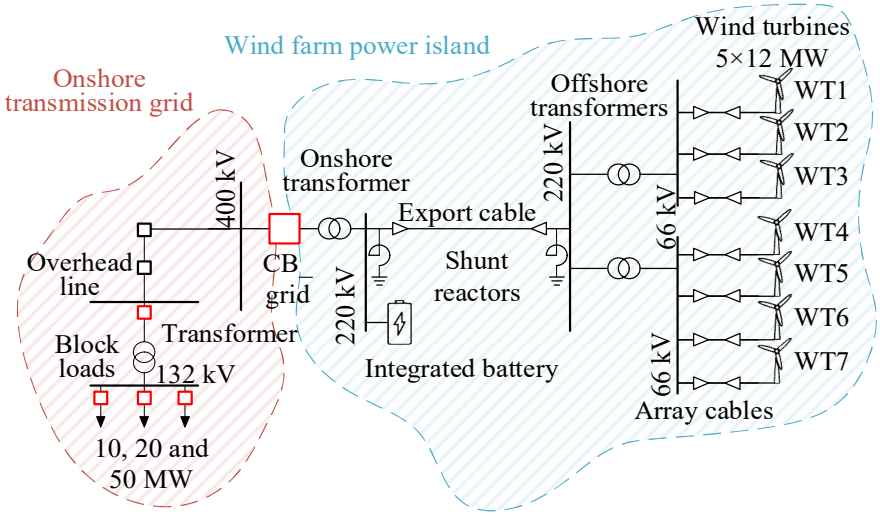

Figure 4-1. Case study of the offshore wind farm with an integrated battery used for the black-start analysis [C4], [92].

The size of the integrated BESS+STATCOM, i.e., 50 MW/100 Mvar, is assumed following [42], as it was used in combination with an OWF of similar nameplate power capacity of the OWF benchmark applied in this case, i.e., 420 MW. However, it is not the objective of this investigation to optimize the size of the storage required. The BESS is assumed adequately large, i.e., the size is not necessarily optimal for the OWF modeled and the case selected.

Ref. [E1], [93] studied the sizing of an ESS to be co-located with an OWF for black-start purposes. Historical long-term wind data has been analyzed and power flow studies show that even considering a 90% service availability, the active power rating of the BESS can be reduced to a minimal extent and even discarded if a large OWF is considered (GW scale) and only 10- or 20-MW block loads are black-started.

Nevertheless, the considerations are not related to the energy capacity of the storage, but rather to the converter active power output. Furthermore, the potential of large OWFs could be exploited for a higher amount of block loads (theoretically the OWF full capacity), if an ESS can counterbalance the time without wind generation. Therefore, further research is suggested.

Offshore Wind Farm and Storage Model

The OWF used in this case study is connected to the onshore transmission grid via a 220/400 kV, 430 MVA transformer. This is highlighted in blue in Figure 4-1. At the 220-kV bus, assumed to be part of the onshore substation of the wind farm, the 50 MW/100 MWh BESS with 100 MVAr STATCOM capability is connected to the system. It is assumed that the BESS has one 33/220 kV, 120 MVA transformer to connect the onshore substation. This BESS is represented as a large, centralized unit located at the onshore substation of the OWF for the advantages discussed in Chapter 2, where it is assumed that the location onshore comports the reduction of costs in operation and maintenance in comparison to locating the unit offshore.

At the 220-kV bus, the OWF 400/220 kV, 420 MVA onshore transformer is connected. All transformers inlcude the saturation characteristics in their models. The export cable of the OWF is also connected at the 220-kV onshore bus. The length chosen is 75 km, as it represents a relatively long cable for modern, large OWFs that are far from shore such as the Hornsea projects in the UK, but without necessitating a midpoint reactive compensation station. The export cable is assumed to be made of a 35 km land cable and a 40 km sea cable. These are modeled by a frequency-dependent model in PSCAD since they can reveal critical cable behavior during transient events. Due to the amount of reactive power produced by the export cable, there are 300 Mvar shunt compensation at the onshore end and 90 Mvar at the offshore end.

In this OWF model, there are two offshore transformers at 220/66 kV with power rated at 200 and 270 MVA respectively for two WT clusters. There are 35 WTs rated at 12 MW (for a total of 420 MW wind power capacity) and arranged in seven strings, each string having five WTs. There are two WT clusters where the strings are arranged, one having three strings (WT1-3) and the other having four strings (WT4-7).

Two different types of three-core sea cables connect the WTs composing one string, respectively of 500 mm^2 and 150 mm^2 cable cross sections. The three first WTs on the feeder are connected via the 500 mm^2, while the last two apply the 150 mm^2 cables. It is assumed that the cable length between WTs is constant and equal to 5 km.

During the design phase of an OWF, detailed simulation studies are important to check the interoperability between WTs and the overall system. However, the computational requirements can be excessive. By using aggregation techniques for some parts of the

OWF (for example, the WT strings), computational time can be reduced while keeping the relevant level of details in the analysis.
Therefore, it is decided to aggregate the WT strings, and these are modeled as seven individual feeders with one 60 MW aggregated WT each, as shown in Figure 4-2.

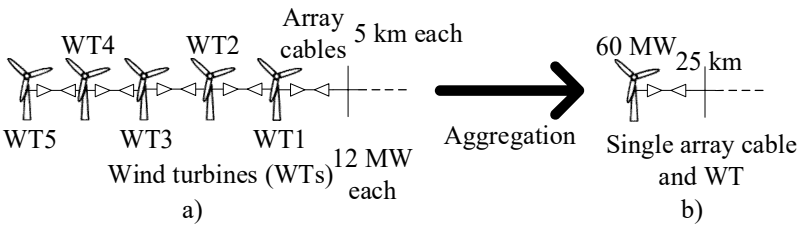

Figure 4-2. Aggregation of wind turbines and array cables: a) whole string and b) single wind turbine resulting from the aggregation.

The aggregated collection cables are modeled via the equivalent T model, where the shunt capacitance is assumed to be entirely lumped in the middle of the cable. While half of the line resistance and reactance are assumed at both sides of the shunt capacitance. Due to the T modeling of the cable, the capacitive charging current is flowing through half of the cable, avoiding the lumped capacitor at the beginning of the cable typical of the PI model. An advantage of this aggregated model is lower computational time and speed up the simulation execution. However, this can cause a misrepresentation of the energization phenomenon, since large groups of WTs are energized at the same time, while in reality, it will be one WT at a time. Accordingly, it can be discussed that the success of this energization in these simulations, therefore, is harder to achieve as a larger unit is energized at once. In contrast, the process is made of more and smaller steps in real life.

Onshore Transmission Grid Model

The onshore grid (highlighted in the red area in Figure 4-1) is assumed as a radial system made of a 400-kV OHL modeled by frequency-dependent models and a 400/132 kV, 420 MVA transformer. The saturation characteristics of this transformer are also included. At the 132-kV level, three block loads (modeled as resistors) are connected and rated at 10, 20, and 50 MW to show the load pickup capability of the system. This is assumed as a demonstration of the black-start capabilities of the system, but it is assumed that a higher number of block loads can be covered by the OWF capacity when the wind is available for the necessary time. This representation of the onshore grid, with both block loads and lines and transformers, is chosen to challenge the islanded network which must comply with the requirements for a black start, i.e., minimum 20 MW block loads capability and 100 Mvar reactive power capability.

The list of the equipment of the full model depicted in Figure 4-1 with their rating is summarized in Table 4-1.

Table 4-1. Ratings of the equipment implemented in the studied system [C4], [92].

Equipment	Ratings	Number of units
Offshore wind farm (OWF)	430 MW	1
Wind turbine (WT)	12 MW	35 (5 WTs in 7 arrays)
Battery energy storage system (BESS)	50 MW/100 Mvar	1
BESS transformer	33/220 kV, 112 MVA	1
WT transformer	66/0.69 kV, (5*)12 MVA	7
Onshore transformer (in the OWF)	400/220 kV, 420 MVA	1
Offshore transformers	220/66 kV, 200, 270 MVA	2
Onshore reactor	190 Mvar	1
Offshore reactor	130 Mvar	1
AC export cable	220 kV, 75 km	1
Array cables	66 kV, 12 km	7
Overhead line (OHL)	400 kV, 50 km	1
Onshore transformer (in the power grid)	400/132 kV, 420 MVA	1
Block loads	132 kV, 10, 20, and 50 MW	3

4.1.2. CONVERTER MODELS

Inverter Model

Three-phase electrical models for both GFL and GFM inverters are developed including their interfaces to the three-phase transmission network. The power-electronic inverter of the BESS and WTs has been modeled by assuming the DC-bus voltage to be constant, and thus, the inverter main circuit is applied as a three-phase controllable voltage source with the filter impedance. The simplification of a constant DC-link voltage assumes that all the power needed during the operation can be extracted from the DC link. This means that the converter model can be simplified, omitting the representation of the power electronic switches and their modulation.As shown in Figure 4-3, the magnitude V_i ($i = a,b,c$) and phase angle δ_i of the inverter internal voltage $V_i\angle\delta_i$ are the output of the controller, for both GFM and GFL. The

three-phase measurements for voltages $V_{gi}\angle\delta_{gi}$ and currents $I_{gi}\angle\phi_{gi}$ are the controller inputs.

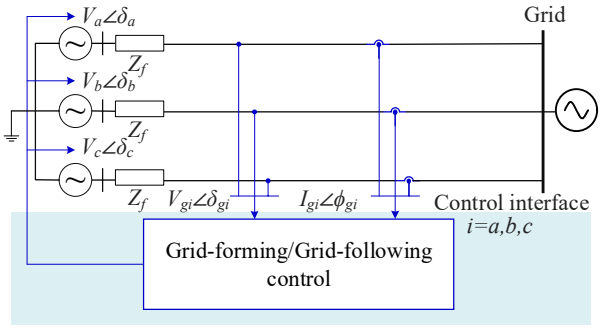

Figure 4-3. Inverter equivalent circuit and controller.

The controllers work in the synchronous reference frame (*dq*-frame) rotating at the rated frequency (50 Hz) and the regulators are proportional-integral (PI) controllers. PI controllers are widely applied and well-known for their ease of tune and flexibility. The Laplace domain (*s* domain) is often used for converter design analysis, which applies transfer functions. This analysis is done in the continuous domain, which is a common assumption when the sampling rate of the controller is very fast, and thus, the discretization can be neglected for simplification. [C3], [80]

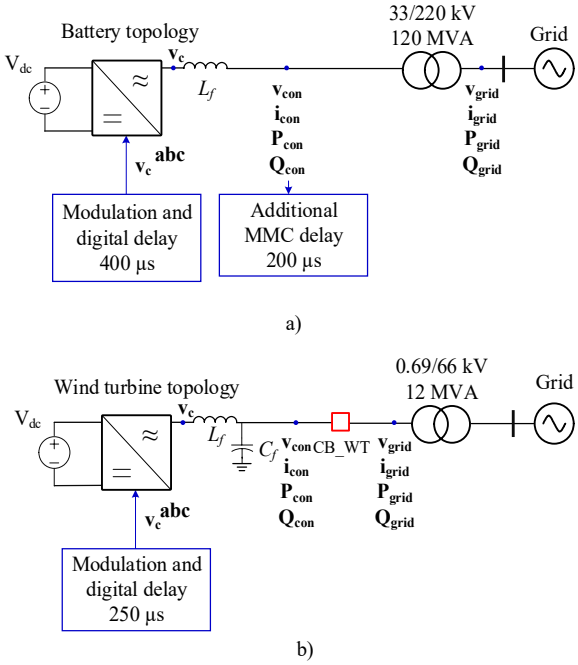

Figure 4-4. Converter topology used in the system for: a) the battery storage and b) for the wind turbine [C4], [92].

The hardware parameters inplemented in the models of the BESS and the WTs are listed in Table 4-2 and Table 4-3, respectively.

Table 4-2. Converter hardware parameters implemented in the battery model.

Parameter name	Parameter value
Rated power [MW/MVAr]	50 MW/100 MVAr
Filter inductance [pu]	0.05
Filter series resistance [pu]	0.003
Transformer rating [MVA]	120
Transformer inductance [pu]	0.1
Transformer resistance [pu]	0.002

Table 4-3. Converter hardware parameters implemented in the wind turbine model.

Parameter name	Parameter value
Rated power [MW]	12
Filter inductance [pu]	0.1
Filter series resistance [pu]	0.005
Filter capacitance [pu]	0.08
Filter parallel resistance [pu]	0.003
Transformer rating [MVA]	12
Transformer inductance [pu]	0.1
Transformer resistance [pu]	0.005

Grid-Forming Controller Dynamic Model

As presented in the previous chapter, the GFM control applied in this thesis is the PSC with additional inertia and damping [91]. As shown in Figure 4-5, PSC controls the voltage magnitude V and frequency f of the inverter internal voltage according to the Q-V droop control and power synchronization loop (PSL), respectively. P^*, Q^*, and $v_{ac}{}^*$ are the reference values for active power, reactive power, and voltage magnitude. The reference values for active and reactive power are unknown for a procedure such as a soft charge. However, these reference values can be kept at 0 as the droop characteristics of the controllers will generate the internal setpoint for the controller [94]. The Q-V droop control mitigates circulating reactive power between paralleled GFM inverters, and the PSL forms the grid phase angle. As suggested in [40], a virtual resistor is added for active damping. A current limiter is added to the control to prevent the current of the inverter to exceed the 10% limit and avoid damage to the power electronic switches.

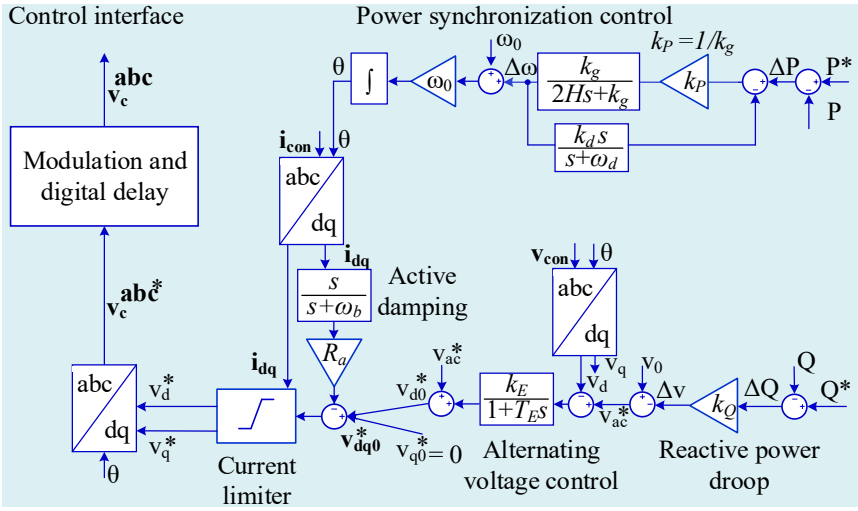

Figure 4-5. Grid-forming control based on power synchronization control implemented for the energy storage system and the wind turbines in the benchmark model [J3], [95].

The controller parameters applied for this system are shown in Table 4-4.

Table 4-4. Controller parameters implemented in the grid-forming converters.

Parameter name	**Parameter value**
Power-synchronization loop (PSL)	
Virtual mechanical damping constant $\boldsymbol{k_d}$ [pu]	0.02
Damping angular frequency $\boldsymbol{\omega_d}$ [rad/s]	16
Inertia constant H [pu]	5
Rated angular frequency $\boldsymbol{\omega_0}$ [rad/s]	2π•50
Reactive power droop control	
Reactive power droop gain [pu]	10
Active damping	
Active resistance R_a [pu]	0.05
Active damping coefficient [rad/s]	0.2
Alternating voltage control	
Filter gain k_E [pu]	1
Filter time constant T_E [s]	0.05
Rated voltage magnitude v_0 [pu]	1

Grid-Following Controller Dynamic Model

The topology of the GFL controller implemented is taken from CIGRE C4.49 and includes the standard components of GFL control, i.e., the inner current control and the PLL. Figure 4-6 shows the control blocks of the chosen GFL control.

The outer loop of this controller consists of an active power/frequency droop, which is chosen to autonomously support the OWF system frequency and avoid the use of higher-level controls. Furthermore, the AC voltage at the WT bus is regulated, to support the remote buses and reduce the reactive power load from the other units of the system, especially the BESS.

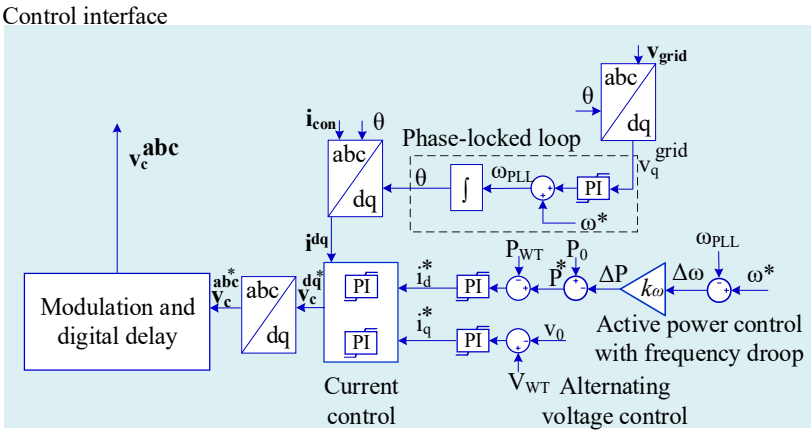

Figure 4-6. Grid-following control implemented for the wind turbines in the benchmark model [J3] [95].

The controller parameters applied for this system are shown in Table 4-5.

Table 4-5. Controller parameters implemented in the grid-following converters.

Parameter name	**Parameter value**
Phase-locked loop (PLL)	
PLL proportional gain [pu]	0.1
PLL integral gain [1/s]	2
PLL filter [rad/s]	500
Rated angular frequency ω^* [rad/s]	2π•50
Current control	
Current control proportional gain [pu]	0.2
Current control integral gain [1/s]	5
Current control feed-forward gain [pu]	0.85
Current control active damping gain [pu]	0.5
Active power control with frequency droop	
Active power control proportional gain [pu]	10.2
Active power control integral gain [pu]	0.02
Frequency droop gain [pu]	0.06
Alternating voltage control	
Voltage control proportional gain [pu]	10.2
Voltage control integral gain [1/s]	0.02
Rated voltage magnitude v_0 [pu]	1

4.2. BLACK-START SYSTEM CONFIGURATIONS

The procedure with two configurations to achieve the provision of black start by OWFs are presented and compared. Additionally, several variations of the case studies are presented to show the resilience of the overall strategy. In the first configuration, a standard, modern OWF equipped with conventional (GFL) WTs is integrated with a BESS with GFM control. In this way, the black-start procedure can only be only initiated by the BESS. The second configuration consists of a fully GFM OWF with additional GFM storage. In this case, the BESS can also be one of the black-starters of the OWF, but higher resilience is reached as the WTs can carry on the procedure without the BESS. A schematic of the two configurations is shown in Figure 4-7. Both configurations are presented in the following sections. Two system configurations are presented and referred to as Configuration 1 and Configuration 2.

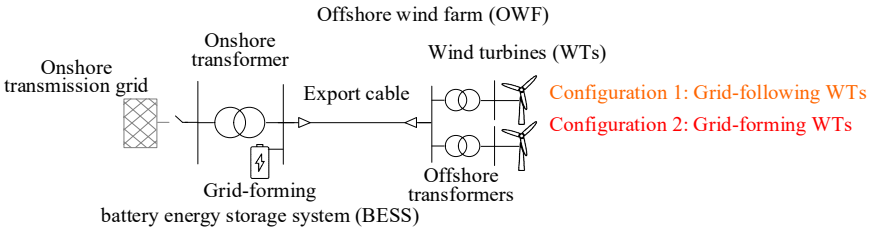

Figure 4-7. Two configurations to perform black start services by offshore wind farms with integrated battery storage [J3], [95].

Synchronization of Several Grid-Forming Units

Since PSC controls the phase angle based on the active power flow of the converter, before the converter is connected to the system, a backup PLL must provide the synchronization input to the converter when more than one GFM unit is presented in the system. After the converter is connected, the PLL is replaced by the PSC. In the switching of control parameters, the two angles may differ. Hence, the bump of the transfer must be minimized. Therefore, the scheme presented in Figure 4-8 is implemented in the WT controllers, which must follow the angle generated by the BESS. The bumpless transfer is proposed to handle the above situation. Once there is an error between the two angles, the scheme integrates the error and feeds back a term to cancel the integral action (integral time constant: 1000 s^{-1} and no proportional gain) of the PSC [12].

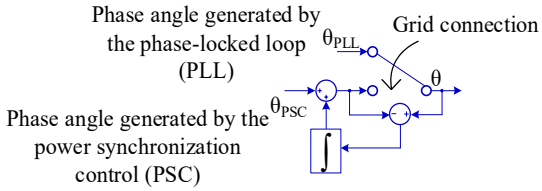

Figure 4-8. Bumpless transfer between the phase-locked loop and the power synchronization control implemented in the wind turbines [39], [C4], [92].

4.3. BLACK-START OPERATIONAL AND CONTROL PHILOSOPHY

The objective of the OWF operational philosophy is to provide the OWF developer the overall concept and operation of the OWF during black-start provision. Having as a reference the grid code requirements and the design guidelines briefly presented in Chapter 2, and the black-start stages showed in Chapter 3, the flowchart in Figure 4-9 clarifies what can be expected on a high level when the black-start procedure has to be carried out.

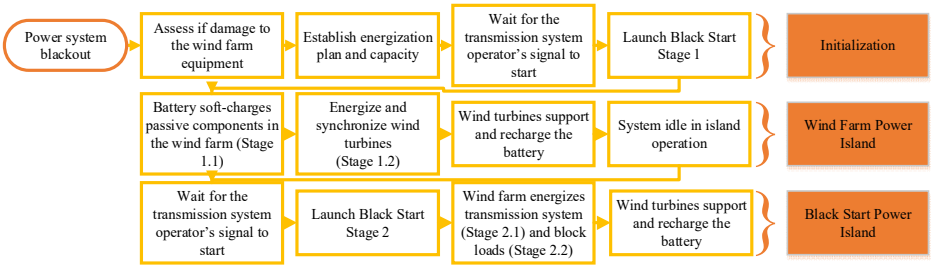

Figure 4-9. Flowchart schematizing the main steps of the implemented black-start procedure for the wind farm operator [C3], [80].

The start is represented by an event such as a power system blackout. It is assumed that following the blackout, also the OWF+BESS system is completely shut down. The first step for the OWF operator is to assess the damage to the system and afterward establish the plan for re-energization and the capacity of the OWF to be used. For example, if only a part of the OWF can take part in the black-start procedure. When the TSO selects its own restoration plan and decides that the OWF will take part in it, the signal from the TSO will be given to start.

In that instance, there is a certain amount of time when the OWF operator has to be ready to provide the service, i.e., 2 hours for NGESO, as explained in Chapter 2. During this time, the OWF has to create its islanded system to be ready to supply the black-start service when the TSO will give the signal to restore the onshore transmission grid. This will initiate Stage 1, Wind Farm Power Island, of the black-start procedure. It is proposed in this project to have the BESS firstly black-start itself together with the passive components of the OWF by soft-charge. Afterward, the WT will be energized. Based on the available power, the WTs will contribute to sustaining the power island and recharging the BESS if needed. Until the TSO gives the signal to black-start the onshore transmission grid, the OWF+BESS system will idle in island mode.

When the TSO signal arrives, Stage 2, Black Start Power Island, will take place. Here the energization of passive reactive components and block loads will begin by connecting one piece of equipment at a time.

Stage 3 of the procedure, i.e., Power Island Re-Synchronization, is not shown in these simulations as the focus is given to the capability to energize block loads. Stage 3 study is however relevant, and it is considered in the proposals for further work. It is proposed that as part of the control philosophy, the BESS takes the central role of the operation, being the main unit to black-start itself and the passive components of the OWF first. The converters are proposed to be equipped with autonomous control, in order to enable the control coordination based on the grid variations and avoid the use of further control interface.

As shown in the modeled controllers in Figure 4-5 and Figure 4-6, droop regulation is implemented to allow autonomous control.

The benchmark system that has been implemented in shown in Figure 4-10, where the black-start stages correlate to the part of the system to be energized.

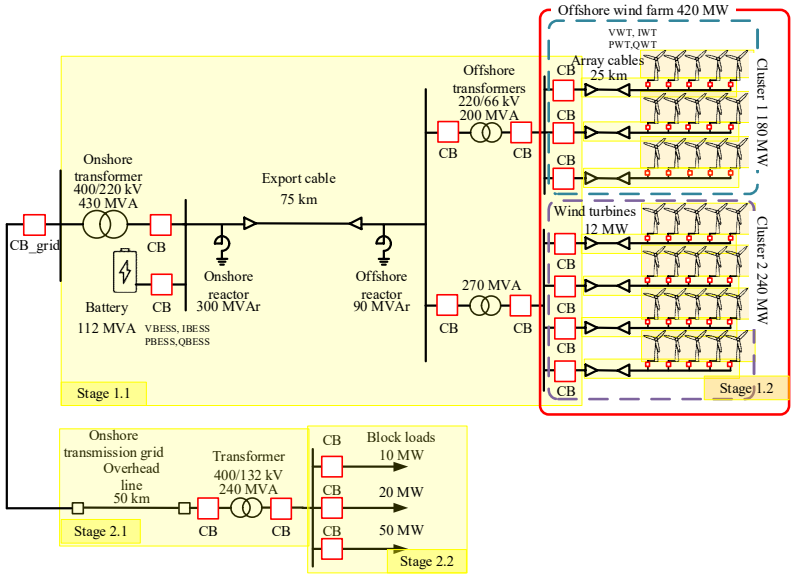

Figure 4-10. Case study of the offshore wind farm with an integrated battery used for the black-start analysis for Configuration 1 and 2 with related stages (CB =circuit breaker).

4.4. CONFIGURATION 1: GRID-FORMING BATTERY AND GRID-FOLLOWING WIND TURBINES

The sequence of events shown in the base case for Configuration 1 is summarized in Table 4-6.

Table 4-6. Events simulated for the base case of Configuration 1 (grid-forming battery storage and grid-following wind turbines) of the black-start procedure [J3], [95].

Event	Stage	Instant [s]	Event	Stage	Instant [s]
Initialization, all units shutdown	-	0.0	Overhead line is connected	2.1	4.5
BESS soft-charge	1.1	0.1-0.5	Onshore transformer is connected	2.1	5.5
WT1 is connected	1.2	1.0	10-MW block load is connected	2.2	10.0
WT2 is connected	1.2	1.5	20-MW block load is connected	2.2	11.5
WT3 is connected	1.2	2.0	50-MW block load is connected	2.2	13.0
WT4 is connected	1.2	2.5	Simulation concluded	-	15.0
WT5 is connected	1.2	3.0			
WT6 is connected	1.2	3.5			
WT7 is connected	1.2	4.0			

In Figure 4-15 the complete black-start procedure for Configuration 1 is shown from the three-phase voltage, current, active, and reactive power from the BESS point of connection. In Figure 4-16, the same electrical parameters for Configuration 1 are presented for the first group of aggregated WTs, i.e., WT1. The stages of the black-start procedure will be referred to in order to explain the results.

4.4.1. STAGE 1: WIND FARM POWER ISLAND

The black-start procedure starts with the overall OWF+BESS system, together with a part of the onshore transmission network shutdown. Before being able to black start the grid, the OWF+BESS must be powered up and work in island mode.

4.4.1.1 Stage 1.1: Soft-Charge of Passive Components

From the state of complete shutdown, the GFM converter must be the source initiating the procedure, i.e., the BESS. It is assumed that the BESS has the necessary energy and power requested for this operation, and it works in the nominal range of SOC.

The initial energization of the OWF may start by, for example, a common sequential switching procedure or by soft-charge, i.e., the procedure whereby the converter is controlled to slowly ramp-up the voltage from 0 to 1 pu while the whole passive network is connected.

In OWFs, the presence of sea cables introduces a significant shunt capacitance to the system, which in turn results in a low natural or resonant frequency. Furthermore, the presence of transformers also leads to harmonic currents due to their non-linear magnetic characteristics. When initially energized, the transformer may draw a transient inrush current that contains many harmonic components. Therefore, a sustained overvoltage could be excited by one of the harmonic components of the inrush current, if this is close to the resonant frequency of the power system depending upon the damping levels. This may cause operational problems and result in the abortion of the black start, where it is especially critical as the OWF is in island mode, so the loading of the system is negligible and the presence of 100% inverter-based resources may result in a weak-source system.

Another challenge may be represented by the zero-missing phenomenon when energizing a cable and a shunt reactor, which could be problematic for system protection. To avoid such obstacles, the black-start procedure is begun by soft-charge, i.e., by letting the BESS slowly ramp up the voltage from 0 to 1 pu while the passive network of the OWF is connected. In this way, all the circuit breakers (CBs) in the blue area of Figure 4-1 are closed, except for the CB connecting the OWF to the grid, i.e., CB_grid, and the CBs of the WTs, i.e., CB_WT in Figure 4-4-b. This is referred to as Stage 1.1.

In the base case in Figure 4-11-a, the voltage of the BESS is shown, where the soft-charge procedure takes place between 0.1 and 0.5 s. At 0.507 s, the voltage reaches 1.02 pu to then settles at 1.0 pu after 1 cycle. This small difference is due to the converter control that reaches 1 pu and after this transient phenomenon settles to steady state. Similar behavior is seen in the other electrical quantities. In fact, in Figure 4-11-b, the BESS current goes at first at 0.35 pu to settle at 0.33 pu. A more marked change is visible is the active power in Figure 4-11-c, which initially reaches 14 MW to then lower to 9.6 MW, while the reactive power reaches the peak of 36.9 Mvar and then goes to 35.5 Mvar.

The reactive power is absorbed by the BESS, and it is the surplus reactive power produced by the cable even though the shunt reactors are connected. The amount of active power that the BESS must supply initially is relatively low in comparison with the amount of reactive power, which is important to consider when designing the converter rating of the BESS, which could function as an integrated STATCOM for dynamic reactive power compensation. Once the BESS has energized the OWF passive components, the black start can proceed with Stage 1.2, i.e., the connection of the WTs.

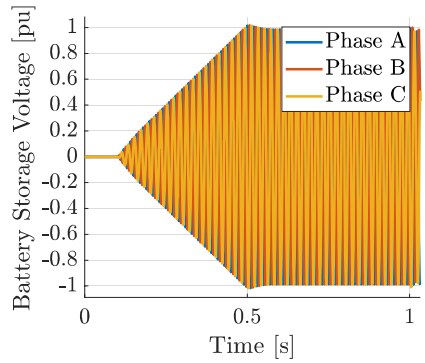

a)

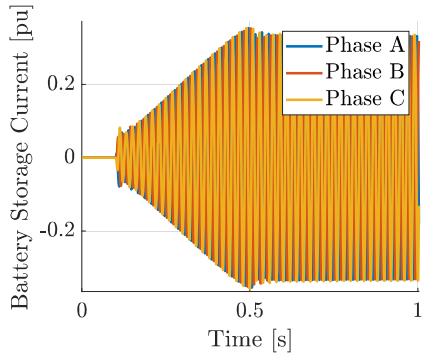

b)

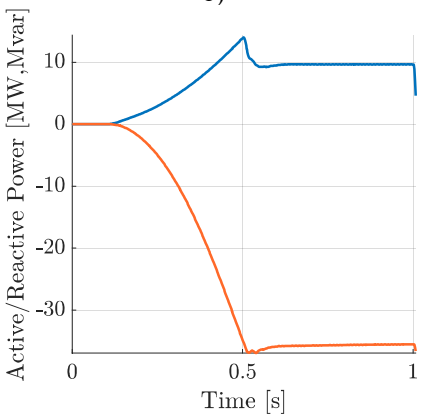

c)

Figure 4-11. Three-phase electrical measurements for Stage 1.1 of the black-start procedure seen from the battery storage point of connection; a) voltage, b) current; c) active power (blue), and reactive power (orange).

4.4.1.2 Stage 1.2: Connection and Energization of Wind Turbines

It is assumed that there is enough wind available, and all the WTs are in a favorable position to start, once the black start procedure must begin. The electrical parameters measured from the BESS and from the WT side of CB_WT are shown in Figure 4-12. Following the sequence presented in Table 4-6, the first WT is connected at 1 s. The real energization of WTs comprises several mechanical and electrical steps and related transients with different ramp-up rates (longer for the mechanical parts, for example). This procedure can take many seconds and even minutes for a single WT unit. For the aim of this simulation, this procedure is simplified by assuming that the WT voltage on the WT side of the CB_WT can be synchronized with the grid voltage while the WT is in standalone mode to reduce the switching transient once the CB is closed. This is only a simplification to replicate the procedure, having the model of the WT grid-side converter modeled as a controlled voltage source. The droop settings on the WT controller allow the WTs to participate in the share of active and reactive power automatically when sensing the voltage and frequency of the grid, helping the BESS to maintain the power island. Figure 4-12-a shows the phase-to-line voltage for the BESS, while Figure 4-12-b shows the phase-to-line voltage for the WT and before 1 s, this is the standalone voltage created for synchronization purposes, so it can be disregarded since the participation of the WT to the black-start procedure is simulated after the connection to the system at 1 s. Before the connection of WT1, the standalone voltage is at 1.09 pu, which results in an unperfect synchronization, with Phase B reaching -1.23 pu at 1.001 s. This would be unacceptable as it violates the ±10% voltage requirement. However, this result depends on the way the WT start-up process has been implemented by creating a standalone voltage before the WT is connected to the rest of the circuit. It is expected that in reality, where only one WT is energized at a time, lasting several minutes, and active and reactive power ramp rates are specified, the switching operation of the WTs can be controlled more smoothly.

Figure 4-12Figure 4-16-c shows the current of the BESS, which goes from 0.35 to 0.23 pu, thanks to the WT sharing the load of the islanded system. Figure 4-12Figure 4-16-c the current of WT1 that goes from 0 to 0.16 pu in 0.1 s. In Figure 4-12-f, it is seen that the WT1 generates 3 MW and absorbs 9.2 Mvar, sharing the load with the BESS that is shown in Figure 4-12-e.

Figure 4-15 shows the whole black-start simulation for Configuration 1 measured at the BESS terminals. Furthermore, Figure 4-16 shows the same parameters measured at the WT1 terminals. The following aggregated WTs are connected every 0.5 s and each of them contributes to the load sharing of the system, leaving the BESS to generate 2.8 MW and absorb 7 Mvar at 4.2 s, as seen in Figure 4-15-c. While the WT1 supplies 0.9 MW and absorbs 4.2 Mvar at 4.2 s, as seen in Figure 4-16, equally as the others. Now that the OWF is fully energized, the OWF+BESS system can move forward to Stage 2, i.e., the actual black start of the transmission network.

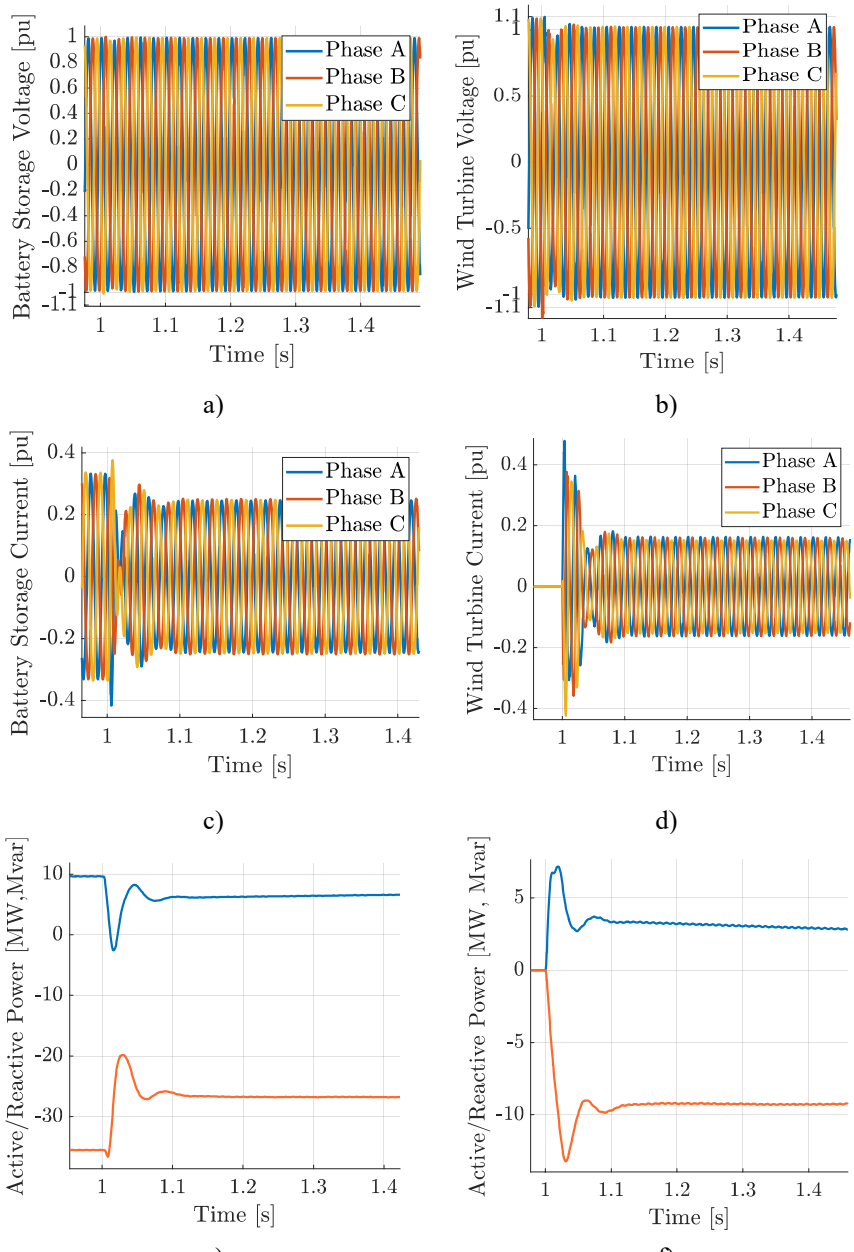

Figure 4-12. Three-phase electrical measurements for Stage 1.2 of the black-start procedure seen from the battery storage and the wind turbine point of connection; a) battery storage voltage, b) wind turbine voltage, c) battery storage current, d) wind turbine current, e) battery storage active power (blue) and reactive power (orange), and f) wind turbine active power (blue) and reactive power (orange).

4.4.2. STAGE 2: BLACK START POWER ISLAND

Stage 2 of the black start by an OWF starts with the closure of CB_grid, which in this simulation takes place at 4.5 s.

4.4.2.1 Stage 2.1: Energization of Passive Components

In this case study, a 50-km OHL is energized first. Figure 4-13-a shows that the BESS voltage is affected minimally by this switching operation, as the highest peak is around 1.04 pu for Phase C, which is within the limits. Furthermore, the voltage waveforms recover from the distortions after 1.5 cycles. Figure 4-13Figure 4-16-b shows instead that the WT voltage surpasses its limit, reaching 1.15 pu at 4.509 s on Phase A. Nevertheless, the voltage waveform stabilizes at 1 pu with a sinusoidal shape in less than 2.5 cycles. The current for both BESS and WTs increases slightly to compensate for the reactive power being exchanged when the OHL is energized.

At 5.5 s, the energization of the onshore transformer takes place. Energizations of large transformers like this (240 MVA), can take several seconds to reach a steady state. Therefore, this is the switching operation, which is simulated the longest, having the next one at 10 s. The transformer energization results in both overvoltage and overcurrent for the BESS, as seen in Figure 4-13-a and Figure 4-13-c, respectively. This is expected due to the saturation of the transformer magnetic core and consequent inrush currents. The current limiter of the BESS shows limitations, and this is one of the disadvantages of not having an explicit current controller in the GFM topology.

The highest current peak seen in Figure 4-13-c is on Phase A at 1.16 pu at 5.57 s, with significant distortions. The current gets lower and goes back to sinusoidal after 4 s, where it is at 0.16 pu.

A transformer is a highly inductive load, and Figure 4-13-e shows the reactive power of the BESS going from 20.6 to 11 Mvar absorbed. As the BESS and the WTs reach a steady state, the following step of the black start can be initiated. As the main purpose of system restoration is to restore consumption, the energization of the block load can be considered the most important stage of the procedure.

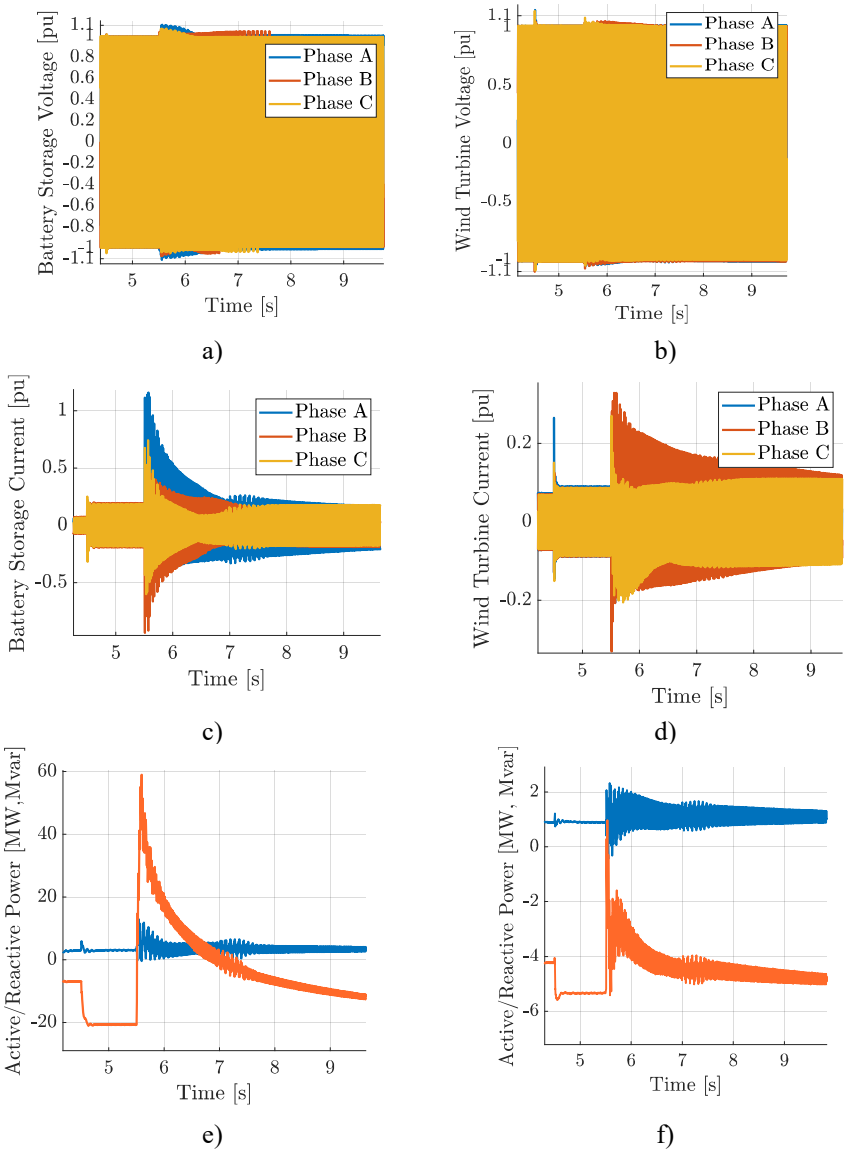

Figure 4-13. Three-phase electrical measurements for Stage 2.1 of the black-start procedure seen from the battery storage and the wind turbine point of connection; a) battery storage voltage, b) wind turbine voltage, c) battery storage current, d) wind turbine current, e) battery storage active power (blue) and reactive power (orange), and f) wind turbine active power (blue) and reactive power (orange).

4.4.2.2 Stage 2.2: Energization of Block Loads

The grid code requirements for Great Britain require a minimum of 20-MW block load to be energized. Also, 10 and 50 MW block loads are energized in this case. Figure 4-14 shows voltage, current active and recative power for both BESS and WT1.

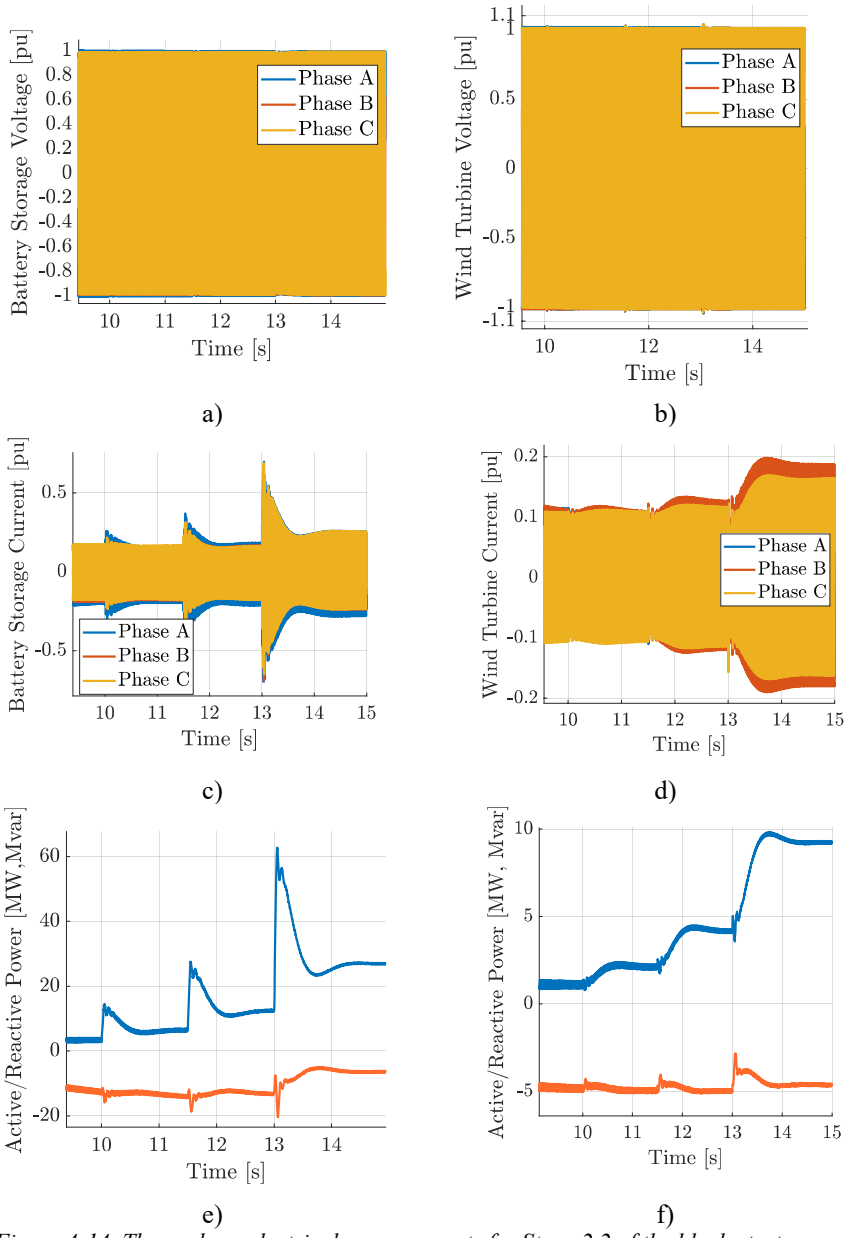

Figure 4-14. Three-phase electrical measurements for Stage 2.2 of the black-start procedure seen from the battery storage and the wind turbine point of connection; a) battery storage voltage, b) wind turbine voltage, c) battery storage current, d) wind turbine current, e) battery storage active power (blue) and reactive power (orange), and f) wind turbine active power (blue) and reactive power (orange).

The connection of block loads results in a minimal change for the BESS voltage, which is unaltered, as seen in Figure 4-14Figure 4-15-a. The BESS active power goes from 4.3 to 7.1 MW as shown in Figure 4-14-e, while the WT1 current goes from 4.6 to 4.8 MW, as presented in Figure 4-14-d, where the remaining load is shared with the other WTs. The connection of the 20-MW and the 50-MW block loads take place at 11.5 and 13 s, respectively. Both events exceed no limits for either BESS or WTs. The energization of block loads from the OWF can ideally continue until the system is completely restored or the full capacity of the OWF is reached (assuming favorable wind conditions). Overall, the black-start procedure carried out by an OWF with integrated BESS with Configuration 1 could complete the restoration. The OWF is not contributing with high generation in this example, but if the wind is available, it is a possibility. Thus, it will be shown in the case study with Configuration 2.

The full simulation results for three-phase voltage, current, active, and reactive power for both BESS and WT1 are shown in Figure 4-15 and Figure 4-16, respectively.

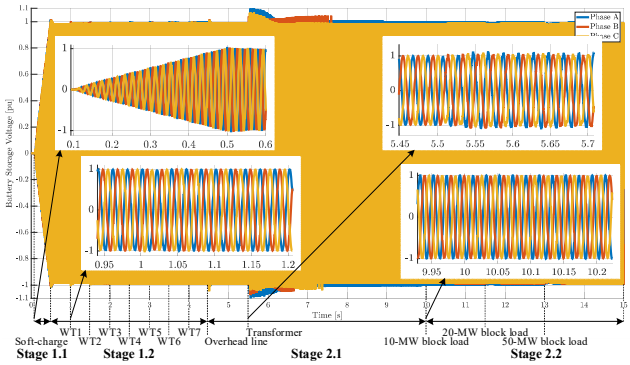

a)

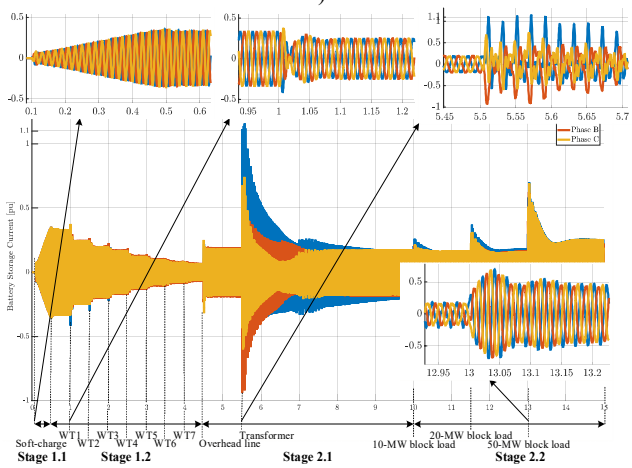

b)

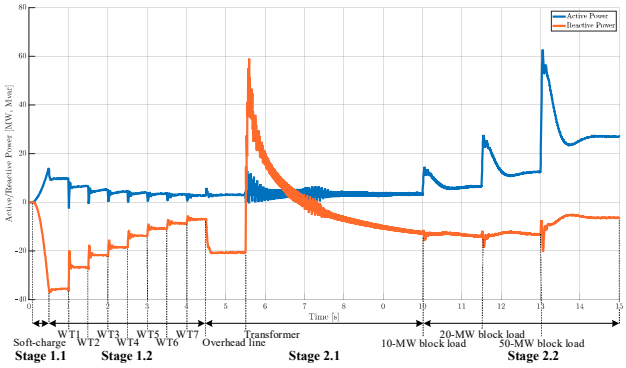

c)

Figure 4-15. Black-start strategy performed with the offshore wind farm in Configuration 1 (grid-forming battery and grid-following wind turbines) showed from the battery terminals: a) voltage; b) current and c) active (blue) and reactive (orange) power [J3], [95].

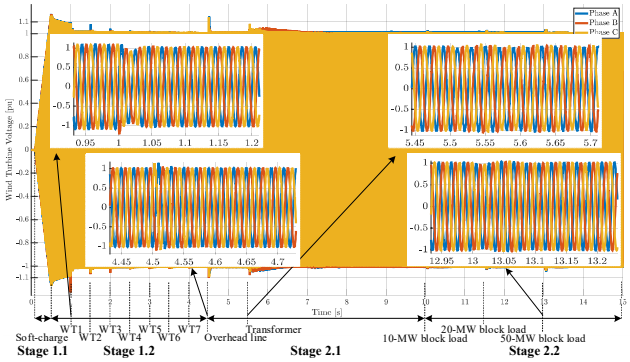

a)

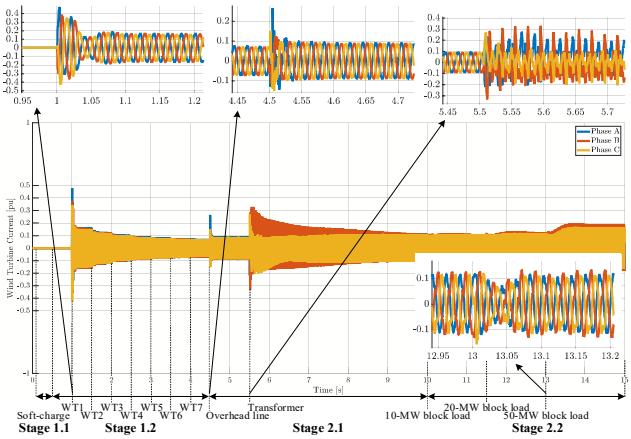

b)

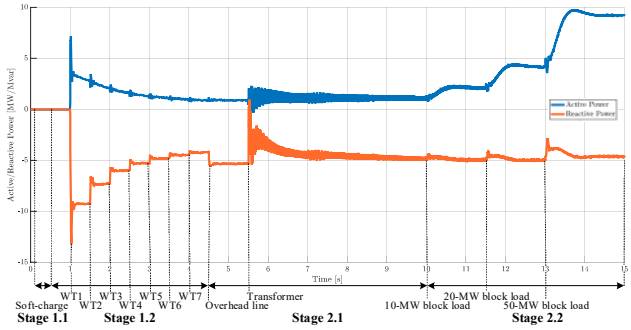

c)

Figure 4-16. Black-start strategy performed with the offshore wind farm in Configuration 1 (grid-forming battery and grid-following wind turbines) showed from the turbine terminals: a) voltage; b) current and c) active (blue) and reactive (orange) power [J3], [95].

4.4.3. NO INERTIA EMULATION IN THE GRID-FORMING CONTROL

The emulation of inertia is one of the requirements clearly introduced in the black-start grid codes for non-conventional power plants. One key feature of the PSC with VSM variation is the application of virtual inertia and damping in the control loop. To show a comparison of the classic PSC against the PSC with VSM design, the same case study as in the previous section, i.e., Configuration 1 is shown, however, without implementing the VSM loop in the GFM controller of the BESS. Since the inertia rovision is related to the active power, the energization of block loads is chosen to illustrate better the impact of the inertia loop. Figure 4-17 shows the three-phase voltage, current, active, and reactive power for the BESS and WT1 for the whole simulation.

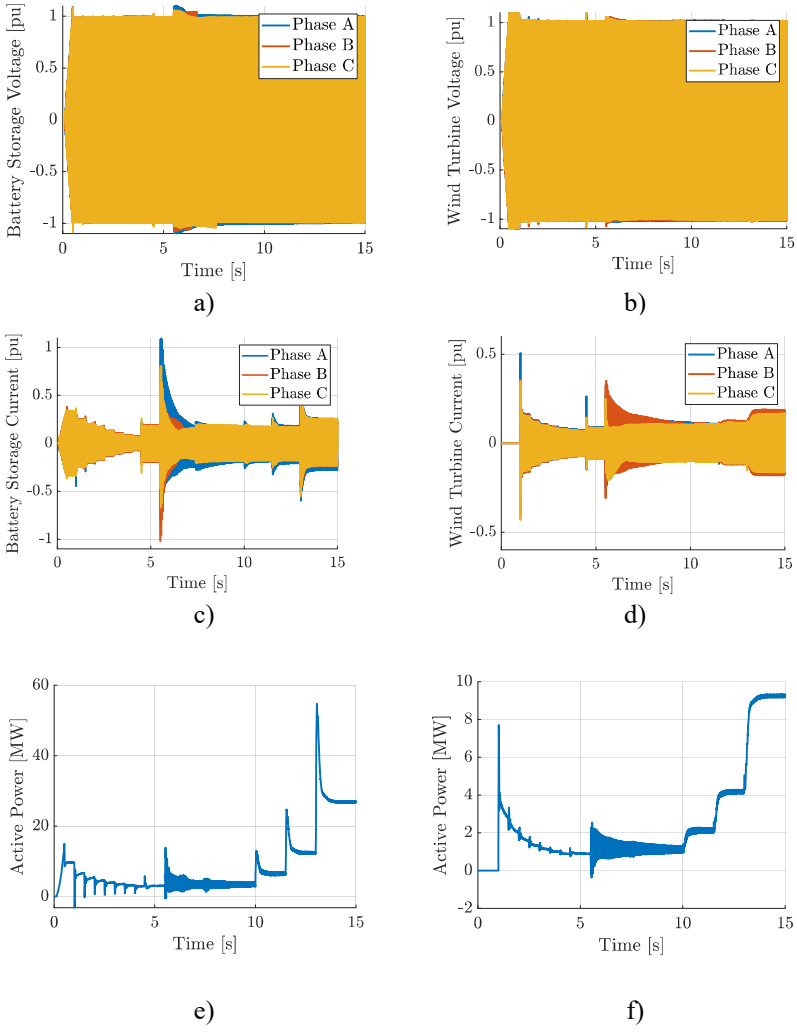

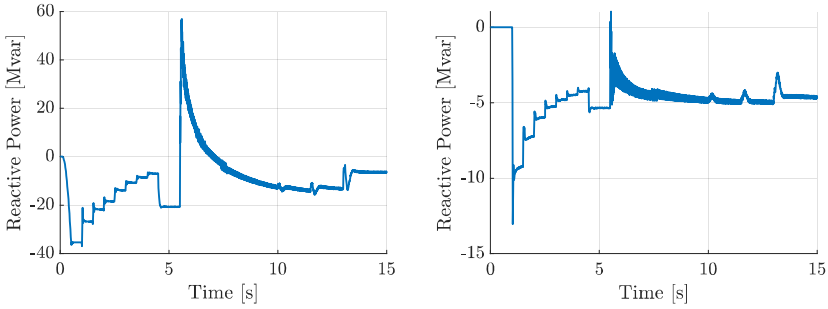

g) h)

Figure 4-17. Three-phase electrical measurements for black-start procedure in Configuration 1 without inertia emulation in the grid-forming controller seen from the battery storage and the wind turbine point of connection; a) battery storage voltage, b) wind turbine voltage, c) battery storage current, d) wind turbine current, e) battery storage active power, f) wind turbine active power, g) battery reactive power, and h) wind turbine reactive power.

Figure 4-17-a to Figure 4-17-d may appear similar to the previous case. However, in Figure 4-17-e and Figure 4-17-f, it is shown that the active power oscillations are slightly increased in comparison to the results shown in Figure 4-15-c and Figure 4-16-c, especially during block loading. This is shown in Figure 4-18.

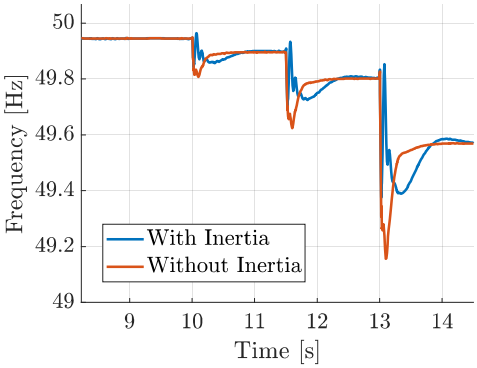

Figure 4-18. Comparison of the frequency swings during block loading (Stage 2.2) in Configuration 1.

4.5. CONFIGURATION 2: GRID-FORMING BATTERY AND GRID-FORMING WIND TURBINES

The sequence of events shown in the base case for Configuration 2 is summarized in Table 4-7. Initial results of this configuration are presented in [C4], [92].

Table 4-7. Events simulated for the demonstration of Configuration 2 (grid-forming battery storage and grid-forming wind turbines) of the black-start procedure [J3], [95].

Event	Stage	Instant [s]	Event	Stage	Instant [s]
Initialization, all units shut down	-	0.0	Overhead line is connected	2.1	15.0
BESS soft charge	1.1	0.1-0.5	Onshore transformer is connected	2.1	17.0
WT1 is connected	1.2	1.0	10-MW block load is connected	2.2	22.0
WT2 is connected	1.2	3.0	20-MW block load is connected	2.2	24.0
WT3 is connected	1.2	5.0	50-MW block load is connected	2.2	26.0
WT4 is connected	1.2	7.0	Simulation concluded	-	30.0
WT5 is connected	1.2	9.0			
WT6 is connected	1.2	11.0			
WT7 is connected	1.2	13.0			

Due to the slower dynamics of the GFM control, implemented in this case in all the WTs, this simulation is longer than Configuration 1.

As in the previous analysis, Figure 4-22 shows the entire black-start procedure for Configuration 2 from the BESS electrical parameters. While Figure 4-23 shows the same electrical parameters for Configuration 2 but is seen from the first group of aggregated WTs, i.e., WT1.

4.5.1. STAGE 1: WIND FARM POWER ISLAND

4.5.1.1 Stage 1.1: Soft-Charge of Passive Components

In this configuration, it is proposed to start the black-start procedure in the same fashion as in Configuration 1. This is mainly because the black start from the WTs implies the energization of the array cables, which are usually connected as a single string, which is energized at a single instance string by string. It may be challenging for a single WT to energize the array cable, due to the cable reactive loading. Therefore, it has not been included in this analysis but could be investigated as a future work where either the WT capability curve is designed to be able to energize at once

the cable or the cable is segmented in smaller parts to allow the first WT to energize two sections and after another WT, and so on. Therefore, the BESS soft-charge procedure is not repeated in this section, as the difference from grid-following to grid-forming control is not relevant for this step.

4.5.1.2 Stage 1.2: Connection and Energization of Wind Turbines

After the soft charge is completed as in the previous configuration, the WTs can be energized. As seen in Figure 4-19-a, the connection of the WTs has minimal impact on the BESS voltage, which is stable at around 1 pu during the whole procedure. Figure 4-19-b shows the same pre-connection voltage as in the previous configuration for WT1, thus it can be neglected as, once connected, the WT voltage passes from 1.06 to 1.0 pu at 1.02 s.

In this configuration, the droop parameters of the WTs are also tuned to show a higher contribution from the WTs, assuming favorable wind conditions, to also show the recharging of the BESS from the WTs. Figure 4-19-c shows the BESS current going from 0.33 to 0.21 pu, and Figure 4-19-e shows that the BESS active power generation drops from 9.7 to 2.7 MW, while the reactive power goes from -35.6 to -25.7 Mvar at 2.8 s, i.e., when WT1 is energized and in steady state.

From the WT1, complementary parameters are presented, as in Figure 4-19-d the current goes from 0 to 0.23 pu, and Figure 4-19-f shows active and reactive power going from 0 to 6.8 MW and -11.1 Mvar respectively.

The other WT groups are energized every 2 s, and when all the seven groups are connected and in a steady state at 14.8 s, the BESS only supplies 0.5 MW and 2.5 Mvar as seen in Figure 4-22-c. Notably, the oscillations connected with the switching of the WTs are reduced with every group of WTs connected. This could be due to the characteristics of GFM converters to work better in weak grid conditions, which is the result of many converter-based resources connected to one isolated system, as in this case.

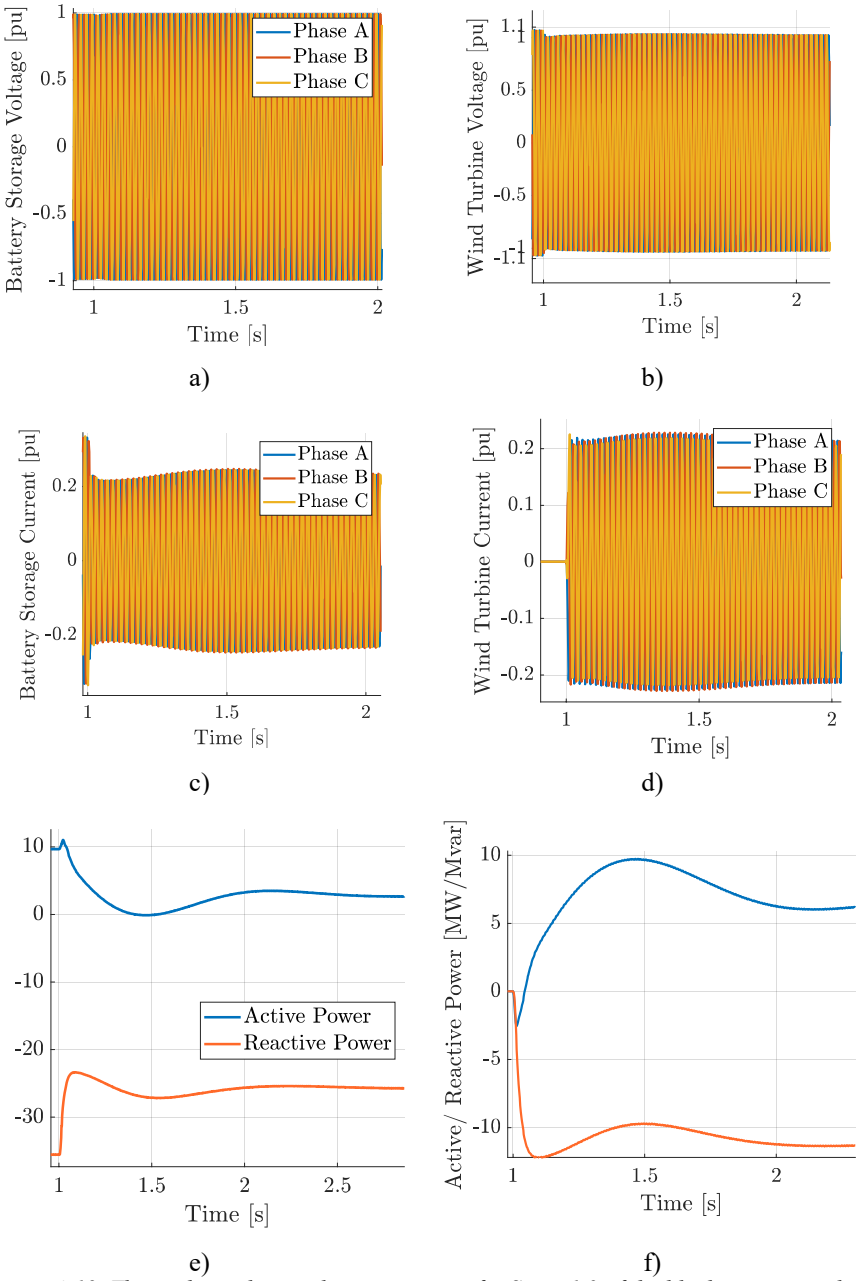

Figure 4-19. Three-phase electrical measurements for Stage 1.2 of the black-start procedure for Configuration 2 seen from the battery storage and the wind turbine point of connection; a) battery storage voltage, b) wind turbine voltage, c) battery storage current, d) wind turbine current, e) battery storage active power (blue) and reactive power (orange), and f) wind turbine active power (blue) and reactive power (orange).

4.5.2. STAGE 2: BLACK START POWER ISLAND

Similar to Configuration 1, after the OWF is working in island mode, Stage 2 can take place together with the actual restoration of the system.

4.5.2.1 Stage 2.1: Energization of Passive Components

At 15 s, the OHL is connected to the OWF system, which results in an overvoltage of 1.05 pu for the BESS, as shown in Figure 4-20Figure 4-22-a, and 1.1 pu for WT1 as seen in Figure 4-20-b. At 17 s, the connection of the transformer takes place, and this also results in an overvoltage of 1.03 pu for the BESS, as shown in Figure 4-20-a, and 1.12 pu for WT1 as seen in Figure 4-20-b. The inrush current reaches 1.09 pu for Phase A the BESS, as shown in Figure 4-20-c and 0.44 pu for Phase B WT1 as shown in Figure 4-20-d.

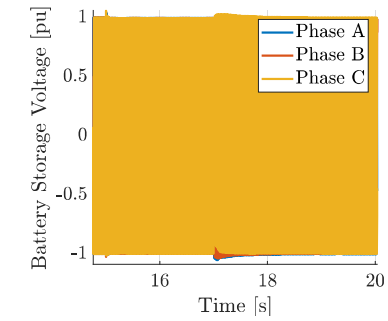

a)

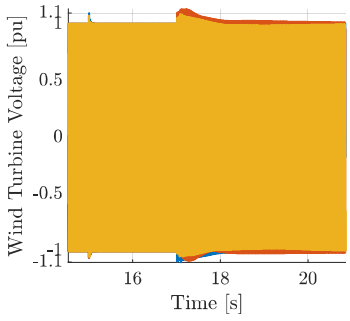

b)

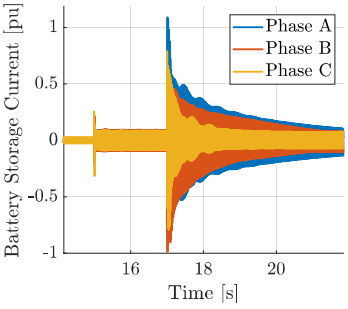

c)

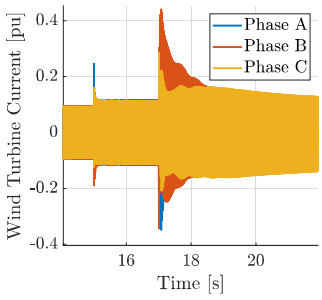

d)

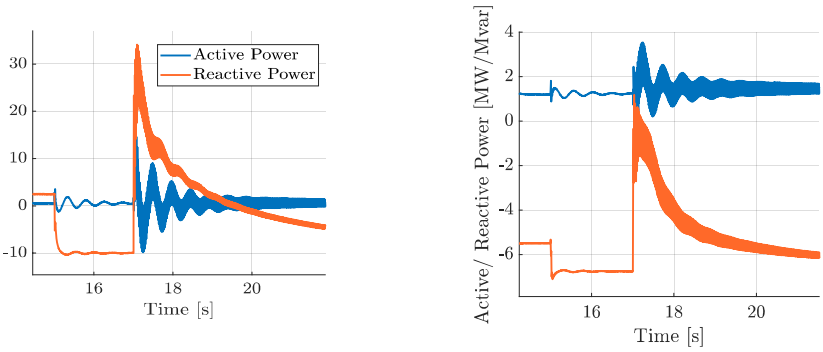

e) f)

Figure 4-20. Three-phase electrical measurements for Stage 2.1 of the black-start procedure seen from the battery storage and the wind turbine point of connection; a) battery storage voltage, b) wind turbine voltage, c) battery storage current, d) wind turbine current, e) battery storage active power (blue) and reactive power (orange), and f) wind turbine active power (blue) and reactive power (orange).

4.5.2.2 Stage 2.2: Energization of Block Loads

The connection of block loads results in higher oscillations in the reactive power than what was seen in Configuration 1, but it is an expected change due to the nature of the GFM control, which does not directly control the active power, while instead controls the frequency via an inertial response, reducing its oscillations. Figure 4-21 shows the results of this stage for both BESS and WT1.

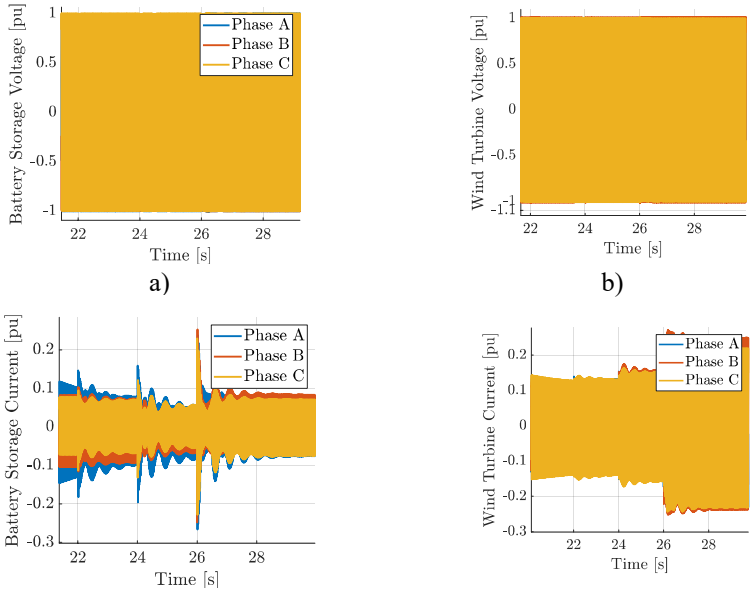

a) b)

c) d)

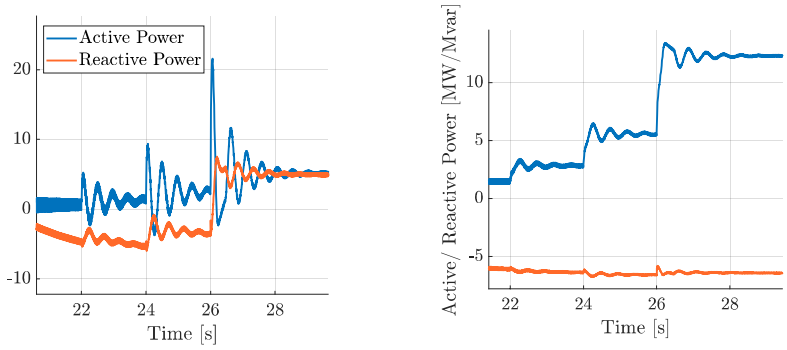

e) f)

Figure 4-21. Three-phase electrical measurements for Stage 2.2 of the black-start procedure seen from the battery storage and the wind turbine point of connection; a) battery storage voltage, b) wind turbine voltage, c) battery storage current, d) wind turbine current, e) battery storage active power (blue) and reactive power (orange), and f) wind turbine active power (blue) and reactive power (orange).

It is shown that booth BESS and WT1 can handle the energization of 10, 20 and 50 MW block loads seamlessly.

The results for the entire black-start procedure for Configuration 2 can be seen in Figure 4-22 for the BESS and in Figure 4-23 for WT1. Both figures include the three-phase voltage, current, active, and reactive power measured at the terminals of the related equipment.

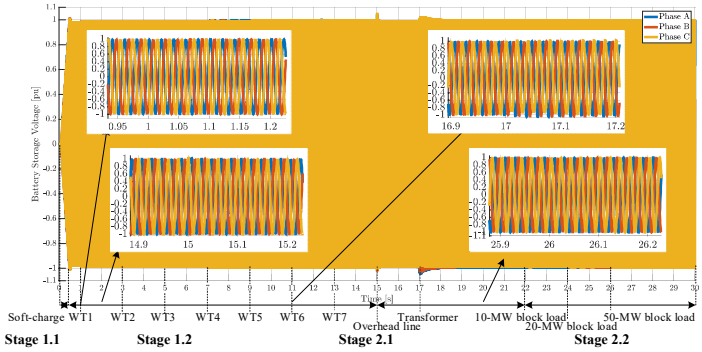

a)

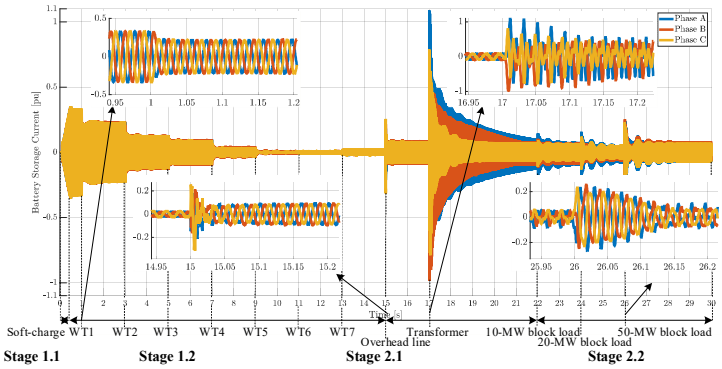

b)

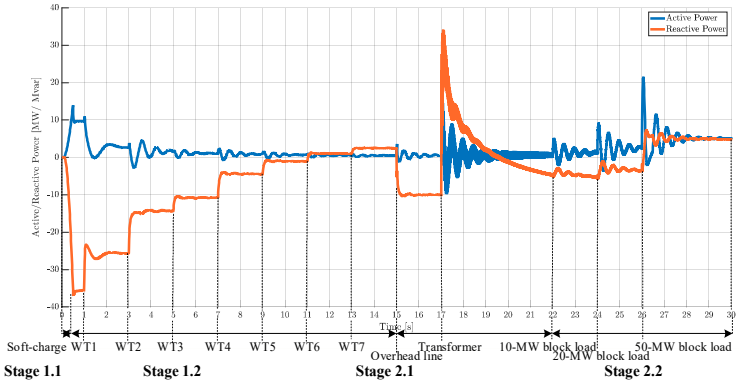

c)

Figure 4-22. Black start strategy performed with the offshore wind farm in Configuration 1 (grid-forming battery and grid-following wind turbines) from the battery terminals: a) voltage; b) current and c) active (blue) and reactive (orange) power [J3], [95].

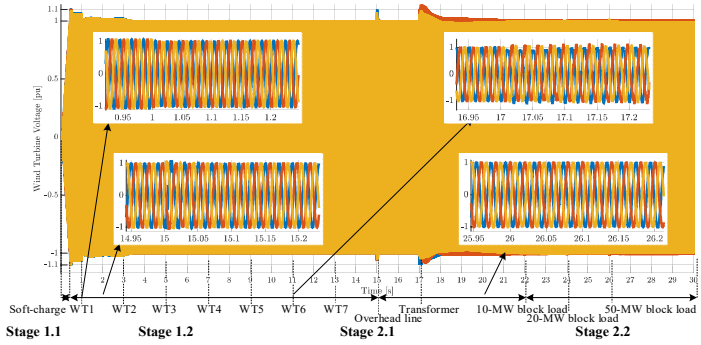

a)

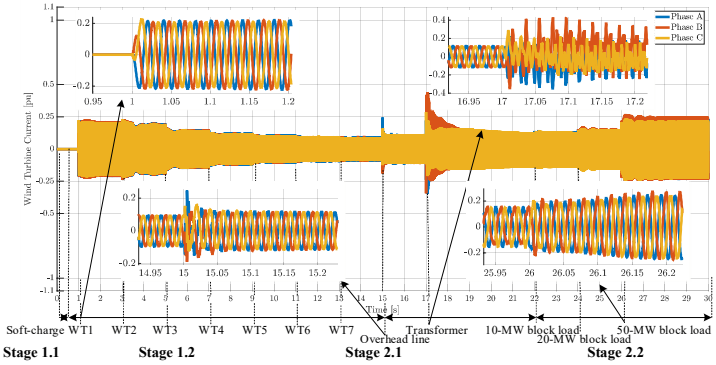

b)

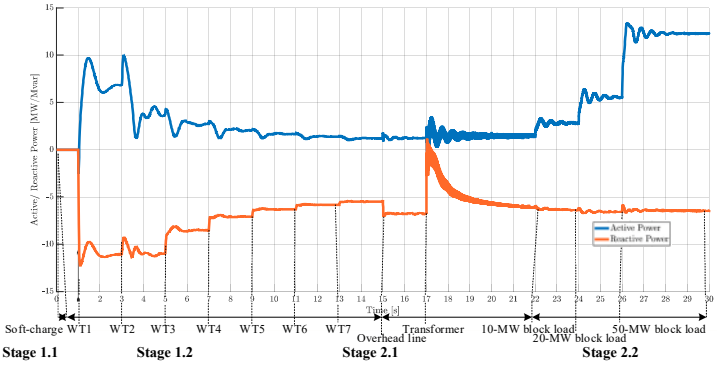

c)

Figure 4-23. Black start strategy performed with the offshore wind farm in Configuration 2 (grid-forming battery and grid-forming wind turbines) from the turbine terminals: a) voltage; b) current and c) active (blue) and reactive (orange) power [J3], [95].

4.6. STRATEGY VARIATIONS AND SENSITIVITY ANALYSIS

Due to the practical differences that there may be with equipment and the random nature of the blackout event as well, in this section, the analysis of different aspects seen in the previous base case is shown.

4.6.1. ENERGIZATION OF WIND TURBINE TRANSFORMER SEPARATELY FROM SOFT-CHARGE

In the proposed black-start procedure, it is suggested to also connect the WT transformer to the passive system when shut down and then have the BESS soft charge it. Thus, the energization of the WT transformer separately from the soft charge is shown here to compare. In both the previous strategies, it has been assumed that it is possible to configure the WT to have first its transformer connected and soft charged, and then the WT itself can be connected. As an alternative case, it is shown how the BESS can soft charge the system, also excluding the WT. Only one WT and respective transformer are simulated in this case, i.e., not an aggregated array as previously shown. The results of this variation are shown in Figure 4-24. In this simulation, the soft charge of the system from the BESS takes place from 0 to 0.5 s. At 0.6 s, the WT transformer is connected, and at 6 s the WT and controller are connected and synchronized. Figure 4-24-a shows that the BESS voltage is stable at 1 pu, and Figure 4-24-b shows that the inrush currents from the transformer are manageable, reaching 0.35 pu on Phase A at the highest. Figure 4-24-c shows that the connection of the WT transformer results in oscillation that gets damped in approximately 1 s, settling at 6.1 MW, therefore not challenging the system. In Figure 4-24-d it can be seen that the reactive load on the BESS during the soft charge settles at -39.9 Mvar, higher than the -35.5 Mvar, due to the lack of transformers connected to the islanded network in this instance. Therefore, the energization of the WT transformer separately from the soft charge is feasible but results in a higher reactive loading on the BESS which is already significant. It is shown that the separate energization of the WT transformer is possible, especially since these are 12 MVA transformers, which means that they are not very large and thus result in fewer challenges. This is possible, however, not recommended as the advantages of this procedure are far less than the disadvantages. The inrush currents and possible excitation of the system resonance are one concern, together with the sympathetic interactions, once the second WT transformer has to be energized, as well as the others.

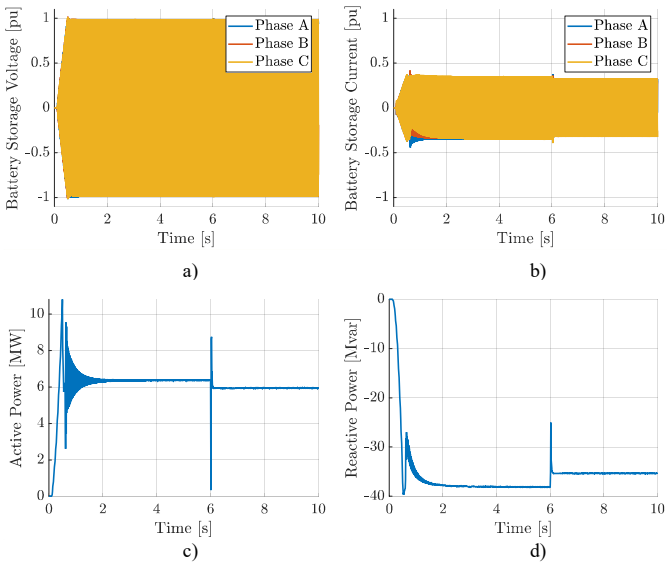

Figure 4-24. Energization of wind turbine transformer separately from the soft-charge seen from the battery storage: a) voltage, b) current, c) active power, and d) reactive power.

4.6.2. SOFT-CHARGE WITH DIFFERENT TIME RATES

The energization of the OWF islanded network via soft-charge by the BESS has been shown with ramp-up from 0.1 to 0.5 s (thus, 0.4 s from 0 to 1 pu) in the base case presented previously. For comparison, three different time lengths of soft charge are here presented to analyze the sensitivity of the procedure concerning this different parameter. Two faster time rates of soft-charge are used, i.e., 0.05 s and 0.2 s. These are shown in Figure 4-25 and Figure 4-26 respectively. Both may be possible for the BESS; however, not preferred, as the faster operation reduces the advantages of implementing it in the first place.

For the soft charge in 0.05 s, Figure 4-25-a shows that the BESS voltage reaches 1.1 pu at 0.16 s, to then settle at 1 pu at 0.3 s. While Figure 4-25-b shows that the current reaches 0.78 pu on Phase B to then settle at 0.33 pu. Figure 4-25-c shows that the active power reaches the high value of 44 MW (14 MW in the base case) to then settle at 6 MW. Also, the reactive power has a high overshoot, reaching -49 Mvar at 0.24 s to then settle at 35.5 Mvar.

Figure 4-26-a shows the BESS voltage when the soft-charge duration is 0.2 s, and it results as well in an overvoltage at 1.1 pu. Figure 4-26-b shows how the BESS current reaches 0.6 pu at 0.31 s. Figure 4-26-c presents the overshoot of the active power at

27 MW, while Figure 4-26-d shows the reactive power peak at -45 Mvar. All in all, the transition is seen as softer due to the lower time rate, as expected.

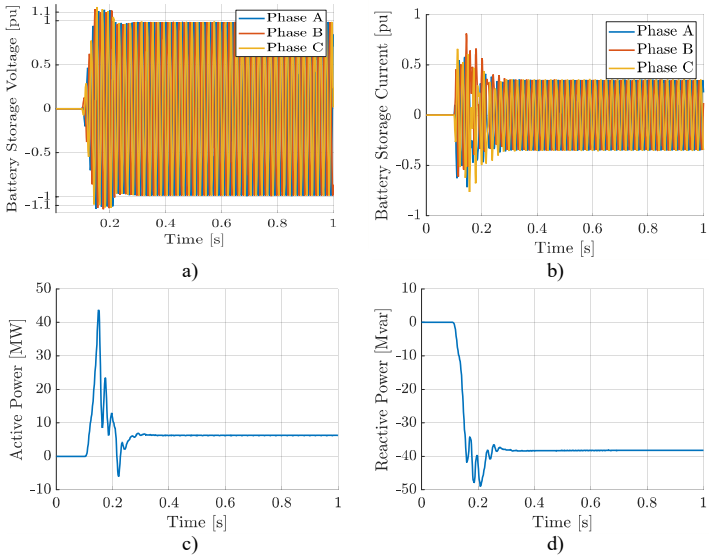

Figure 4-25. Soft-charge in 0.05 s: a) voltage, b) current, c) active power, and d) reactive power.

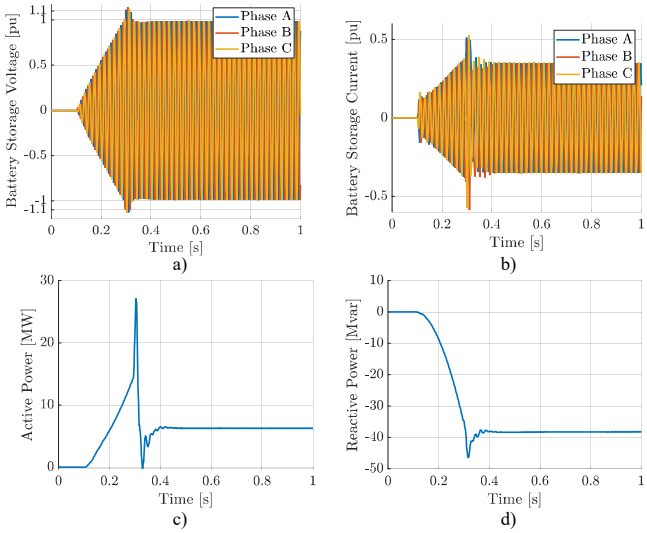

Figure 4-26. Soft-charge in 0.2 s: a) voltage, b) current, c) active power, and d) reactive power.

To avoid overvoltage, the lower time rate of 0.4 s shown in the base case is sufficient. For comparison, an even slower time rate of 0.8 s is shown in Figure 4-27. Figure 4-27-a shows the BESS voltage that seamlessly goes from 0 to 1 pu, while Figure 4-27-b shows similar results for the current. Figure 4-27-c and Figure 4-27.d show the active and reactive power respectively, which result in the smallest overshoot seen in the active power at 8.5 MW before settling at 6 MW.

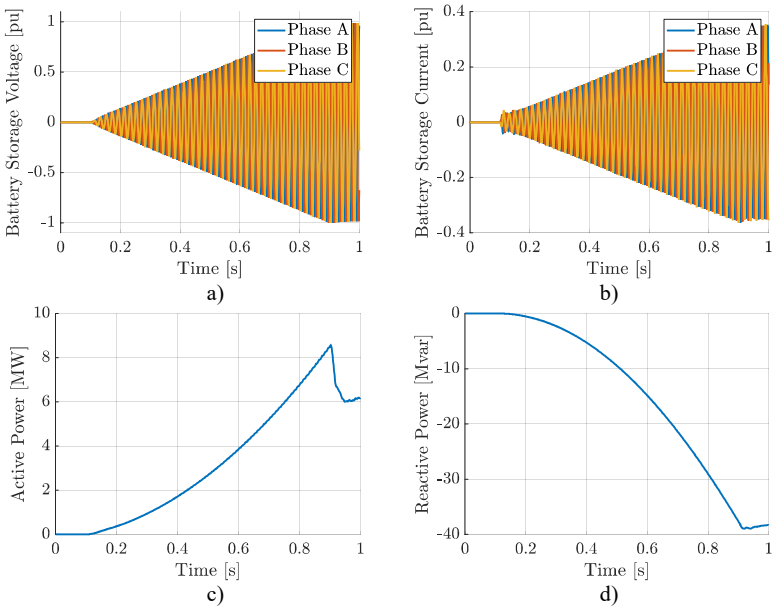

Figure 4-27. Soft charge in 0.8 s: a) voltage, b) current, c) active power, and d) reactive power.

4.6.3. ENERGIZATION OF LONGER TRANSMISSION LINE

Configuration 1

As the onshore transmission system to be restored is unknown, it is important to test the capabilities of the OWF system to black-start different types of system scenarios. It is chosen to double the length of the OHL modeled, to give an example. Figure 4-28 shows the connection of the OHL performed by Configuration 1. Despite the change implemented, the system can carry out with the performance.

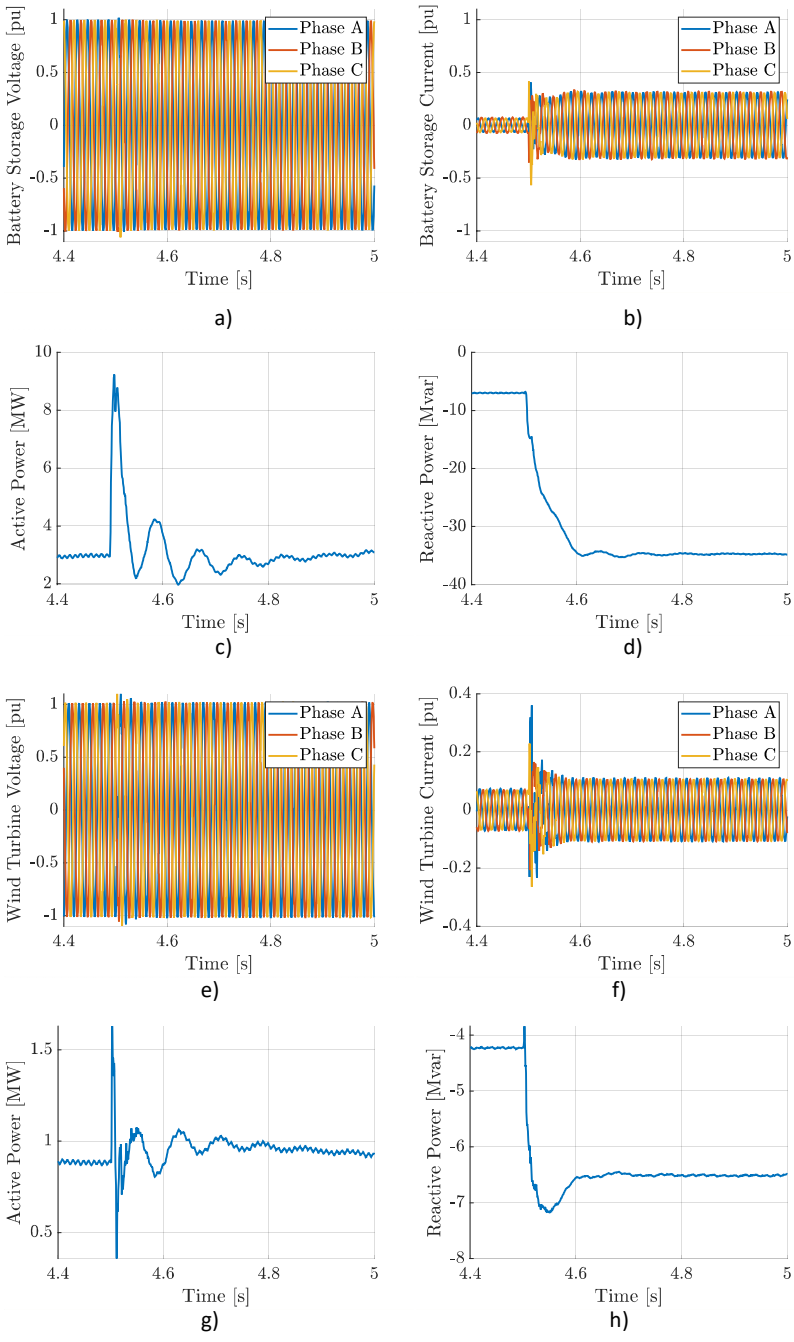

Figure 4-28. Energization of 100 km overhead line during Configuration 1: a) battery voltage, b) battery current, c) battery active power, d) battery reactive power, e) wind turbine voltage, f) wind turbine current, g) wind turbine active power and h) battery reactive power.

Configuration 2

Similar to what is shown for Configuration 1, also Configuration 2 can accept the long OHL. In Figure 4-29, the BESS and WT parameters show the energization of the 100 km OHL.

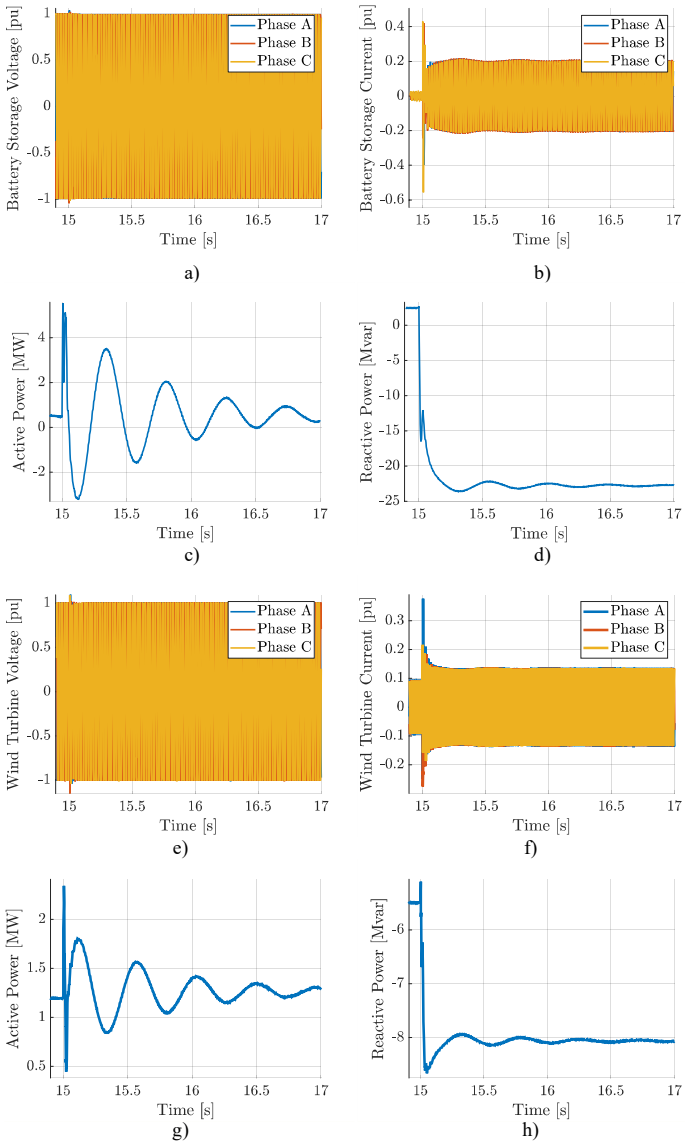

Figure 4-29. Energization of 100 km overhead line during Configuration 2: a) battery voltage, b) battery current, c) battery active power, d) battery reactive power, e) wind turbine voltage, f) wind turbine current, g) wind turbine active power and h) battery reactive power.

4.6.4. APPLICATION OF SINGLE-POLE SWITCHING TO ENERGIZE THE ONSHORE TRANSMISSION GRID TRANSFORMER

As shown for both Configuration 1 and 2, the energization of the large onshore transformer in the transmission network caused an overvoltage and overcurrent to the BESS. Since the impact of such distortions depends greatly on the phase angle of the source voltage, the application of three-phase CBs that can operate with single-pole switching, i.e., each phase can be switched separately from the others, is investigated. Sometimes, this practice is also referred to as a point of wave (POW) switching, as the switching instant is applied to a certain point of the voltage waveform, rather than a specific time. In this way, instead of the three phases switching at the same given instant, they switch at slightly different times but when the phase angle of the source voltage is controlled. Since this case regards transformer energization, the phase angle to minimize the transient due to the energization, ideally eliminate, is when the voltage is crossing zero [96].

For both configurations, the exact switching times have been set in the CBs applying the single-pole switching and the simulation has been repeated.

Configuration 1

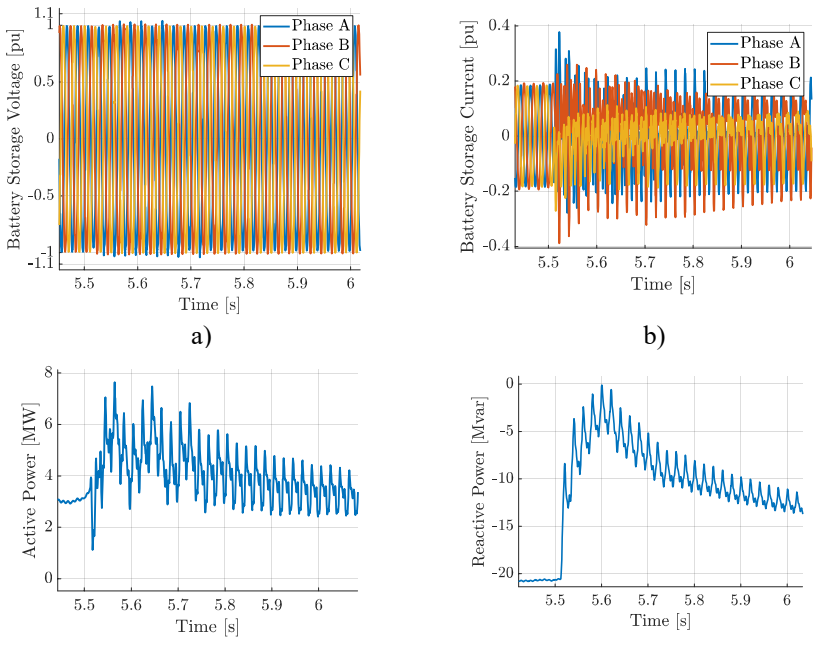

Figure 4-30. Three-phase electrical measurements for the battery storage application of single-pole switching to energize the onshore transmission grid transformer; a) voltage, b) current, c) active power, and d)reactive power.

Figure 4-30 shows the BESS three-phase electrical parameters during the energization of the onshore transmission grid transformer at 5.5 s. More specifically, Figure 4-30-a shows the voltage, Figure 4-30-b shows the current, while Figure 4-30-c and Figure 4-30-d show respectively the active and reactive power measured at the BESS PCC.

Comparing Figure 4-30-a to Figure 4-20-a, it can be seen that the magnitude of the voltage magnitude during the transient is reduced by the application of the single-point operation of the circuit breaker, having the highest voltage peak at 1.01 pu on Phase A at 5.57 s, while originally surpassing 1.1 pu. The largest improvement is seen in the current waveform, as the current is reduced to a maximum of 0.43 pu for Phase B, as seen in Figure 4-30-b, while before exceeding as well 1.1 pu as shown in Figure 4-20-c. Consequently, also the active and reactive power peaks are reduced as seen in Figure 4-30-c and Figure 4-30-d respectively.

Configuration 2

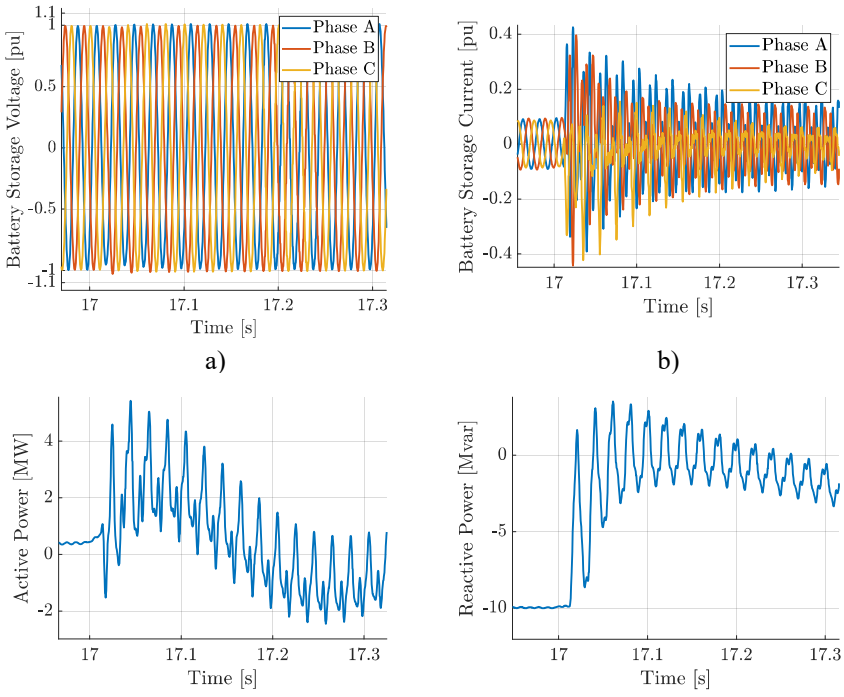

Figure 4-31. Three-phase electrical measurements for the battery storage application of single-pole switching to energize the onshore transmission grid transformer; a) voltage, b) current, c) active power, and d)reactive power.

Similarly to the previous configuration, Figure 4-31 shows the BESS three-phase electrical parameters during the energization of the onshore transmission grid transformer at 17 s for Configuration 2. More specifically, Figure 4-31-a shows the

voltage, Figure 4-31-b shows the current, while Figure 4-31-c and Figure 4-31-d show respectively the active and reactive power measured at the BESS PCC.

Comparing Figure 4-31-a to Figure 4-13-a, it can be seen that the magnitude of the voltage magnitude during the transient is reduced by the application of the single-point operation of the circuit breaker, having the highest voltage peak at 1.01 pu on Phase A at 17.03 s, while originally surpassing 1.1 pu. The largest improvement is seen in the current waveform, as the current is reduced to a maximum of 0.43 pu for Phase B, as seen in Figure 4-30-b, while before exceeding as well 1.1 pu as shown in Figure 4-13-c. Consequently, also the active and reactive power peaks are reduced as seen in Figure 4-30-c and Figure 4-30-d respectively.

The application of single-point operation for the CB results in satisfactory transients that do not exceed any limitations. Nevertheless, the application of this technique requires more costly and sophisticated hardware. While an optimized controller tuning may reduce the impact of this event, it is thus recommended for future work.

4.7. SUMMARY

An OWF+BESS has been designed and tested to perform a black start using an integrated ESS with only power electronic-based components. For the black start, power electronic converters must operate in island mode, and regulate the system frequency and voltage, with at least one grid-forming unit. This is in opposition to the well-known GFL operation in which renewable-based resources are controlled to extract the maximum available power. The black start capability of the proposed control system is possible through the integration of a grid-forming BESS, that performs the initial system energization and boosts the availability to perform a black start even when there is no wind.

The challenge of a system with multiple converters working in island mode, where local losses and generation must be carefully balanced when connecting new parts of the system has been presented. A solution is proposed in terms of two different configurations that can achieve this procedure, i.e., Configuration 1 consisting of a grid-forming BESS integrated into an OWF with grid-following WTs and Configuration 2 consisting of both grid-forming BESS and WTs. These ensure that the black start procedure can be carried out completely until the connection of block loads up to 50 MW.

The proposed strategies are applied to a case study where a 420-MW OWF with integrated BESS black starts a transmission system made of an OHL, a transformer, and three block loads. The modeling of this case study is presented to illustrate the proposed control system operation and simulation results are presented to validate the proposal. Also, a configuration variation and sensitivity analysis has been performed to demonstrate the stability of the black start procedure despite varying parameters.

The selection of the most suitable configuration for the OWF developer to implement is left as future work, as both strategies can complete a black start. Further controller design studies may achieve higher capabilities for the system, where grid-forming control may be able to perform in weaker systems than grid-following control.

The results show that an OWF can be controlled to perform a black start without relying on additional diesel generators. The grid-forming BESS can soft-charge passive components and synchronize the grid-following/grid-forming WTs in an isolated system. Since this synchronization is independent of active power, it can be performed even for varying wind power scenarios. If active power was used for synchronization in this scenario, the system would be unstable since the equal frequency required for synchronization would demand equal power increments. Once the WTs are started, the actual black start of the transmission grid can take place and, energizing up to 50 MW block loads, the black-start process is completed. For future work, the strategy used for Configuration 2 can be analyzed when starting from the WTs, applying the BESS only if support is necessary.

Having a real OWF project, the worst-case inrush currents during the black start procedure, especially while energizing large transformers, can be estimated, and compared against capability curves and current limits of the active equipment. This will lead to defining the optimized procedure to reduce the loading on such equipment based on reduced generator terminal voltage, automatic voltage regulator tuning and regulation of the reactive power compensation, and overall, the optimal sizing of the grid-forming BESS and WTs.

5. CONCLUSIONS

In this chapter, the main conclusions of this Ph.D. dissertation are given. Its contributions and the proposed future research for implementing black-start capabilities by offshore wind farms are listed.

5.1. OVERALL SUMMARY

The main research focus of this Ph.D. thesis is enabling the integration of black-start capabilities into OWFs, where the future power-electronic-based power system can rely on non-conventional resources to perform restoration services. To this end, several challenging issues for the black start have been studied, and the corresponding discussions and solutions have been proposed, especially by selecting proper wind farm system configurations and control strategies. The research outcomes of the Ph.D. thesis are summarized as follows.

In *Chapter 1*, the challenging issues about the integration of power-electronic-based resources into the future power system have been discussed, based on which the objectives of this Ph.D. thesis are proposed. On one hand, RESs are needed to reduce CO_2 emissions and contrast climate change. On the other hand, their black-start capability is not ready for industrial deployment yet. The use of advanced control methods like GFM control and additional equipment like ESSs can provide black-start capabilities with superior and robust performance. Although the main idea of the implementation of black-start provision by OWFs is to enable the system to emulate actual SGs during restoration, different wind farm system configurations and control strategies may be used. As a result, control and operational philosophies among these OWFs will be different as well.

In *Chapter 2*, an overview of a generic OWF structure is presented and a brief description of common energization methods for normal and abnormal operation of the wind farm is given. This gives input on what the black start of the OWF may look like. For example, during the first energization, the power comes from the transmission grid, hence from onshore to offshore. Furthermore, in abnormal operations, mobile/auxiliary diesel generators are deployed on single WTs to avoid damage. Subsequently, an investigation of grid code requirements for a black start is given. In terms of actual applications, no RESs are performing black start, and thus, following grid codes. Nevertheless, NGESO is considering amending the grid code to include the black start capabilities of RESs. The requirements considered the relaxation of the current grid codes for conventional power plants to adapt them to renewable-based resources, and so are shown in *Chapter 2*. These requirements show the gaps that OWFs have to comply with. A main concern is the availability requirement, which being at 90% may be high for an OWF, which can solely rely on the wind. Therefore, given the overview of wind farm system configurations for a

black start, it is proposed to use additional equipment with increased availability, like SGs or ESSs. Given the need to move away from fossil fuels, the application of GFM ESSs is preferred. Therefore, two main system configurations are explored; the combination of an OWF equipped with GFL WTs with a GFM BESS, and the combination of an OWF equipped with GFM WTs with a GFM BESS. These two systems composed of OWF+BESS represent hybrid power plants whose control and operation have to be properly defined.

In *Chapter 3*, the chosen configurations for black start by an OWF are applied to outline the stages that the OWF+BESS system has to go through as a black-start source. These stages are three and are defined as 1) Wind Farm Power Island, when the OWF+BESS is black-started and disconnected from the onshore transmission grid, thus working in islanding mode; 2) Black Start Power Island, when the OWF+BESS system starts energizing parts of the onshore transmission network, but still working in islanding mode; 3) Power Island Re-Sync, when the OWF+BESS power island has to synchronize with the other power islands or the main grid that was not shutdown to go back to a state of restored normal operation. To complete these stages, the OWF in the chosen configurations has firstly to be able to black start itself, which may be possible only when applying GFM control to the converters of the system. Thus, an overview of the most common control topologies for GFM control is shown, and the selected GFM control, i.e., PSC with additional VSM implementation is described.

Therefore, the overall black-start procedure is shown for the two implemented configurations where EMT simulations are applied in *Chapter 4*. The benchmark model is described, and it consists of an HVAC-connected OWF rated at 420 MW. The simulation results are used to show the operation philosophy, where communication-free controllers are used to define the lower-level dynamics automatically. The implementation of improved energization strategies, like soft-charge of the reactive components and single pole operation of the CBs, are applied to avoid the stresses on the equipment coming from conventional switching operation. Especially, the energization of large transformers on the onshore transmission grid can be challenging, as soft-charge cannot be applied, and the saturation of the transformer can result in large inrush currents that may harm the power-electronic switches of the converters. Overall, the two black-start procedures carried out with the two system configurations can complete the restoration procedure and energize both passive reactive components and black loads in the onshore transmission network.

5.2. MAIN CONTRIBUTIONS

The contributions of this Ph.D. study gather both academic and industrial outcomes. The main contributions can be summarized as follows:

1. Analysis of the grid code requirements for future OWFs with black-start capabilities. Presented in Chapter 2 and in [J2], [60].
2. Implementation of design guidelines for the future OWFs as hybrid systems with integrated ESSs with black-start capability. Discussed in Chapter 2.
3. Definition of possible system configurations that can be implemented in OWFs to allow black-start operation. Described in Chapter 2 and in [C1], [3].
4. Development of the control philosophy for an OWF with integrated EESs capable of working in island mode and providing black-start services. Outlined in Chapter 4 and [C3], [80], [C4], [92], [J3], [95].
5. Definition of the operational philosophy in the form of flowcharts for an OWF with integrated EESs capable of working in island mode and providing black-start services. Illustrated in Chapter 4 and [C3], [80], [C4], [92], [J3], [95].

5.3. FUTURE WORK

During this three-year project, the main work has focused on the presented work condensed in this thesis based on a series of choices and considerations. Since there are many aspects that have been left unexplored, the work done during this Ph.D. project may be continued with the following research activities:

- Investigate the synchronization of the Black Start Power Island with other power islands during Stage 3 (Power Island Re-Sync) to complete the restoration procedure.
- Study the short-circuit capability of an OWF as the black-start source.
- Analyze and quantify the inertia provision of the OWF as a black-start provider to be able to handle active loads.
- Investigation of a similar strategy but with grid-forming STATCOM, possibly with ultracapacitors, instead of BESS with integrated STATCOM in order to save costs.
- Research on the services that an ESS can achieve in grid-connected mode to increase the revenue of the OWF.
- Implement protection strategies that can work during soft-charge, island operation, and black start in general.
- Analysis of the harmonic performance of the system and proposal of passive or active harmonic filtering tailored for the black-start procedure.
- Proposals for grid-forming control design to ensure stability with a large degree of uncertainty considered. The uncertainty shall consider changes in the grid structure, as well as the connection of unknown active elements.
- Study of fault-ride-through strategies in grid-forming mode.
- The design of distributed control strategies for OWFs considering the available fast communications. Using just a centralized controller is possible to control all the WTs of an OWF. It may mean a performance increment in any operation carried out in an OWF.

- Study of the ratio of grid-forming to grid-following in an OWF to ensure stability and to ensure the capability to carry out some operations such as black start.
- Control strategies that estimate in-rush currents during the black start procedure and achieve fast mitigation of the inrush current.
- Investigate emergency responses during abnormalities in the grid to develop an islanding detection approach and avoid the shutdown of the OWF when a blackout in the grid takes place.

LITERATURE LIST

[1] United Nations, “Goal 7 | Sustainable Development Goals,” [Online]. Available: https://sdgs.un.org/goals/goal7. [Accessed 2022 April 1].

[2] U. Knight, "The 'Black Start' Situation," in *Power Systems in Emergencies - From Contingency Planning to Crisis Management*, ISBN 978-0-471-49016-6, John Wiley & Sons, 2001.

[3] D. Pagnani, Ł. Kocewiak, J. Hjerrild, F. Blaabjerg and C. L. Bak, "Overview of Black Start Provision by Offshore Wind Farms," in *46th Annual Conference of the IEEE Industrial Electronics Society*, Singapore, pp. 1-6, 2020.

[4] CIGRE SC C2, "Power System Restoration – World Practices & Future Trends," *CIGRE Science and Engineering Journal,* vol. 14, no. June, pp. 1-17, 2019.

[5] International Renewable Energy Agency (IRENA), "Future of Wind: Deployment, Investment, Technology, Grid Integration and Socio-Economic Aspects," Abu Dhabi, 2019.

[6] P. Kundur and O. P. Malik, Power System Stability and Control, 2nd ed., McGraw-Hill Education, 2022.

[7] A. D. Hansen, "Generators and Power Electronics for Wind Turbines," in *Wind Power in Power Systems*, John Wiley & Sons, 2012, pp. 73-103.

[8] F. Blaabjerg, R. Teodorescu, M. Liserre and A. V. Timbus, "Overview of Control and Grid Synchronization for Distributed Power Generation Systems," *IEEE Transactions on Industrial Electronics,* vol. 53, no. 5, pp. 1398-1409, 2006.

[9] X. Wang and F. Blaabjerg, "Harmonic Stability in Power Electronic-Based Power Systems: Concept, Modeling, and Analysis," *IEEE Transactions on Smart Grid,* vol. 10, no. 3, pp. 2858-2870, 2019.

[10] Ł. Kocewiak, R. Blasco-Giménez, C. Buchhagen, J. B. Kwon, Y. Sun, A. Svchwanka Trevisan, M. Larsson and X. Wang, "Overview, Status and Outline of Stability Analysis in Converter-based Power Systems," in *19th Wind Integration Workshop*, Online, pp. 1-10, 2020.

[11] J. Rocabert, A. Luna, F. Blaabjerg and P. Rodriguez, "Control of Power Converters in AC Microgrids," *IEEE Transactions on Power Electronics,* vol. 27, no. 11, pp. 4734-4749, 2012.

[12] M. Kesraouia, N. Korichib and A. Belkadi, "Maximum Power Point Tracker of Wind Energy Conversion System," *Renewable Energy,* vol. 36, no. 10, pp. 2655-2662, 2011.

[13] L. Shuai, R. Sharma, K. H. Jensen, J. N. Nielsen, D. Murcia, S. Pirzada, P. Brogan and P. Godridge, "Eigenvalue-based Stability Analysis of Sub-synchronous Oscillation in an Offshore Wind Power Plant," in *17th Wind Integration Workshop*, Stockholm, Sweden, pp. 1-8, 2018.

[14] C. Bunchhagen, M. Greve, A. Menze and J. Jung, "Harmonic Stability - Practical Experience from a TSO," in *15th Wind Integration Workshop*, Vienna, Austria, p. 16, 2016.

[15] H. Urdal, R. Ierna, J. Zhu, C. Ivanov, A. Dahresobh and D. Rostom, "System Strength Considerations in a Converter Dominated Power System," *IET Renewable Power Generation,* vol. 9, no. 1, pp. 10-17, 2015.

[16] M. G. Taul, X. Wang, P. Davari and F. Blaabjerg, "Current Limiting Control with Enhanced Dynamics of Grid-Forming Converters during Fault Conditions," *IEEE Journal of Emerging and Selected Topics in Power Electronics,* vol. 8, no. 2, pp. 1062-1073, 2020.

[17] M. Chen, "Modeling and Control of Solid-State Synchronous Generator," Aalborg University Publishing House. PhD series, The Faculty of Engineering and Science, Aalborg, Denmark, 2021.

[18] World Energy Council, "E-storage: Shifting from cost to value. Wind and Solar applications," London, United Kingdom, 2016.

[19] I. Todorović, "Europe is halfway into closing all coal power plants by 2030," Balkan Green Energy News, 25 March 2021. [Online]. Available: https://balkangreenenergynews.com/europe-is-halfway-into-closing-all-coal-power-plants-by-2030/. [Accessed 1 August 2022].

[20] C. Owens, "Black Start – Restarting The Grid From Scratch," The Blackout Report, 4 July 2019. [Online]. Available: https://www.theblackoutreport.co.uk/2019/07/04/black-start/. [Accessed 1 September 2022].

[21] U.S.-Canada Power System Outage Task Force, "Final Report on the August 14, 2003 Blackout in the United States and Canada: Causes and Recommendations," Washington, DC, 2004.

[22] Central Electricity Regulatory Commission, "Report on the Grid Disturbances on 30 and 31 July 2012," New Delhi, India, 2012.

[23] AEMO, "Black System South Australia 28 September 2016," Melbourne, Australia, 2017.

[24] J. Molina Guzmán, "Análisis de Falla del Sistema Eléctrico Nacional. Pérdida Total del Sistema. Dia 07/03/2019," Caracas, Venezuela, 2019.

[25] G. Shaw, "A massive power outage left over 48 million people in the dark across entire countries in South America," Business Insider, 16 June 2019. [Online]. Available: https://www.businessinsider.com/power-outage-south-america-argentina-uruguay-2019-6?r=US&IR=T. [Accessed 17 August 2022].

[26] Energy Institute of University of Texas at Austin, "The Timeline and Events of the February 2021 Texas Electric Grid Blackouts," Austin, Texas, 2021.

[27] Hydro-Québec, "A look at the outages caused by the May 21 derecho," 14 June 2022. [Online]. Available: https://news.hydroquebec.com/en/press-releases/1841/a-look-at-the-outages-caused-by-the-may-21-derecho/?fromSearch=1. [Accessed 17 August 2022].

[28] Elkraft System (now Energinet), "Strømafbrydelsen i Østdanmark og Sydsverige 23. september 2003," Fredericia, Denmark, 2003.

[29] Commissione di indagine istituita con decreto del Ministro delle Attività Produttive, "Black-out del Sistema Elettrico Italiano del 28 Settembre 2003," Rome, Italy, 2003.

[30] D. Pagnani, F. Blaabjerg, C. L. Bak, F. Faria da Silva, Ł. Kocewiak and J. Hjerrild, "Offshore Wind Farm Black Start Service Integration: Review and Outlook of Ongoing Research," *Energies,* vol. 13, no. 23, pp. 6286-, 2020.

[31] National Grid Electricity System Operator, "Black Start from Non-Traditional Generation Technologies," Warwick, United Kingdom, 2019.

[32] J. Marchgraber and W. Gawlik, "Investigation of Black-Starting and Islanding Capabilities of a Battery Energy Storage System Supplying a Microgrid Consisting of Wind Turbines, Impedance- and Motor-Loads," *Energies,* vol. 13, no. 5170, pp. 1-24, 2020.

[33] L. Liu, J. Wu, Z. Mi and C. Sun, "A Feasibility Study of Applying Storage-Based Wind Farm as Black-Start Power Source in Local Power Grid," in *2016 International Conference on Smart Grid and Clean Energy Technologies (ICSGCE)*, Chengdu, China, pp. 257-261, 2016.

[34] National Grid Electricity System Operator, "Demonstrationn of Black Start from DERs (Live Trials Report) Part 1," Warwick, United Kingdom, 2021.

[35] S. Cherevatskiy, S. Zabihi, R. Korte and H. Klingenberg, "A 30 MW Grid Forming BESS Boosting Reliability in South Australia and Providing Market Services on the National Electricity Market," in *18th Wind Integration Workshop*, Dublin, pp. 1-8, 2019.

[36] S. Cherevatskiy, S. Sproul, S. Zabihi, R. Korte, H. Klingenberg, B. Buchholz and A. Oudalov, "Grid Forming Energy Storage System addresses Challenges of Grids with High Penetration of Renewables (A Case Study)," in *CIGRE Paris 2020*, Paris, France, pp. 1-13, 2020.

[37] The National HVDC Center, "Maximising HVDC Support for GB Black Start and System Restoration," Scottish Hydro Electric Transmission, Glasgow, UK, 2019.

[38] G. Xu, L. Tu, H. Lan and C. Xia, "Analysis on HVDC Start-Up in System Black-Start," in *2015 5th International Conference on Electric Utility Deregulation and Restructuring and Power Technologies (DRPT)*, Changsha, China, pp. 1705-1709, 2015.

[39] L. Zhang, L. Harnefors and H.-P. Nee, "Power-Synchronization Control of Grid-Connected Voltage-Source Converters," *IEEE Transactions on Power Systems,* vol. 25, no. 2, pp. 809-820, 2009.

[40] L. Harnefors, M. Hinkkanen, U. Riaz, F. M. M. Rahman and L. Zhang, "Robust Analytic Design of Power-Synchronization Control," *IEEE Transactions on Industrial Electronics,* vol. 66, no. 8, pp. 5810-5819, 2019.

[41] S. K. Chaudhary, R. Teodorescu, J. R. Svensson, Ł. Kocewiak, P. Johnson and ,. B. Berggren, "Islanded Operation of Offshore Wind Power Plant using IBESS," in *2021 IEEE Power and Energy Society General Meeting*, online, pp. 1-5, 2021.

[42] S. K. Chaudhary, R. Teodorescu, J. R. Svensson, Ł. Kocewiak, P. Johnson and B. Berggren, "Black Start Service from Offshore Wind Power Plant using IBESS," in *2021 IEEE Madrid PowerTech*, online, pp. 1-6, 2021.

[43] F. Zhao, X. Wang, Z. Zhou, L. Harnefors, J. Svensson, Ł. Kocewiak and M. P. Gryning, "Control Interaction Modeling and Analysis of Grid-Forming Battery Energy Storage System for Offshore Wind Power Plant," *IEEE Transactions on Power Systems,* vol. 37, no. 1, pp. 497-507, 2022.

[44] F. Zhao, X. Wang, Z. Zhou, L. Harnefors, J. R. Svensson and Ł. H. Kocewiak, "Comparative Study of Battery-based STATCOM in Grid-Following and Grid-Forming Modes for Stabilization of Offshore Wind Power Plant," *Electric Power Systems Research,* vol. 212, no. November, pp. 1-7, 2022.

[45] S. Bernal-Perez, R. Blasco-Gimenez, S. Añó-Villalba and T. Abeyasekera, "Providing Auxiliary Power when a High-Voltage Link is Non-Functional". United States of America Patent US20190260208A, 26 October 2017.

[46] Ö. Göksu, O. Saborío-Romano, N. A. Cutululis and P. Sørensen, "Black Start and Island Operation Capabilities of Wind Power Plants," in *17th Wind Integration Workshop*, Berlin, Germany, pp. 1-4, 2017.

[47] PROMOTioN Project, "D3.7: Compliance Evaluation Results using Simulations," https://www.promotion-offshore.net/fileadmin/PDFs/D3.7_Compliance_evaluation_results_using_simulations.pdf, 2020.

[48] S. Bernal-Perez, S. Añó-Villalba, R. Blasco-Gimenez and J. Rodríguez-D'Derlée, "Off-Shore Wind Farm Grid Connection using a Novel Diode-Rectifier and VSC-Inverter based HVDC Transmission Link," in *IECON 2011-37th Annual Conference on IEEE Industrial Electronics Society*, Melbourne, Australia, pp. 3186-3191, 2011.

[49] A. Jain, J. N. Sakamuri and N. A. Cutululis, "Grid-forming Control Strategies for Black Start by Offshore Wind Power Plants," *Wind Energy Science,* vol. 5, pp. 1297-1313, 2020.

[50] L. Yu, R. Li and L. Xu, "Distributed PLL-Based Control of Offshore Wind Turbines Connected with Diode-Rectifier-Based HVDC Systems," *IEEE Transactions on Power Delivery,* vol. 33, no. 3, pp. 1328-1336, 2018.

[51] T. Noguchi, H. Tomiki, S. Kondo and I. Takahashi, "Direct Power Control of PWM Converter without Power-Source Voltage Sensors," *IEEE Transactions on Industry Applications,* vol. 34, no. 3, pp. 473-479, 1998.

[52] J. Martínez-Turégano, S. Año-Villalba and S. Bernal-Pérez, "Mixed Grid-Forming and Grid-Following Wind Power Plants for Black Start Operation," in *17th Wind Integration Workshop*, Stockholm, Sweden, pp. 1-6, 2018.

[53] J. Martínez-Turégano, S. Añó-Villalba, S. Bernal-Pérez and R. Blasco-Giménez, "Small-Signal Stability and Fault Performance of Mixed Grid-Forming and Grid-Following Offshore Wind Power Plants connected to a HVDC-Diode Rectifier," *IET Renewable Power Generation,* vol. 14, no. 12, pp. 1-10, 2020.

[54] M. Aten, R. Shanahan, F. Mosallat and S. Wijesinghe, "Dynamic Simulations of a Black Starting Offshore Wind Farm Using Grid Forming Converters," in *18th Wind Integration Workshop*, Dublin, Ireland, pp. 1-8, 2019.

[55] REN21, "Renewables Global Status Report," 2022.

[56] J. Hjerrild, S. Sahukari, M. Juamperez, Ł. Kocewiak, M. A. Vilhelmsen, J. Okholm, M. Zouraraki and T. Kvarts, "Hornsea Projects One and Two – Design and Execution of the Grid Connection for the World's Largest Offshore Wind Farms," in *CIGRE Symposium*, Aalborg, Denmark, pp. 1-11, 2019.

[57] J. Dakic, M. Cheah-Mane, O. Gomis-Bellmunt and E. Prieto-Araujo, "HVAC Transmission System for Offshore Wind Power Plants Including Mid-Cable Reactive Power Compensation: Optimal Design and Comparison to VSC-HVDC Transmission," *IEEE Transactions on Power Delivery,* vol. 36, no. 5, pp. 2814-2824, 2021.

[58] National Grid ESO, "Black Start Technical Requirements and Assessment Criteria," National Grid Electricity System Operator, Warwick, 2019.

[59] National Grid Electricity System Operator, "Appendix 1 - Technical Requirements and Assessment Criteria for the ESR Wind Tender 2022," Warwick, United Kingdom, 2022.

[60] D. Pagnani, Ł. Kocewiak, J. Hjerrild, F. Blaabjerg and C. L. Bak, "Challenges and Solutions in Integrating Black Start into Offshore Wind Farms," in *19th Wind Integration Workshop*, Online, pp. 1-8, 2020.

[61] D. Pagnani, Ł. Kocewiak, J. Hjerrild, F. Blaabjerg and C. L. Bak, "Integrating Black Start Capabilities into Offshore Wind Farms by Grid-Forming Batteries," *IET Renewable Power Generation,* vol. Early Access, no. Early Access, pp. 1-12, 2023.

[62] K. S. Nielsen, "Method of start up at least a part of a wind power". United States of America Patent 8,000,840, 16 August 2011.

[63] P. Egedal, S. Kumar and K. S. Nielsen, "Black start of wind turbine devices". Unites States of America Patent 9,509,141, 29 November 2016.

[64] Y. Zhao, T. Zhang, L. Sun, X. Zhao, L. Tong, Wang, L., J. Ding and Y. Ding, "Energy Storage for Black Start Services: A Review," *International Journal of Minerals Metallurgy and Materials,* vol. 29, no. 4, pp. 691-704, 2022.

[65] R. L. Hales, "First Black Start on Germany's Grid," CleanTechnica, 15 August 2017. [Online]. Available: https://cleantechnica.com/2017/08/15/first-black-start-germanys-grid/. [Accessed 17 August 2022].

[66] A. Colthorpe, "California Battery's Black Start Capability Hailed as 'Major Accomplishment in the Energy Industry'," Energy Storage News, 17 May 2017. [Online]. Available: https://www.energy-storage.news/california-batterys-black-start-capability-hailed-as-major-accomplishment-in-the-energy-industry/. [Accessed 17 August 2022].

[67] C. Li et al., "Method for the Energy Storage Configuration of Wind Power Plants with Energy Storage Systems used for Black-Start," *Energies,* vol. 11, no. 12, pp. 3394 (1-16), 2018.

[68] W. Liu and Y. Liu, "Enabling Wind Farm to be Black-Start Source by Energy Storage," *IET The Journal of Engineering,* vol. 2019, no. 18, pp. 5138-5141, 2019.

[69] L. Weipeng and L. Yutian, "Energy Storage Sizing by Copula Modelling Joint Distribution for Wind Farm to be Black-Start Source," *IET Renewable Power Generation,* vol. 13, no. 11, pp. 1882-1890, 2019.

[70] A. Roscoe, T. Knueppel, R. Da Silva, P. Brogan, I. Gutierrez, J. Perez Campion, D. Elliott and P. Crolla, "Practical Experience of Providing Enhanced Grid Forming Services from an Onshore Wind Park," in *19th Wind Integration Workshop*, Online, pp. 1-6, 2020.

[71] L. Huang, C. Wu, D. Zhou, L. Chen, D. Pagnani and F. Blaabjerg, "Challenges and Potential Solutions of Grid-Forming Converters Applied to Wind Power Generation System," *Frontiers in Energy Research,* vol. 11, pp. 1-14, 2023.

[72] C. Li, R. Burgos, I. Cvetkovic, D. Boroyevich, L. Mili and P. Rodriguez, "Evaluation and Control Design of Virtual-Synchronous-Machine-based STATCOM for Grids with High Penetration of Renewable Energy," in *2014 IEEE Energy Conversion Congress and Exposition (ECCE)*, Pittsburgh, PA, USA, pp. 5652-5658, 2014.

[73] M. R. A. Wara and A. H. M. A. Rahim, "Supercapacitor E-STATCOM for Power System Performance Enhancement," in *2019 International Conference on Robotics,Electrical and Signal Processing Techniques (ICREST)*, Dhaka, Bangladesh, pp. 69-73, 2019.

[74] M. Nuhic and G. Yang, "A Hybrid System Consisting of Synchronous Condenser and Battery - Enhanced Services for Weak Systems," in *IEEE PES Innovative Smart Grid Technologies Europe (ISGT-Europe)*, Bucharest, Romania, pp. 1-5, 2019.

[75] H. T. Nguyen, G. Yang, A. H. Nielsen and P. H. Jensen, "Combination of Synchronous Condenser and Synthetic Inertia for Frequency Stability Enhancement in Low-Inertia Systems," *IEEE Transactions on Sustainable Energy,* vol. 10, no. 3, pp. 997-1005, 2019.

[76] Y. Katsuya, Y. Mitani and K. Tsuji, "Power System Stabilization by Synchronous Condenser with Fast Excitation Control," in *International Conference on Power System Technology (PowerCon)*, Perth, WA, pp. 1563-1568, 2000.

[77] V. Knap, S. K. Chaudhary, D. Stroe, M. Świerczynski, B. Craciun and R. Teodorescu, "Sizing of an Energy Storage System for Grid Inertial Response and Primary Frequency Reserve," *IEEE Transactions on Power Systems,* vol. 31, no. 5, pp. 3447-3456, 2016.

[78] S. A. Nasar and F. C. Trutt, Electric Power Systems, Cleveland: CRC Press, 1999.

[79] F. Shixiong et al., "Influence of Synchronous Condenser Transient Parameters on Voltage Stability of HVDC," in *13th IEEE Conference on Industrial Electronics and Applications (ICIEA)*, Wuhan, pp. 2015-2020, 2018.

[80] J. Jia, G. Yang, A. H. Nielsen, E. Muljadi, P. Weinreich-Jensen and ,. V. Gevorgian, "Synchronous Condenser Allocation for Improving System Short-Circuit Ratio," in *5th International Conference on Electric Power and Energy Conversion Systems (EPECS)*, Kitakyushu, pp. 1-5, 2018.

[81] D. Pagnani, Ł. Kocewiak, J. Hjerrild, F. Blaabjerg and C. L. Bak, "Control Principles for Island Operation and Black Start by Offshore Wind Farms integrating Grid-Forming Converters," in *2022 24th European Conference on Power Electronics and Applications (EPE'22 ECCE Europe)*, pp. 1-11, 2022.

[82] E. Alegria, T. Brown, E. Minear and R. H. Lasseter, "CERTS Microgrid Demonstration with Large-Scale Energy Storage and Renewable Generation," *IEEE Transactions on Smart Grid,* vol. 5, no. 2, pp. 937-943, 2014.

[83] North American Electric Reliability Corporation (NERC), "Grid-Forming Technology," December 2021. [Online]. Available: https://www.nerc.com/comm/RSTC_Reliability_Guidelines/White_Paper_Grid_Forming_Technology.pdf. [Accessed 23 March 2022].

[84] J. Svensson, "Synchronisation Methods for Grid-Connceted Voltage Source Converters," *IEE Proceedings - Generation, Transmission and Distribution,* vol. 148, no. 3, p. 229–235, 2001.

[85] M. Durrant, H. Werner and K. Abbott, "Model of a VSC HVDC Terminal Attached to a Weak AC System," in *2003 IEEE Conference on Control Applications, 2003. CCA 2003*, Istanbul, Turkey, pp. 178-182, 2003.

[86] H. Konishi, C. Takahashi, H. Kishibe and H. Sato, "A Consideration of Stable Operating Power Limits in VSC-HVDC Systems," in *7th International Conference on AC-DC Power Transmission*, London, U.K., pp. 102-106, 2001.

[87] P. Fischer, "Modelling and Control of a Line-Commutated HVDC Transmission System Interacting with a VSC STATCOM," Ph.D. Dissertation, Royal Inst. Technol., Stockholm, Sweden, 2007.

[88] L. Harnefors, M. Bongiorno and S. Lundberg, "Input-Admittance Calculation and Shaping for Controlled Voltage-Source Converters," *IEEE Transactions on Industrial Electronics,* vol. 54, no. 6, p. 3323–3334, 2007.

[89] D. Jovcic, L. A. Lamont and L. Xu, "VSC Transmission Model for Analytical Studies," in *2003 IEEE Power Engineering Society General Meeting (IEEE Cat. No.03CH37491)*, Toronto, ON, Canada, pp. 1737-1742, 2003.

[90] S. D'Arco and J. Suul, "Virtual Synchronous Machines - Classification of Implementations and Analysis of Equivalence to Droop Controllers for Microgrids," in *2013 IEEE PowerTech*, Grenoble, France, 2013.

[91] L. Yu, R. Li and L. Xu, "Distributed PLL-Based Control of Offshore Wind Turbines Connected with Diode-Rectifier-Based HVDC Systems," *IEEE Trans. Power Deliv. ,* vol. 33, no. 3, pp. 1328-1336, 2017.

[92] L. Zhang, "Modeling and Control of VSC-HVDC Links Connected to Weak AC Systems," Royal Institute of Technology - School of Electrical Engineering, Stockholm, Sweden, 2010.

[93] D. Pagnani, Ł. Kocewiak, J. Hjerrild, F. Blaabjerg, C. L. Bak, R. Blasco-Giménez and J. Martínez-Turégano, "Power System Restoration Services by Grid-Forming Offshore Wind Farms with Integrated Energy Storage," in *2023 IEEE Power & Energy Society General Meeting (PESGM) (accepted)*, Orlando, Florida, pp. 1-5, 2023.

[94] N. Halwany, D. Pagnani, M. Ledro, O. I. Idehen, M. Marinelli and Ł. Kocewiak, "Optimal Sizing of Battery Energy Storage to Enable Offshore Wind Farm Black Start Operation," in *21st Wind Integration Workshop*, The Hague, pp. 1-10, 2022.

[95] F. Mandrile, "Next Generation Inverters Equipped with Virtual Synchronous Compensators for Grid Services and Grid Support," Politecnico di Torino, Ph.D. Series, Torino, 2021.

[96] D. Pagnani, Ł. Kocewiak, J. Hjerrild, F. Blaabjerg, C. L. Bak, R. Blasco-Giménez and J. Martínez-Turégano, "Wind Turbine and Battery Storage Interoperability to Provide Black Start by Offshore Wind Farms," *CIGRE Science and Engineering,* pp. 1-19, 2023 (in review).

[97] A. Greenwood, Electrical Transients in Power Systems, Wiley, 1990.

[98] IEC TS 62898-1, "Technical Specification: “Microgrids – Part 1: Guidelines for microgrid projects planning and specification," British Standards Institute, London, United Kingdom, 2017.

PART II – APPENDED PAPER

ISSN (online): 2446-1636
ISBN (online): 978-87-7573-725-3

AALBORG UNIVERSITETSFORLAG